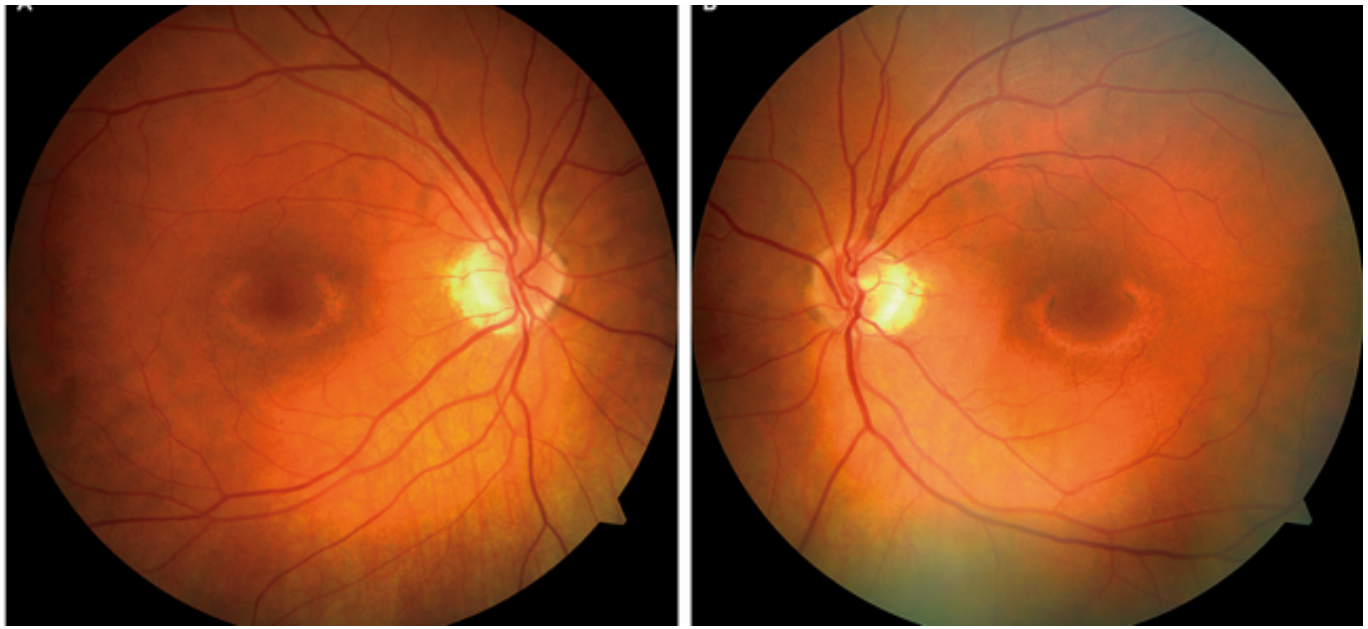
https://www.mdc-berlin.de/de/veroeffentlichungstypen/clinical-journal-club



Als gemeinsame Einrichtung von MDC und Charité fördert das Experimental and Clinical Research Center die Zusammenarbeit zwischen Grundlagenwissenschaftlern und klinischen Forschern. Hier werden neue Ansätze für Diagnose, Prävention und Therapie von Herz-Kreislauf- und Stoffwechselerkrankungen, Krebs sowie neurologischen Erkrankungen entwickelt und zeitnah am Patienten eingesetzt. Sie sind eingelanden, um uns beizutreten. Bewerben Sie sich!



A 60-year-old woman presented to the ophthalmology clinic after noticing central blind spots in the visual fields of both eyes. She had a history of rheumatoid arthritis, which had been treated with hydroxychloroquine for 14 years. The retinal examination showed the pattern below. What is the most likely underlying cause of this abnormality?

Rheumatoid arthritis

Hydroxychloroquine toxicity

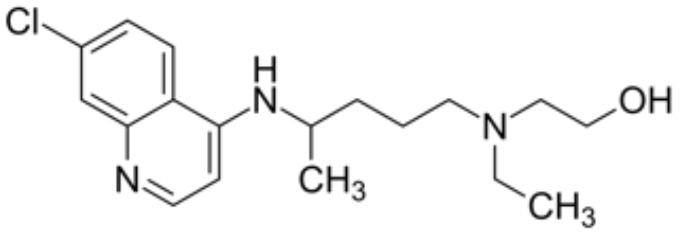
Age-related macular degeneration

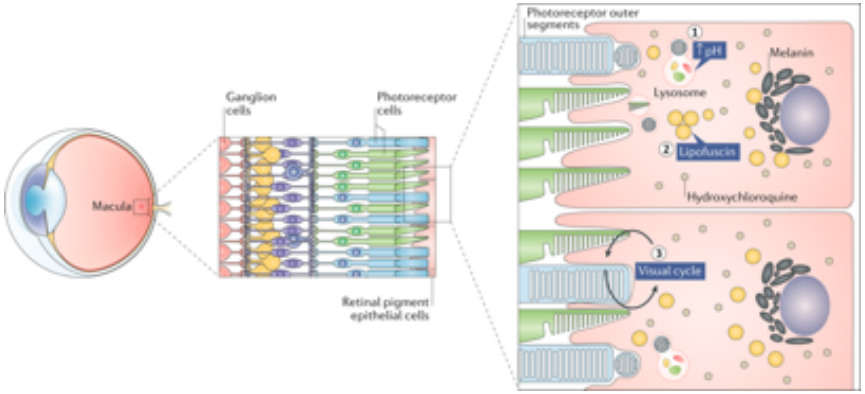
Type 2 diabetes

Bardet-Biedl syndrome

The retinal examination showed a bull's-eye pattern of hypopigmentation in both the right eye (Panel A) and the left eye (Panel B). Visual-field testing showed ring scotomas, and retinal imaging on optical coherence tomography showed corresponding loss of photoreceptors and retinal pigment epithelium, findings that are consistent with bull's-eye maculopathy associated with hydroxychloroquine toxicity.

Hydroxychloroquin ist ein von Chloroquin abgeleiteter und chemisch mit Chinin verwandter Arzneistoff zur Therapie und Prophylaxe der Malaria tropica, der rheumatoiden Arthritis und Kollagenosen wie dem systemischem Lupus erythematodes. Der genaue Wirkungsmechanismus des Hydroxychloroquins ist unbekannt. Hydroxychloroquin hemmt die Häm-Polymerase der Plasmodien und bindet an DNA. Es wird in Plasmodien in ihre Vakuolen aufgenommen. Hydroxychloroquin hemmt den Lebensabschnitt der Plasmodien in den Erythrozyten. Es ist weniger giftig für die Retina als Chloroquin.
Auge Irreversible Retinopathie → Schießscheibenmakulopathie → Ophthalmologische Kontrollen vor und während der Therapie
Reversible Hornhauttrübungen.

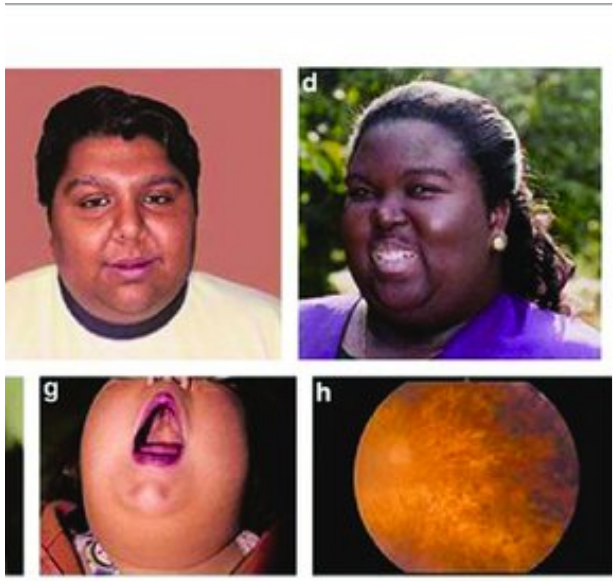




Hydroxychloroquine is thought to cause retinal damage through (1) inhibition of autophagy as a result of increasing retinal pigment epithelial (RPE) cell lysosomal pH and blocking the attachment of autophagosomes to lysosomes. (2) This interference with autophagy also causes an increase in the concentration of lipofuscin in RPE cells, which in turn is linked to photoreceptor degradation. (3) Hydroxychloroquine also inhibits the activity of organic anion transporting polypeptide 1A2 (OATP1A2), which disrupts recycling of all-*trans*-retinol in RPE cells, an important step in the visual cycle.



Das Laurence-Moon-Biedl-Bardet-Syndrom (LMBBS), auch Laurence-Moon-Biedl-Syndrom, ist eine angeborene und unheilbare Entwicklungsstörung auf der Grundlage einer autosomal-rezessiv vererbbaren Genmutation an zwölf möglichen Genen. Es wurden früher zwei Syndromtypen unterschieden: Laurence-Moon-Syndrom und Biedl-Bardet-Syndrom. International wird inzwischen in die Typen 1 bis 12 eingeteilt, je nach dem welches Gen betroffen ist. Das mit hormonellen, insbesondere Gonadotropine betreffende, Störungen zusammenhängende Syndrom gehört zur Gruppe der Ziliopathien.



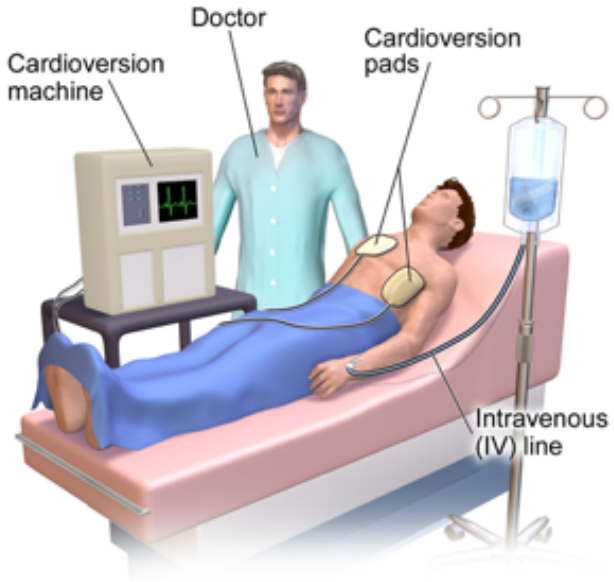
Spitzgaumen

- Gesicht, Augen und Ohren
  - verbreiterte Nasenwurzel
  - kurzer Hals
  - unterdurchschnittliche Zahl der Zähne
  - Retinitis pigmentosa, eine fortschreitende, ggf. zu Blindheit führende, Augenerkrankung
  - Hemeralopie
  - nach unten außen abfallende Lidwinkel
  - Schwerhörigkeit
  - vergleichsweise tief liegende Ohren
- Extremitäten
  - Polydaktylie, häufig der Zehen
- Körper
  - Adipositas (Übergewicht)
  - Diabetes mellitus
  - Arterielle Hypertonie (Bluthochdruck)
  - Minderwuchs
  - Muskelhypotonie (Muskelschwäche)
  - Fehlbildungen der Eierstöcke bzw. Unterentwicklung von Penis (Mikropenis) und Hodensack, Degeneration der Hoden-Tubuli, Leydig-Zell-Hypoplasie (Hypogenitalismus, Hypogonadismus)
  - Fehlbildungen im Bereich der Leber und der Gallenwege
  - Anfälligkeit für Erkrankungen der Nieren, häufig primäre Nierenhypoplasie mit Pyelonephritis und Urämie
- Sonstiges
  - Geistige Behinderung unterschiedlichen Schweregrades
  - Störungen der Motorik
  - Antriebsschwäche
  - verzögerte oder ausbleibende Pubertät

Die elektrische Kardioversion

Unter dem Begriff „elektrische Kardioversion“ versteht man eine Maßnahme zur Wiederherstellung des normalen Herzschlags bei Herzrhythmusstörungen wie Vorhofflimmern. Das Ziel ist es, das Herz wieder in den sogenannten Sinusrhythmus – den normalen, regelmäßigen Herzschlag – zurückzuführen. Vorhofflimmern stellt eine Funktionsstörung dar, bei der die Reizausbreitung unkoordiniert abläuft. Ausgehend vom Sinusrhythmus wird die rhythmische Bewegung des Herzens gesteuert. Mittels der elektrischen Kardioversion wird versucht, eine geordnete Aktivität des Sinusknotens – des elektrischen Taktgebers der Herzaktion – wiederherzustellen, sodass das Herz wieder im Rhythmus schlägt.

Was ist vor der elektrischen Kardioversion bei Vorhofflimmern-Patienten zu beachten?



Cardioversion

Wie wird eine elektrische Kardioversion durchgeführt?

Bei Betroffenen, bei denen das Vorhofflimmern länger als 48 Stunden anhält oder bei unbekannter Dauer, empfiehlt die Europäische Gesellschaft für Kardiologie vor der Kardioversion eine Therapie mit **oralen Antikoagulanzien** für mindestens drei Wochen. Nach dem Eingriff muss die Antikoagulation für weitere vier Wochen beibehalten werden.

Die elektrische Kardioversion wird in der Regel ambulant durchgeführt. Damit beim Eingriff selbst die Verschluckung von Lebensmittelresten oder ähnlichem ausgeschlossen werden kann, ist es notwendig, dass der Patient zum vereinbarten Termin nüchtern in die Klinik bzw. Praxis kommt. Zur Untersuchung sollten Patienten auch daran denken, unter anderem folgende Unterlagen mitzubringen:

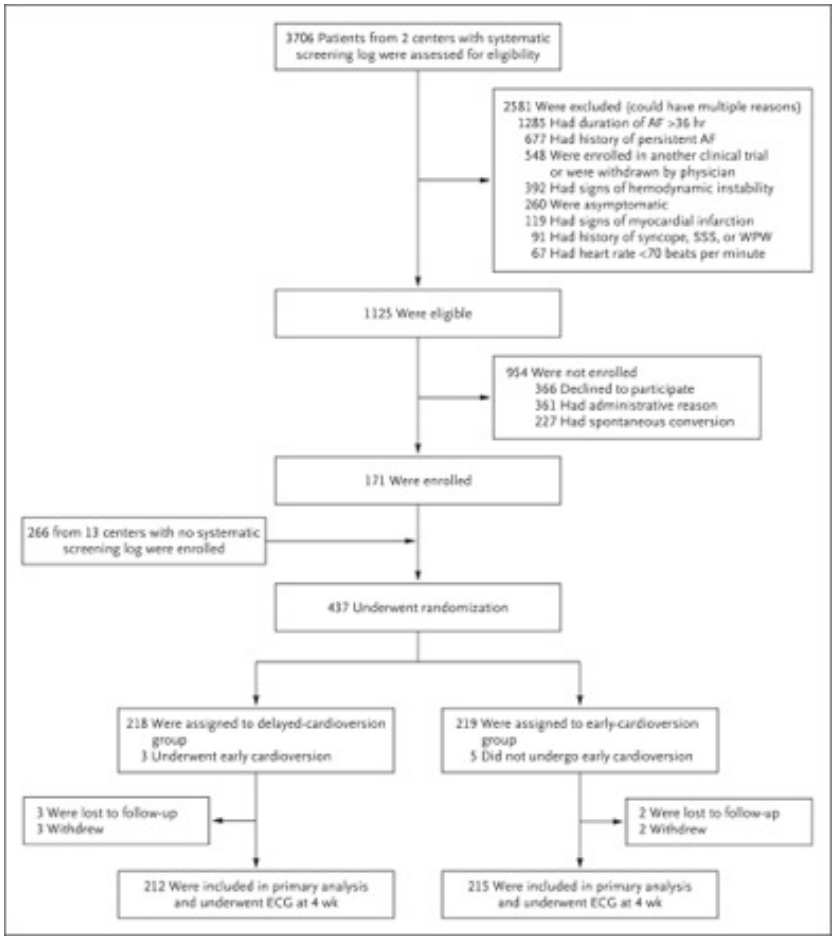
- Eventuell vorhandene Dokumente zu Voruntersuchungen (ggfs. Bescheinigung des unauffälligen Befundes der transösophageale Echokardiographie)
- Medikamentenausweis sowie -liste (ggfs. über den Hausarzt zu erfragen)
- Einweisungsbescheid des Hausarztes



Die elektrische Kardioversion wird unter Kurznarkose durchgeführt und ist somit für den Patienten schmerzfrei. Während der gesamten Behandlung steht der Patient unter EKG-Kontrolle. Mithilfe von Stromstößen (die mit einer wesentlich geringeren Dosis als beispielsweise bei der Defibrillation abgegeben werden) wird der Herzrhythmus zurück in den Sinusrhythmus versetzt. Impulsgeber für die Stromstöße ist dabei der eigene Herzschlag, der vom EKG erfasst wird. So kann das Risiko eines Auftretens von Kammerflimmern reduziert werden.

Early or Delayed Cardioversion in Recent-Onset Atrial Fibrillation

Patients with recent-onset atrial fibrillation commonly undergo immediate restoration of sinus rhythm by pharmacologic or electrical cardioversion. However, whether immediate restoration of sinus rhythm is necessary is not known, since atrial fibrillation often terminates spontaneously. In a multicenter, randomized, open-label, noninferiority trial, we randomly assigned patients with hemodynamically stable, recent-onset (<36 hours), symptomatic atrial fibrillation in the emergency department to be treated with a wait-and-see approach (delayed-cardioversion group) or early cardioversion. The wait-and-see approach involved initial treatment with rate-control medication only and delayed cardioversion if the atrial fibrillation did not resolve within 48 hours. The primary end point was the presence of sinus rhythm at 4 weeks. Noninferiority would be shown if the lower limit of the 95% confidence interval for the between-group difference in the primary end point in percentage points was more than −10.



In the delayed-cardioversion group, patients received rate-control medication and were discharged when their condition was determined to be clinically stable. An outpatient clinic visit was planned for the next day, as close as possible to 48 hours after the onset of symptoms of atrial fibrillation (AF). At this visit, the heart rhythm was reassessed on 12-lead electrocardiography (ECG). If atrial fibrillation was still present, patients were referred to the emergency department for delayed cardioversion. In the early-cardioversion group, patients underwent immediate pharmacologic or electrical cardioversion, depending on their medical history. SSS denotes sick sinus syndrome, and WPW Wolff–Parkinson–White syndrome.

Of the 437 patients who had undergone randomization, 218 were assigned to the delayed-cardioversion group and 219 to the early-cardioversion group (Table). The mean (±SD) age was 65±11 years; 176 patients (40%) were female, and 192 (44%) had a first episode of atrial fibrillation. Palpitations were the most common symptom (87%), followed by exercise-induced fatigue (26%). An increased risk of stroke, as reflected by a CHA_2DS_2-VASc score of 2 or higher, was seen in 279 patients (64%). At enrollment, 175 patients (40%) were taking oral anticoagulant drugs, and in 127 patients (29%) anticoagulation was initiated during the index visit.

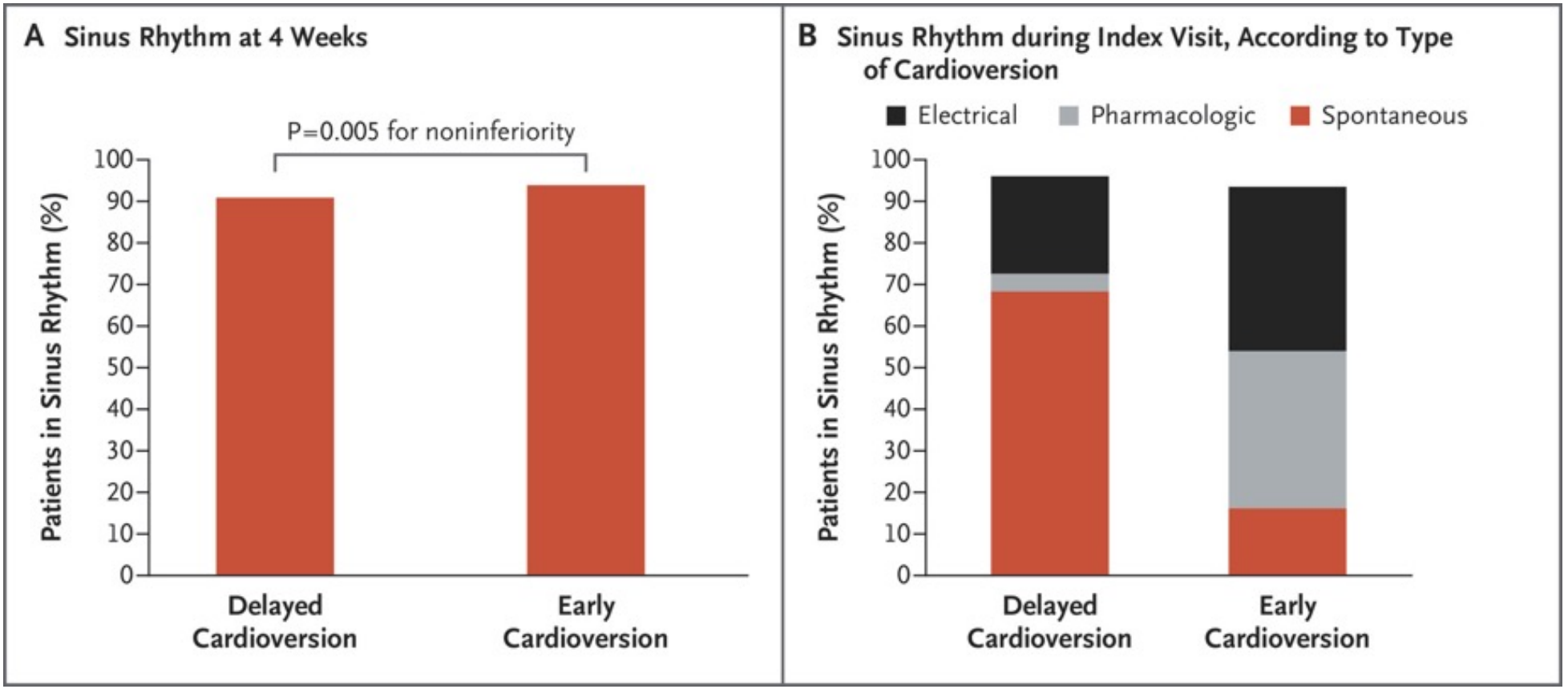
A screening log was kept in two of the trial centers. Of the 3706 patients who had undergone screening, 2581 (70%) were excluded. The most common reasons for exclusion were a duration of atrial fibrillation of more than 36 hours and a history of persistent atrial fibrillation.

Table 1. Characteristics of the Patients at Baseline.*

Characteristic	Delayed Cardioversion (N=218)	Early Cardioversion (N=219)
Age — yr	65±11	65±11
Male sex — no. (%)	131 (60)	130 (59)
Medical history — no. (%)		
Hypertension	118 (54)	133 (61)
Diabetes	21 (10)	25 (11)
Myocardial infarction	24 (11)	13 (6)
Ischemic stroke or transient ischemic attack	12 (6)	15 (7)
CHA_2DS_2-VASc score — no. (%)†		
0	36 (17)	33 (15)
1	47 (22)	42 (19)
≥2	135 (62)	144 (66)
Symptoms — no. (%)		
Palpitations	188 (86)	193 (88)
Exercise-induced fatigue	55 (25)	60 (27)
Dyspnea	56 (26)	44 (20)
Chest pain	54 (25)	44 (20)
Median heart rate during atrial fibrillation (IQR) — beats/min	123 (101–144)	125 (103–143)
Medication use — no. (%)		
Vitamin K antagonist	34 (16)	34 (16)
Non–vitamin K oral anticoagulant	56 (26)	51 (23)
Antiarrhythmic drug	46 (21)	53 (24)

* Plus–minus values are means ±SD. There were no significant differences between the two groups. Percentages may not total 100 because of rounding. Additional details regarding the baseline characteristics are provided in Table S7 in the Supplementary Appendix. IQR denotes interquartile range.

† The CHA_2DS_2-VASc score is a measure of the risk of stroke in patients with atrial fibrillation, with scores ranging from 0 to 9 and higher scores indicating a greater risk. Congestive heart failure, hypertension, an age of 65 years to 74 years, diabetes, and vascular disease are each assigned one point, and previous stroke or transient ischemic attack and an age of more than 75 years are assigned two points.



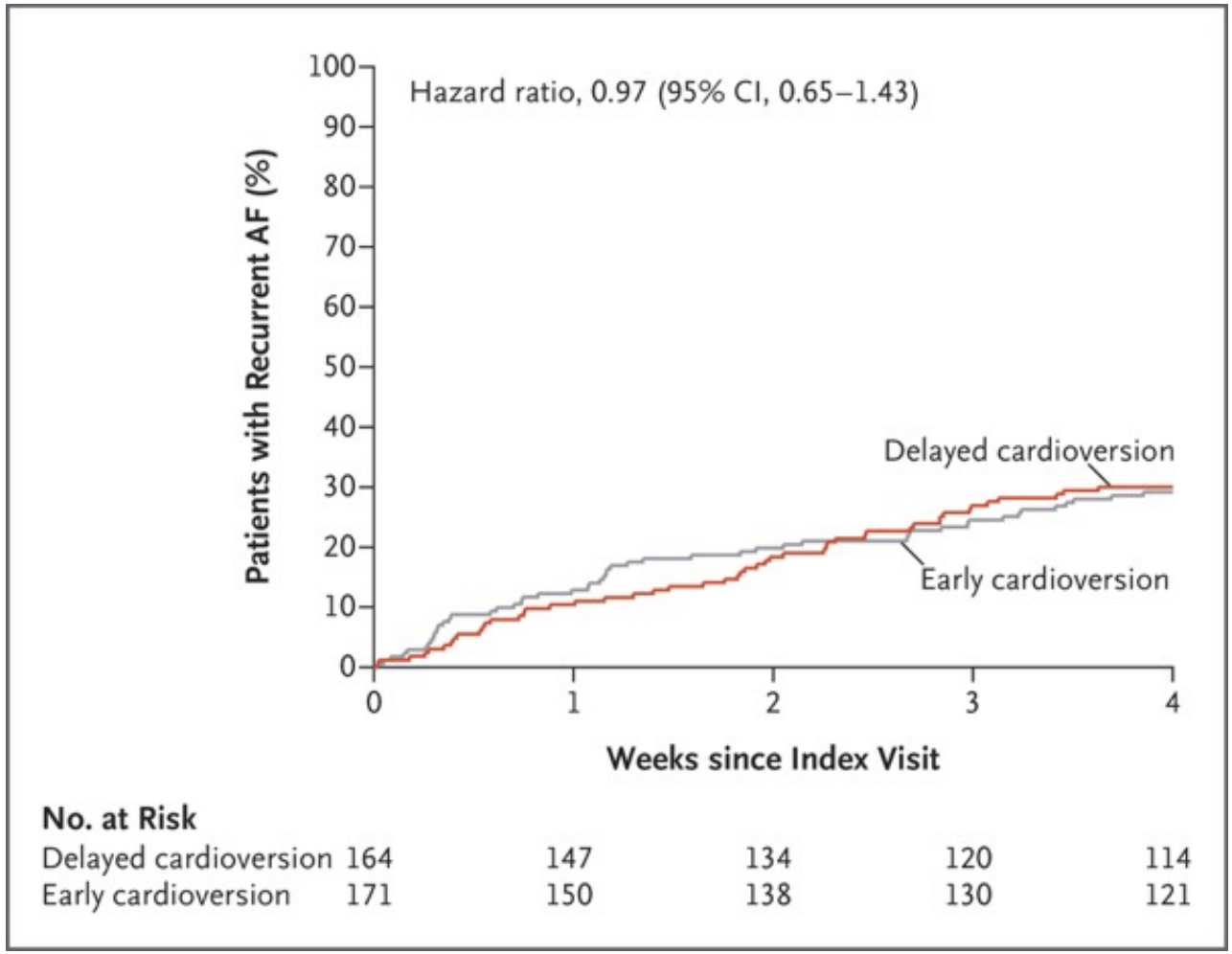
Primary End Point and Distribution of Cardioversion Methods. Panel A shows the percentage of patients with the primary end point (sinus rhythm at 4 weeks after the index visit) among those who were treated with a wait-and-see approach (delayed-cardioversion group) or early cardioversion. Panel B shows the percentage of patients in sinus rhythm according to the method of cardioversion during the index visit. The index visit included the emergency department visit for all patients and a next-day emergency department visit for delayed cardioversion as needed in the patients who were treated with a wait-and-see approach, all as close as possible to 48 hours after symptom onset. In the delayed-cardioversion group, the rate of spontaneous conversion was higher owing to the wait-and-see period. The spontaneous conversions in the early-cardioversion group occurred during preparation for the cardioversion procedure.

Table 2. Cardiovascular Complications during the Index Visit and during 4 Weeks of Follow-up.

Complication	Index Visit*		During 4 Weeks of Follow-up	
	Delayed Cardioversion (N=218)	Early Cardioversion (N=219)	Delayed Cardioversion (N=218)	Early Cardioversion (N=219)
	number of patients			
Admission for heart failure	1	1	0	0
Ischemic stroke or transient ischemic attack	0	0	1	1
Unstable angina or acute coronary syndrome	0	0	3	3
Bradycardia or hypotension	1†	2	2‡	0
Tachycardia	1	1	1§	0

* The index visit was defined as the initial visit to the emergency department for all patients and included a next-day emergency department visit for delayed cardioversion as needed in the patients who were treated with a wait-and-see approach.
† This patient had sinus bradycardia, hypotension, and sinus arrest after delayed cardioversion at 48 hours, which was followed by hospital admission for rhythm observation.
‡ After the infusion of flecainide, one patient had sinus arrest with asystole for 30 seconds, which necessitated temporary chest compressions until a return of spontaneous circulation.
§ This patient had wide QRS tachycardia after the infusion of flecainide.

There were no significant between-group differences with respect to cardiovascular complications. Within 4 weeks after randomization (including during the index visit), 10 cardiovascular complications occurred in the delayed-cardioversion group (including 1 patient with ischemic stroke and 3 with acute coronary syndrome or unstable angina) and 8 in the early-cardioversion group (including 1 patient with transient ischemic attack and 3 with acute coronary syndrome or unstable angina). There were no deaths during follow-up.



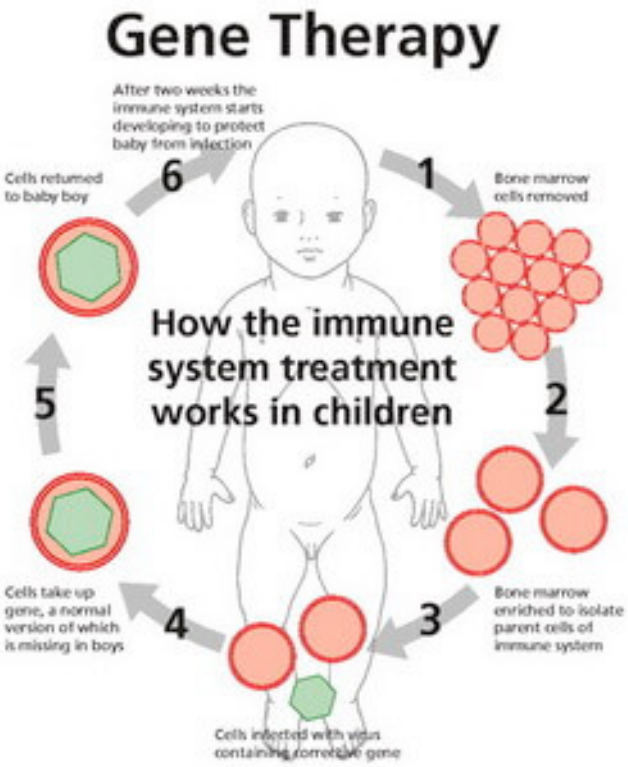
First Recurrence of Atrial Fibrillation. Shown is a Kaplan–Meier analysis of the time until the first recurrence of atrial fibrillation in the two trial groups among 335 patients for whom telemetric ECG monitoring was available. The hazard ratio is for the delayed-cardioversion group as compared with the early-cardioversion group.

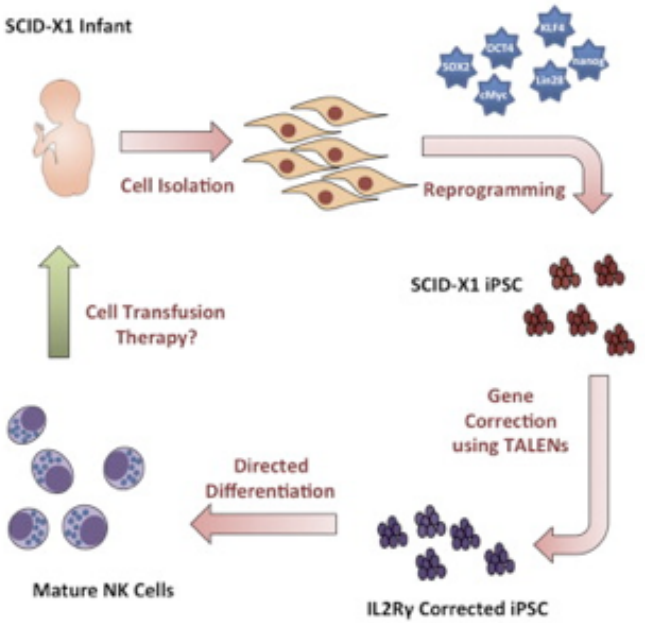
Discussion

Among patients who presented to the emergency department with recent-onset, symptomatic atrial fibrillation, a wait-and-see strategy was noninferior to early cardioversion in obtaining sinus rhythm at 4 weeks after the index visit. Spontaneous conversion frequently occurred in patients in the delayed-cardioversion group and reduced the need for immediate pharmacologic or electrical cardioversion.

The approaches to treating patients with recent-onset atrial fibrillation in the emergency department vary greatly. Early pharmacologic or electrical cardioversion is common practice. However, the wait-and-see strategy, with delayed cardioversion if needed within 48 hours after symptom onset, has several advantages for patients. First, cardioversion (along with its potential complications) may be avoided. Second, the time spent in the emergency department during the initial presentation may be reduced. Third, spontaneous conversions of atrial fibrillation may be observed, leading to fewer misclassifications of persistent atrial fibrillation. This factor may bear consequences for future rhythm-control strategies, which are considered to be less complex in patients with paroxysmal atrial fibrillation than in those with persistent atrial fibrillation. Fourth, patients may have the experience that their arrhythmia terminated by itself, which may broaden their insight into treatment options. Our data suggest that the wait-and-see approach, including a second emergency department visit as needed, is not necessarily more time consuming than early cardioversion. This finding may be due to workup for sedation or drug infusion, waiting time for a sufficient fasting state before electrical cardioversion, or obligatory observation after cardioversion. An unplanned early cardioversion challenges the organization of care in generally overcrowded emergency departments. Pharmacologic cardioversion requires specific expertise in the administration of intravenous antiarrhythmic drugs by the treating cardiologist. Electrical cardioversion requires sedation, involving the expertise of an anesthesiologist. These circumstances may hamper prompt execution of cardioversion, especially since cardioversion in a clinically stable patient is usually not considered to be an emergency procedure. In contrast, almost all the patients in the delayed-cardioversion group could be discharged home after the administration of rate-control medication, regardless of conversion to sinus rhythm.

X-SCID (Severe Combined Immunodeficiency), auch SCID-X1, ist eine Form der Immunschwächekrankheit SCID, bei der durch eine Mutation am gemeinsamen Interleukin-Rezeptor-γ-gen bzw. der durch dieses Gen kodierten gemeinsamen Kette (kurz γc, CD132), mehrere Interleukinrezeptoren nicht mehr funktionsfähig sind. Ein Beispiel ist der Interleukin-2-Rezeptor (IL-2Rγ). Auf Grund dieser Fehler können sich aus hämatopoetischen Stammzellen (Blut-Stammzellen) keine Vorläufer-T-Lymphozyten und keine NK-Zellen entwickeln. Da aber für die Antikörperproduktion durch B-Lymphozyten als Stimulus TH2-Zellen (=eine „Unter-Klasse“ der T-Lymphozyten) essentiell sind, ist nicht nur das zelluläre, sondern auch das humorale Immunsystem nicht arbeitsfähig, also das gesamte adaptive Immunsystem defekt. Das Gen für den Rezeptor ist am X-Chromosom lokalisiert, deshalb die Bezeichnung X-SCID. X-SCID ist die genetische Ursache für etwa 50 % aller SCID-Fälle. Betroffene Patienten sind anfällig für Infektionen jeglicher Art wie Lungenentzündung oder Meningitis und überleben ohne entsprechende medizinische Behandlung (oder Abschirmung in einem sterilen Zelt) nur kurz. Wie bei vielen anderen Immunkrankheiten, z. B. Leukämien, wird klassischerweise eine Zerstörung des gesamten Immunsystems durch Chemotherapie durchgeführt (wobei dies hier kaum nötig ist), anschließend werden durch eine Knochenmarkstransplantation Lymphozyten aus einem geeigneten Spender implantiert, die dann ein neues Immunsystem im Patienten bilden sollen.





Lentiviral Gene Therapy Combined with Low-Dose Busulfan in Infants with SCID-X1

Allogeneic hematopoietic stem-cell transplantation for X-linked severe combined immunodeficiency (SCID-X1) often fails to reconstitute immunity associated with T cells, B cells, and natural killer (NK) cells when matched sibling donors are unavailable unless high-dose chemotherapy is given. In previous studies, autologous gene therapy with γ-retroviral vectors failed to reconstitute B-cell and NK-cell immunity and was complicated by vector-related leukemia. We performed a dual-center, phase 1–2 safety and efficacy study of a lentiviral vector to transfer *IL2RG* complementary DNA to bone marrow stem cells after low-exposure, targeted busulfan conditioning in eight infants with newly diagnosed SCID-X1.

Patient No. (Age at Gene Therapy)	*IL2RG* Mutation	Maternal T-Cell Engraftment	CD3+ Cell Count	CD19+ Cell Count	CD3−CD56+ Cell Count	Medical History	Busulfan Cumulative AUC	CD34+ Cell Dose	VCN of Graft	Follow-up Duration	Status at Last Follow-up†
		% of T cells		*cells/mm³*			*mg×hr/liter*	*no.×10⁻⁶/kg*	*copies/cell*	*mo*	
1 (6 mo)	c.720G→A p. Trp240X	100	3916	1210	40	Neutropenia, CMV, coronavirus	20.0	4.46	0.16‡	24.9	CMV and coronavirus resolved, autoimmune cytopenia had developed but resolved
2 (3 mo)	c.270(−15)A→G IVS2 branch point A splice	0	0	2340	13	Rhinovirus	22.5	8.67	1.13	23.1	No longer receiving IV immune globulin, immunized§
3 (4 mo)	c.876(−1)G→A IVS5 splice	0	10	1138	18	Rhinovirus	20.7	9.26	0.80	20.1	No longer receiving IV immune globulin, immunized§
4 (14 mo)	c.562C→T p. Gln188X	0	0	190	4	Disseminated BCG, legionella, rhinovirus	23.0	6.93	0.35	17.1	Disseminated BCG and legionella resolved, no longer receiving IV immune globulin, immunized
5 (3 mo)	c.677G→A p. Arg266His	0	0	5832	1094	None	22.8	6.02	0.44	15.7	Outpatient
6 (11 mo)	c.903_910del p. Glu302Argfs X11	0	41	1376	19	Disseminated BCG	22.9	4.60	0.17	14.6	Disseminated BCG resolved, no longer receiving IV immune globulin, immunized§
7 (2 (mo)	c.548delT p. Leu183Trpfs X90	42	15	1178	11	Neutropenia	20.4	15.10	1.10	11.1	Outpatient
8 (3 mo)	c.326_340del p.Glu109_ Ser113del	1	4	2590	2	Aphthous ulcers	22.2	6.52	0.36	6.7	Outpatient, ulcers resolved

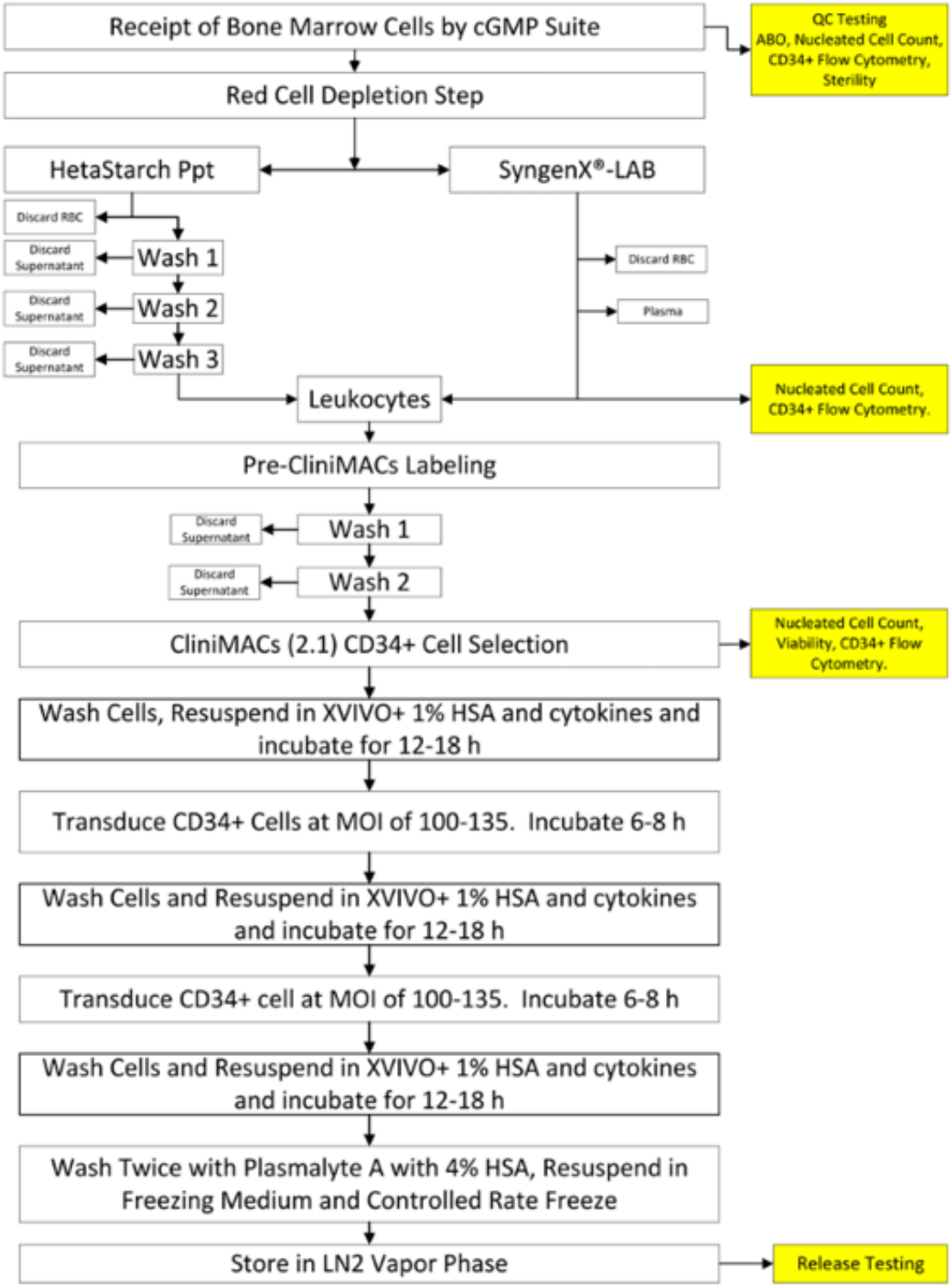

Receipt of Bone Marrow Cells by cGMP Suite
QC Testing
ABO, Nucleated Cell Count, CD34+ Flow Cytometry, Sterility
Red Cell Depletion Step
HetaStarch Ppt
SyngenX®-LAB
Discard RBC
Discard Supernatant
Wash 1
Discard Supernatant
Wash 2
Discard Supernatant
Wash 3
Discard RBC
Plasma
Leukocytes
Nucleated Cell Count, CD34+ Flow Cytometry.
Pre-CliniMACs Labeling
Discard Supernatant
Wash 1
Discard Supernatant
Wash 2
CliniMACs (2.1) CD34+ Cell Selection
Nucleated Cell Count, Viability, CD34+ Flow Cytometry.
Wash Cells, Resuspend in XVIVO+ 1% HSA and cytokines and incubate for 12-18 h
Transduce CD34+ Cells at MOI of 100-135. Incubate 6-8 h
Wash Cells and Resuspend in XVIVO+ 1% HSA and cytokines and incubate for 12-18 h
Transduce CD34+ cell at MOI of 100-135. Incubate 6-8 h
Wash Cells and Resuspend in XVIVO+ 1% HSA and cytokines and incubate for 12-18 h
Wash Twice with Plasmalyte A with 4% HSA, Resuspend in Freezing Medium and Controlled Rate Freeze
Store in LN2 Vapor Phase
Release Testing

Figure S9: Genomic features of vector insertion sites (VIS) in cases 1-5.

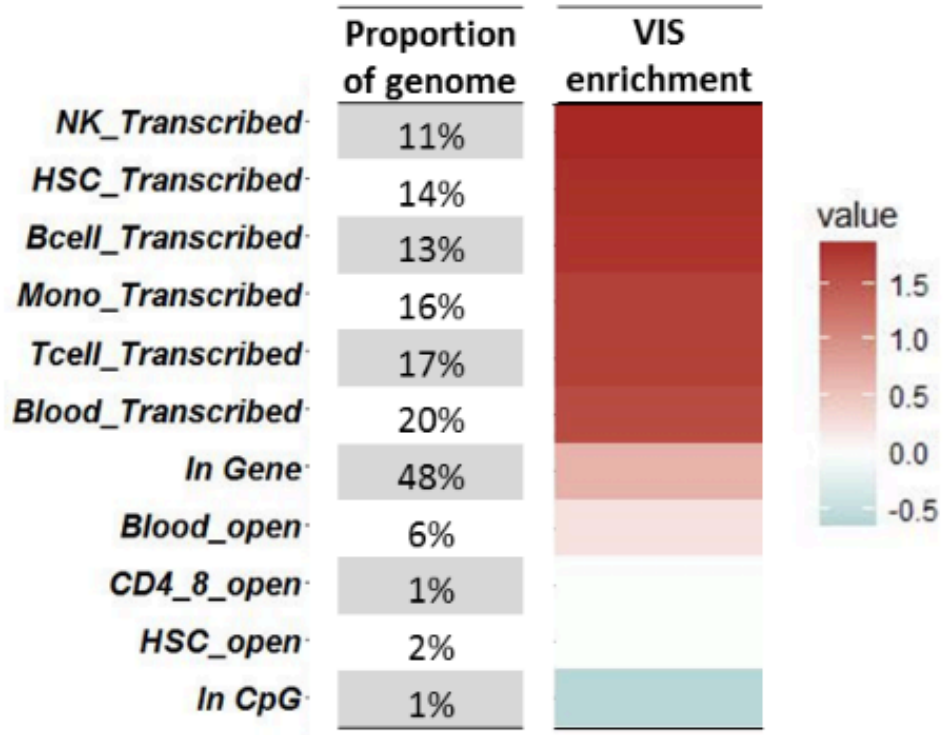


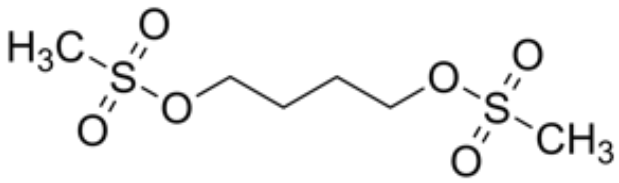
Figure S9: Genomic features of vector insertion sites (VIS) in cases 1-5. The heatmap shows the relative frequency of VIS in the indicated genomic regions, adjusted for their relative proportion within the genome. Red indicates a relative increase in VIS frequency in the indicated genomic areas with a predilection for insertions into regions associated with transcription of blood cell genes and in exons/introns of coding regions. There is a relative depletion of insertions into CpG rich areas typically associated with gene regulator regions.

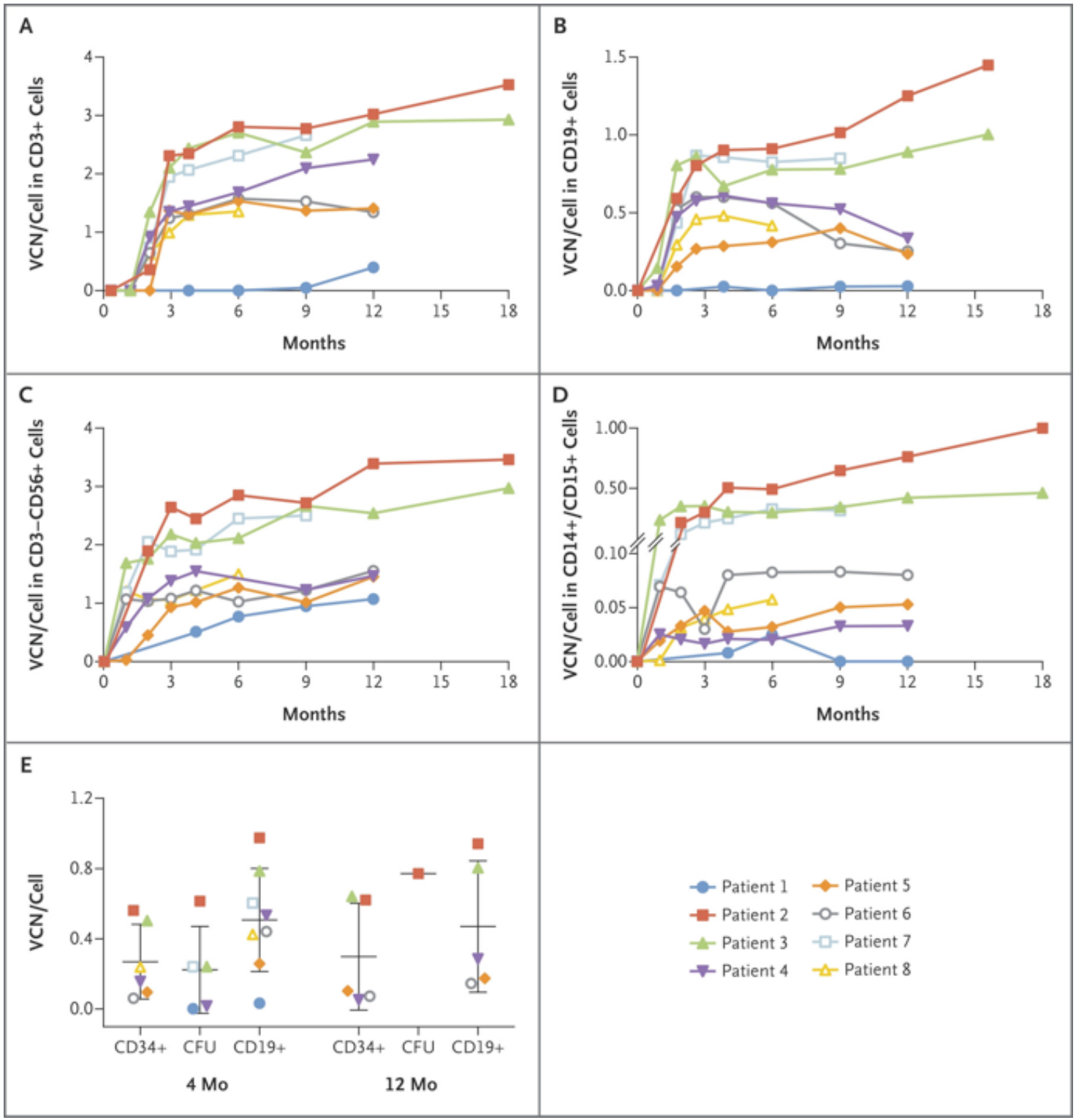
Busulfan ist ein synthetisches Zytostatikum zur Behandlung bestimmter Krebserkrankungen. Es zählt zu den Alkylantien. Busulfan ist ein bifunktionales Alkylans. Die Bifunktionalität ergibt sich aus zwei Methansulfonat-Gruppen, die an den Enden der C4-Kette vorzufinden sind. Die beiden Methansulfonatgruppen stellen gute Abgangsgruppen dar und werden leicht nukleophil substituiert. Alkyliert wird vor allem die DNA, aber auch andere Moleküle in der Zelle können Ziele der Alkylierung durch Busulfan sein. Anwendungsgebiete von Bulsulfan sind die Chronische myeloische Leukämie (CML) und die Konditionierungsbehandlung vor Stammzelltransplantation.

Table S1: Busulfan doses and measured overall exposure by case

Pt No.	Age Mo	1st dose mg/kg	2nd dose mg/kg	Total dose mg/kg	Total AUC mg*hr/L	Adverse Events
1	6	2.59	0.00	2.59	20.0	None
2	3	2.14	2.95	5.09	22.5	None
3	4	2.33	2.39	4.72	20.7	None
4	14	3.08	2.59	5.67	23.0	None
5	3	2.27	2.75	5.02	22.8	Mucositis
6	11	2.59	2.88	5.47	22.9	Mucositis, hair loss
7	2	1.91	0.75	2.66	20.4	None
8	3	2.07	1.56	3.63	22.2	None

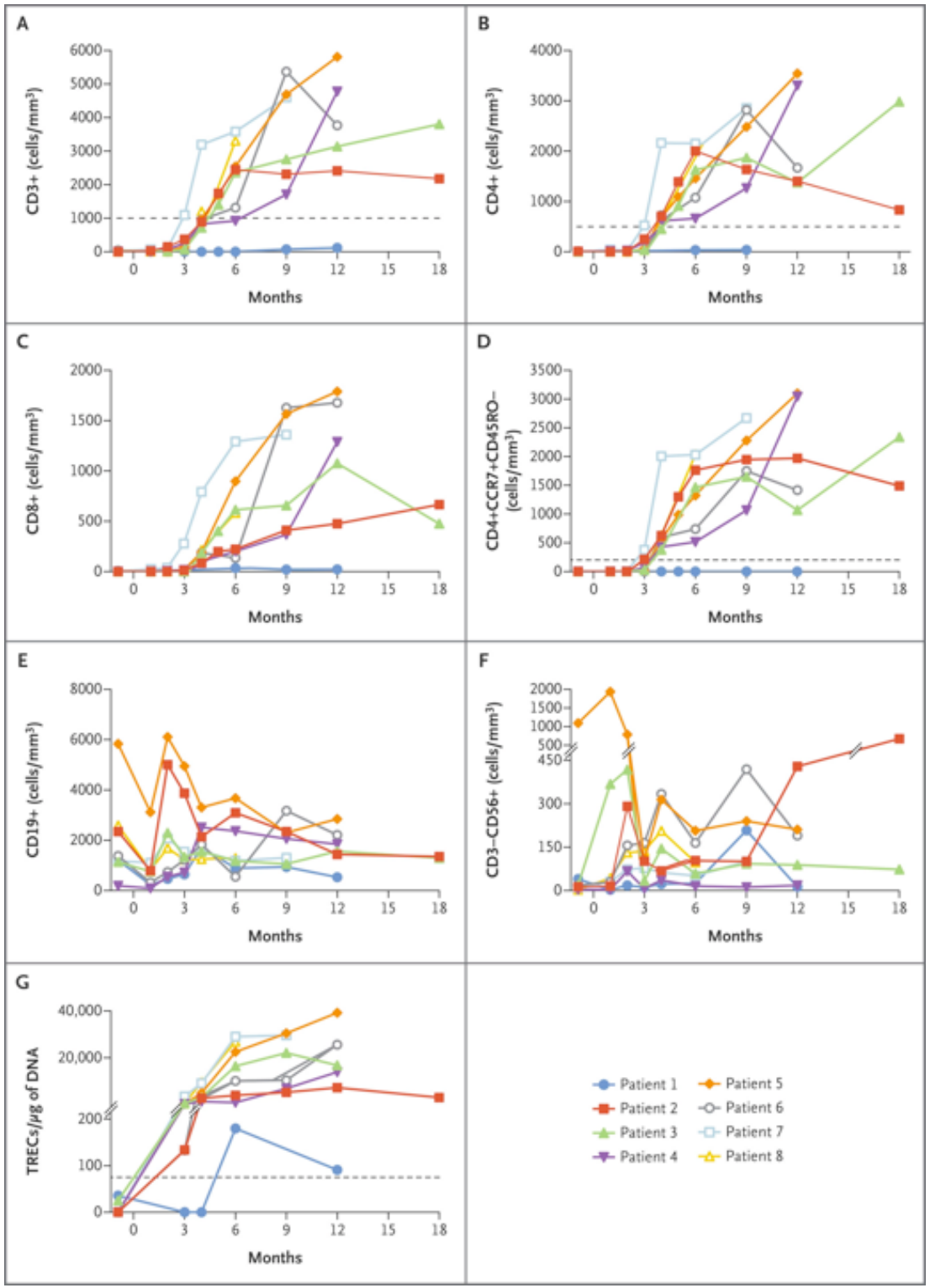
The individual 1st and 2nd doses and total dose are shown for each case. The measured cAUC is also shown for each case and was calculated from multiple peripheral blood samples using standard population pharmacokinetic model. Adverse events are listed in cases where such events occurred.





Vector Marking in Blood and Marrow Cells after Gene Therapy.

Panels A through D show the vector copy number (VCN) per cell in peripheral-blood T-cell (CD3+), B-cell (CD19+), NK-cell (CD3−CD56+), and myeloid-cell (CD14+/CD15+) lineages, respectively, as sorted by flow cytometry, in Patients 1 through 8 at various time points after cell infusion. Panel E shows the results of cells obtained by bone marrow aspiration at 4 and 12 months after gene therapy. The mean vector copy number per cell of selected CD34+ and CD19+ cells is shown. In addition, the mean vector copy number per cell measured in pooled myeloid colony-forming unit (CFU) assays after 14 days of culture is shown.



Immune Reconstitution after Gene Therapy.

Panels A through F show absolute numbers of peripheral-blood immune-cell subsets, as determined by means of standard flow cytometry, over time after cell infusion. Dotted lines indicate values for T-cell counts that are defined in the protocol as representing clinically significant reconstitution at 52 weeks after gene therapy. Panel G shows the quantity of DNA T-cell–receptor excision circles (TRECs) in peripheral-blood mononuclear cells, with a dotted line indicating the lower limit of the normal range. The values above the hash marks on the y axis range from 201 to 40,000.

Discussion

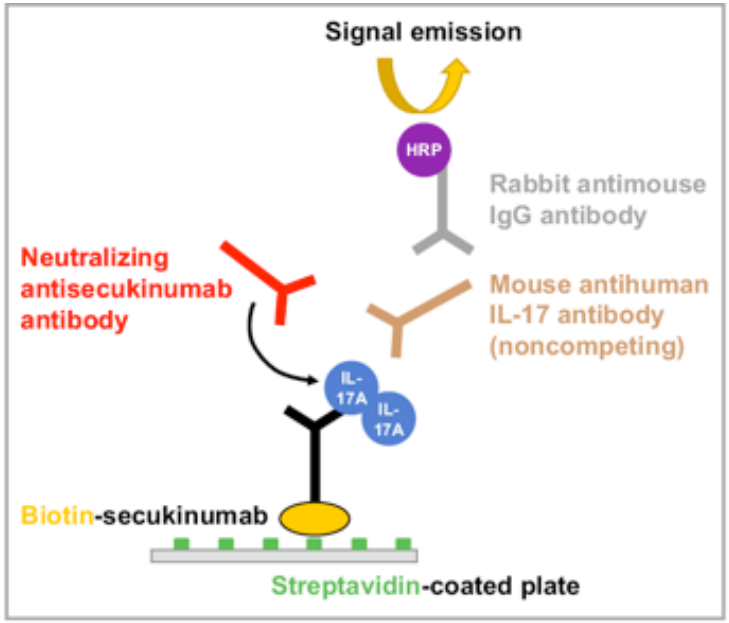
This study showed the successful use of a lentiviral vector combined with low-exposure, targeted busulfan conditioning as the primary treatment in infants with newly diagnosed SCID-X1. This approach led to broad immune reconstitution and efficient vector transduction in diverse lineages, including T cells, B cells, NK cells, myeloid cells, and bone marrow progenitors. This high-level marking was associated with evidence of B-cell reconstitution and restoration of humoral immunity, which has not been achieved in previously reported trials of gene therapy for infants with newly diagnosed SCID-X1. In addition, rapid reconstitution of T cells and NK cells was achieved in most cases, and the overall safety profile was favorable at the time of this interim analysis.

In previous trials that used a γ-retroviral vector without busulfan conditioning to treat newly diagnosed SCID-X1 in infants, durable immune reconstitution was limited to T cells, whereas myeloid-cell, B-cell, and NK-cell marking was relatively low, and patients did not recover humoral immunity.

In conclusion, we found that the combination of a lentiviral vector construct and nonmyeloablative targeted busulfan conditioning in infants with newly diagnosed SCID-X1 resulted in multilineage engraftment of gene-marked cells, with prompt and durable normalization of T-cell immunity and high-level gene marking in B cells and NK cells, with normalization of IgM levels and the development of normal antibody responses. It is hoped that durable, complete adaptive immunity will be achieved in the majority of the patients over time. Successful manufacturing from a stable producer cell line and cryopreservation of the transduced-cell product would streamline the vector production process and facilitate efforts to commercialize product distribution through centralized manufacturing facilities. Long-term follow-up will be required to assess the durability of the immune reconstitution and the persistence of the transferred gene in hematopoietic and immune cells and to monitor the patients for potential late effects of busulfan conditioning and gene therapy.

Neutralisierende Antikörper (NAb) sind Antikörper, die neutralisierend auf die biologische Aktivität eines Pathogens oder eines Toxins wirken. Neutralisierende Antikörper binden meist an Proteine in der Oberfläche einer Zelle des Pathogens (bei Bakterien und Pilzen) bzw. auf der Virusoberfläche bei Viren und hemmt deren Funktion. Nur einen Anteil der nach Infektion oder Impfung gebildeten und an das Pathogen bindenden Antikörper wirkt neutralisierend. Neutralisierende Antikörper sind ein wichtiger Bestandteil der Immunität nach einer Infektion, welche vor erneuter Infektion schützt (sterilisierende Immunität). Die Neutralisation ist eine der drei möglichen Funktionen eines Antikörpers. Beim Subtyp Immunglobulin A ist die Neutralisation die Hauptfunktion. Impfstoffe zur passiven Immunisierung enthalten neutralisierende Antikörper in hohen Konzentrationen. Typische Beispiele für neutralisierende Antikörper sind das Diphtherie-Antitoxin, das nach einer Impfung mit einem Diphtherieimpfstoff gebildet wird, wie auch viele andere Antitoxine. Bei der Therapie der multiplen Sklerose mit Interferon-beta können neutralisierende Antikörper dagegen entstehen, welche die Wirksamkeit der Behandlung mindern. Die neutralisierende Wirkung von Antikörpern kann mit einem Neutralisationstest gemessen werden. Ein Hämagglutinationshemmtest und ein Tierversuch mit passiver Immunisierung und anschließender Infektion (Belastungsversuch) geben Hinweise auf neutralisierende Wirkung.

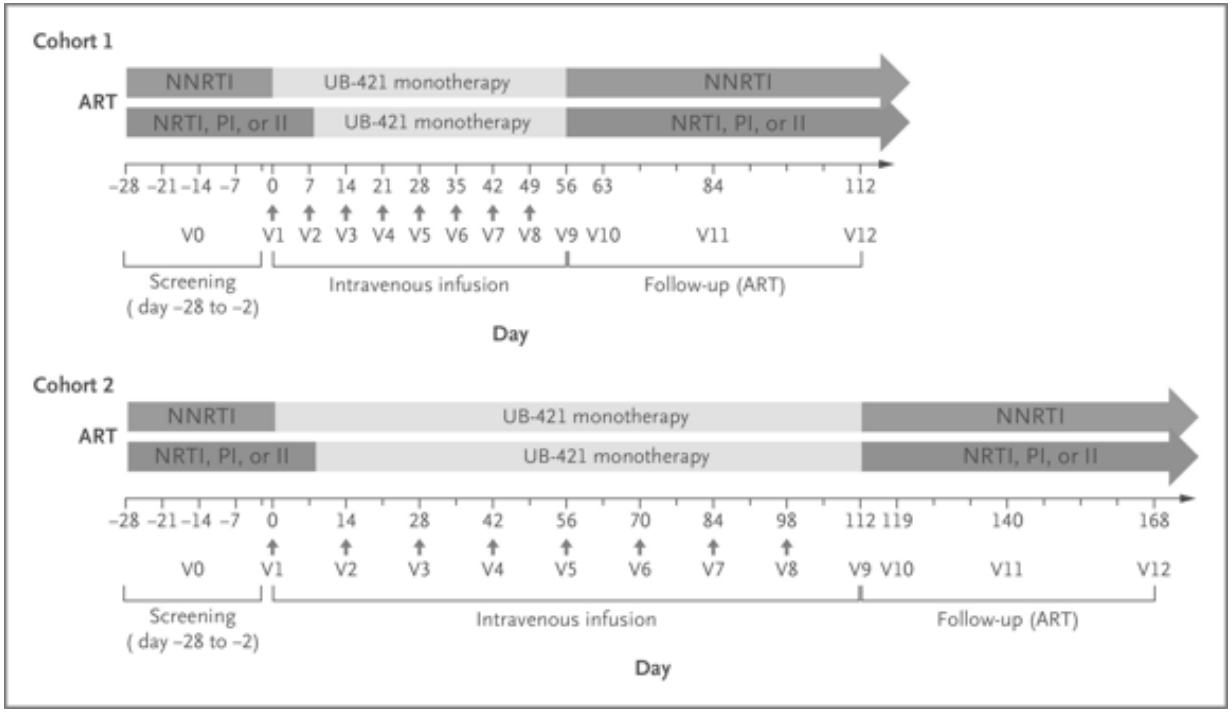




Effect of Anti-CD4 Antibody UB-421 on HIV-1 Rebound after Treatment Interruption

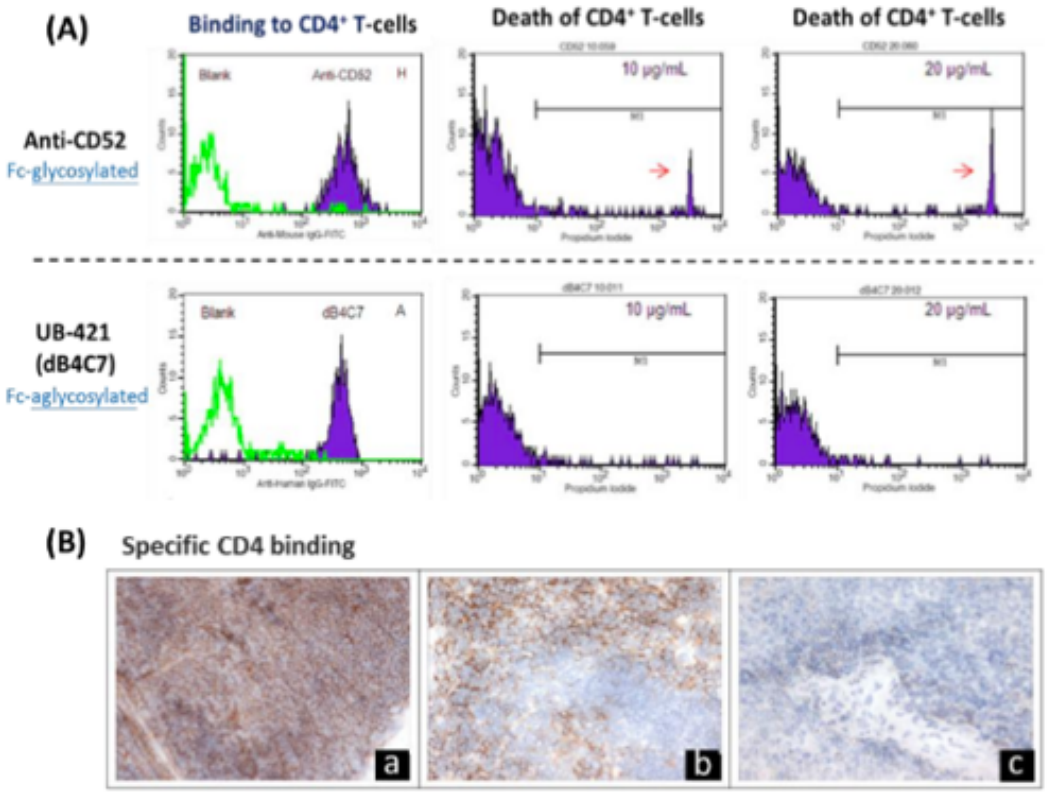
Administration of a single broadly neutralizing human immunodeficiency virus (HIV)–specific antibody to HIV-infected persons leads to the development of antibody-resistant virus in the absence of antiretroviral therapy (ART). It is possible that monotherapy with UB-421, an antibody that blocks the virus-binding site on human CD4+ T cells, could induce sustained virologic suppression without induction of resistance in HIV-infected persons after analytic treatment interruption. We conducted a nonrandomized, open-label, phase 2 clinical study evaluating the safety, pharmacokinetics, and antiviral activity of UB-421 monotherapy in HIV-infected persons undergoing analytic treatment interruption. All the participants had undetectable plasma viremia (<20 copies of HIV RNA per milliliter) at the screening visit. After discontinuation of ART, participants received eight intravenous infusions of UB-421, at a dose of either 10 mg per kilogram of body weight every week (Cohort 1) or 25 mg per kilogram every 2 weeks (Cohort 2). The primary outcome was the time to viral rebound (≥400 copies per milliliter).

UB-421 maintained virologic suppression (during the 8 to 16 weeks of study) in participants in the absence of ART. One participant discontinued therapy owing to a rash.



Participants in the phase 2 study were recruited from three tertiary hospitals designated as AIDS-referring centers in Taiwan. The qualified study participants were antiretroviral therapy (ART)–stabilized, having undetectable plasma viremia (<20 copies of human immunodeficiency virus [HIV] RNA per milliliter) and a CD4+ T-cell count of more than 350 cells per microliter at the screening visit.

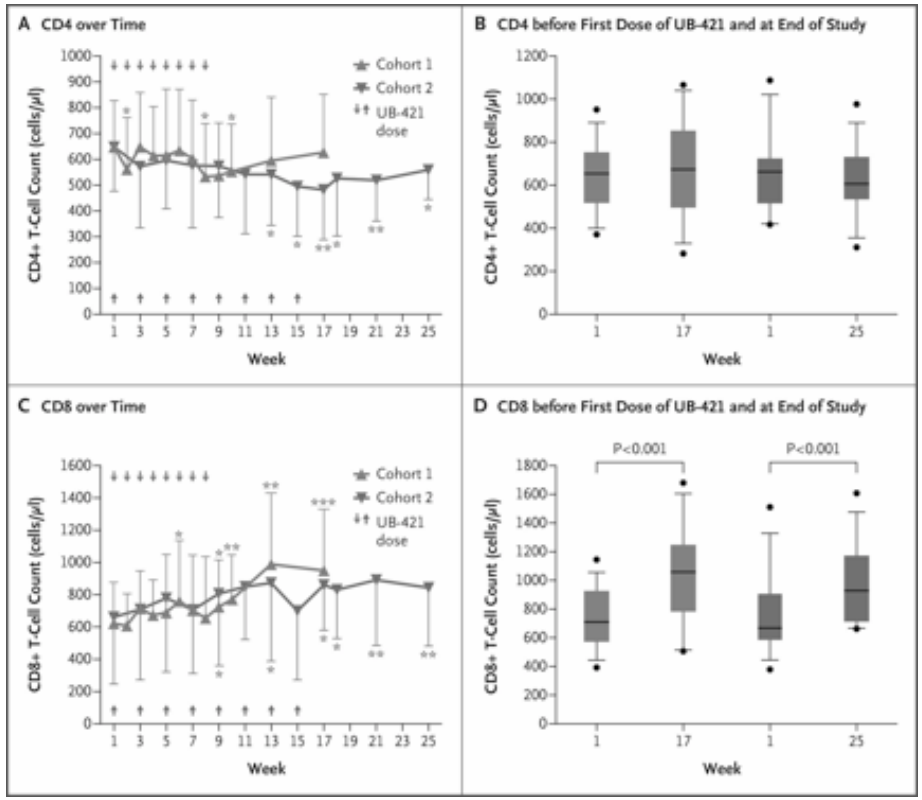
Figure S1. Non-depleting of and specific binding to CD4$^+$ T cells by the Fc-aglycosylated UB-421 mAb



(A) Representative illustrations of a binding of T-cell depleting anti-CD52 mAb to CD4$^+$ T cells in peripheral blood leukocytes (PBL) that leads to dose-dependent cell death, a phenomenon not seen with the Fc-aglycosylated UB-421. The PBLs collected from a healthy human donor were incubated on ice with UB-421 or anti-human CD52 (as positive control) for 30 min, and then incubated with 10% human serum for 2 hours at 37 ^{o}C. The PI-indexed cell death was analyzed on FACS. UB-421 is rendered devoid of carbohydrate structure at Fc region via one amino acid N297H mutation. The Fc aglycosylation is thought to be responsible for the reduction in both complement- and antibody-dependent cytotoxicities (CDC and ADCC, respectively) upon UB-421 binding. The non-T cell depleting UB-421 mAb can effectively coat the CD4$^+$ T cells without destroying them, while the anti-CD52 mAb (Campth-1) did so in a dose dependent manner (red arrows indicate cell death), presumably mediated by CDC, ADCC, and apoptotic

Baseline Characteristics of Study Participants and Adverse Events That Developed during UB-421 Monotherapy.

Variable	Cohort 1 (N=14)	Cohort 2 (N=15)
Baseline characteristics		
Asian race — no. (%)†	14 (100)	15 (100)
Male sex — no. (%)	14 (100)	15 (100)
Median age (range) — yr	35 (25–47)	31 (21–56)
Median weight (range) — kg	70.3 (55–97)	62.3 (46–74)
Median height (range) — cm	175 (168–183)	169 (159–178)
Median duration of HIV infection (range) — yr	5.7 (2.9–17.7)	5.8 (1.3–15.7)
Median duration of ART (range) — yr	4.8 (1.7–16.3)	5.2 (1.3–10.9)
Plasma viremia <20 copies of HIV RNA/ml — no. (%)	14 (100)	15 (100)
Median red-cell count (range) — $\times 10^{-6}/mm^3$	4.1 (3.6–5.0)	4.3 (3.4–5.3)
Median CD4+ T-cell count (range) — cells/mm^3	653 (370–951)	640 (394–1087)
Median CD8+ T-cell count (range) — cells/mm^3	721 (392–1145)	831 (379–1511)
Adverse event of grade 2 or higher — no./total no. (%)‡		
Rash	1/14 (7)	2/14 (14)§
Eosinophilia	1/14 (7)	2/14 (14)§
Bilirubin elevation	1/14 (7)¶	0/14
Alkaline phosphatase elevation	1/14 (7)¶	0/14
γ-Glutamyltransferase elevation	1/14 (7)¶	0/14
Alanine aminotransferase elevation	1/14 (7)¶	1/14 (7)§
Aspartate aminotransferase elevation	1/14 (7)¶	2/14 (14)§



Effects of UB-421 Monotherapy on CD4+ and CD8+ T-Cell Counts during Analytic Treatment Interruption and after Reinitiation of ART.

Data are for 14 participants in Cohort 1 and 13 participants in Cohort 2. Panel A shows the change in CD4+ T-cell counts over time. The counts, which were analyzed with a noninterfering anti–CD4 domain 2 antibody (clone M-T441, Ancell), remained stable in both Cohort 1 (weeks 1 to 17) and Cohort 2 (weeks 1 to 25). Panel B shows CD4+ T-cell counts before the first dose of UB-421 and at the end of the study, when serum UB-421 was no longer detected. The counts, which were measured with an anti–CD4 domain 1 antibody, did not change significantly in either cohort. Panel C shows the change in CD8+ T-cell counts over time. The counts, which were measured by flow cytometry with an anti-CD8 antibody, increased in both cohorts. Panel D shows the CD8+ T-cell counts before the first dose of UB-421 and at the end of the study. The counts, which were determined by standard diagnostic methods at each study site hospital, showed a significant increase in both cohorts.

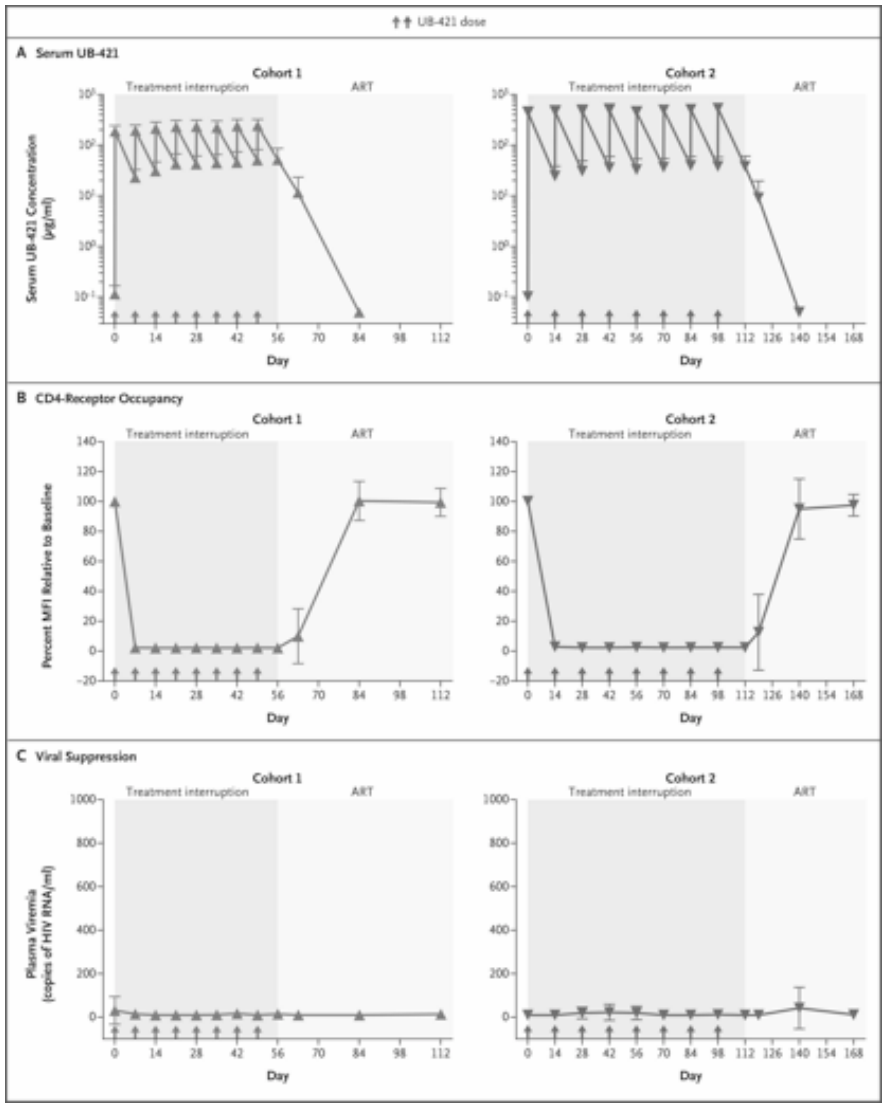
Table 2. Plasma Viremia before and after UB-421 Monotherapy as ART Substitution during Analytic Treatment Interruption.*

Cohort and Participant No.	Visit 0, Day S	Visit 1, Day 0	Visit 2, Day 7	Visit 3, Day 14	Visit 4, Day 21	Visit 5, Day 28	Visit 6, Day 35	Visit 7, Day 42	Visit 8, Day 49	Visit 9, Day 56	Visit 10, Day 63	Visit 11, Day 84	Visit 12, Day 112
						copies of HIV RNA/milliliter							
Cohort 1													
1-1-01	<20	<20	<20	<20	<20	<20	<20	<20	<20	<20	<20	<20	<20
1-1-02	<20	251	25	<20	<20	<20	<20	<20	<20	<20	<20	<20	<20
1-1-03	<20	<20	<20	<20	<20	<20	<20	<20	<20	<20	<20	<20	<20
1-1-04	<20	<20	49	<20	<20	<20	<20	<20	<20	<20	<20	<20	<20
1-1-05	<20	<20	<20	<20	<20	<20	<20	<20	<20	<20	<20	<20	<20
2-1-01	<20	<20	<20	<20	<20	<20	<20	<20	<20	<20	<20	230,000†	1920‡
2-1-02	<20	38	<20	<20	<20	<20	<20	<20	<20	<20	<20	<20	<20
2-1-03	<20	<20	<20	<20	<20	<20	<20	<20	<20	<20	<20	<20	12,000†‡
2-1-04	<20	<20	<20	<20	<20	<20	<20	<20	<20	<20	<20	127,000†	453‡
2-1-05	<20	<20	<20	<20	<20	<20	<20	<20	<20	<20	<20	<20	<20
3-1-01	<20	<20	<20	<20	<20	<20	<20	<20	<20	<20	<20	<20	<20
3-1-02	<20	<20	<20	<20	<20	<20	27	88	<20	<20	<20	<20	<20
3-1-03	<20	<20	<20	<20	<20	<20	<20	<20	<20	51	<20	<20	48
3-1-04	<20	31	<20	<20	<20	<20	<20	<20	<20	<20	<20	<20	<20
	Visit 0, Day S	**Visit 1, Day 0**	**Visit 2, Day 14**	**Visit 3, Day 28**	**Visit 4, Day 42**	**Visit 5, Day 56**	**Visit 6, Day 70**	**Visit 7, Day 84**	**Visit 8, Day 98**	**Visit 9, Day 112**	**Visit 10, Day 119**	**Visit 11, Day 140**	**Visit 12, Day 168**
Cohort 2													
1-2-01	<20	<20	<20	<20	<20	<20	<20	<20	<20	<20	<20	<20	<20
1-2-02	<20	<20	<20	47	142	21	<20	<20	<20	<20	<20	<20	<20
1-2-03	<20	<20	<20	<20	<20	<20	<20	<20	<20	<20	<20	<20	<20
1-2-04	<20	<20	<20	<20	<20	<20	<20	<20	<20	<20	<20	<20	<20
1-2-05	<20	<20	<20	<20	<20	<20	<20	<20	<20	<20	<20	<20	<20
2-2-01	<20	<20	<20	<20	<20	<20	<20	<20	<20	<20	<20	573,000†	1180‡
2-2-02	<20	<20	<20	<20	<20	<20	<20	<20	<20	<20	<20	30,900†	178‡
2-2-03	<20	<20	<20	<20	<20	<20	<20	<20	<20	<20	<20	<20	<20
2-2-04	<20	<20	<20	<20	<20	121	<20	<20	<20	<20	<20	<20	<20
2-2-05	<20	<20	<20	<20	<20	<20	<20	<20	<20	<20	<20	329	<20
3-2-01	<20	<20	<20	101	<20	<20	<20	<20	<20	<20	<20	<20	<20
3-2-02	<20	<20	WC										
3-2-03	<20	<20	<20	<20	WC								
3-2-04	<20	<20	<20	<20	<20	<20	<20	<20	<20	<20	<20	43	29
3-2-05	<20	<20	<20	<20	40	<20	<20	<20	36	<20	<20	<20	<20

* Undetectable plasma viremia was defined as less than 20 copies of HIV RNA per milliliter on day S (screening period between –28 to –2). WC denotes withdrawal of participant with consent.

† Three participants in Cohort 1 and two participants in Cohort 2 chose not to resume the scheduled ART after the last dose of UB-421. The time to plasma viral rebound in these participants was 35 days for two participants and 63 days for one participant in Cohort 1 and 42 days for two participants in Cohort 2. Their plasma viremia subsequently returned to an undetectable level after reinitiation of ART.

‡ Shown are the five participants who restarted ART after viral rebound of more than 1000 copies per milliliter rather than directly after the last dose of UB-421.



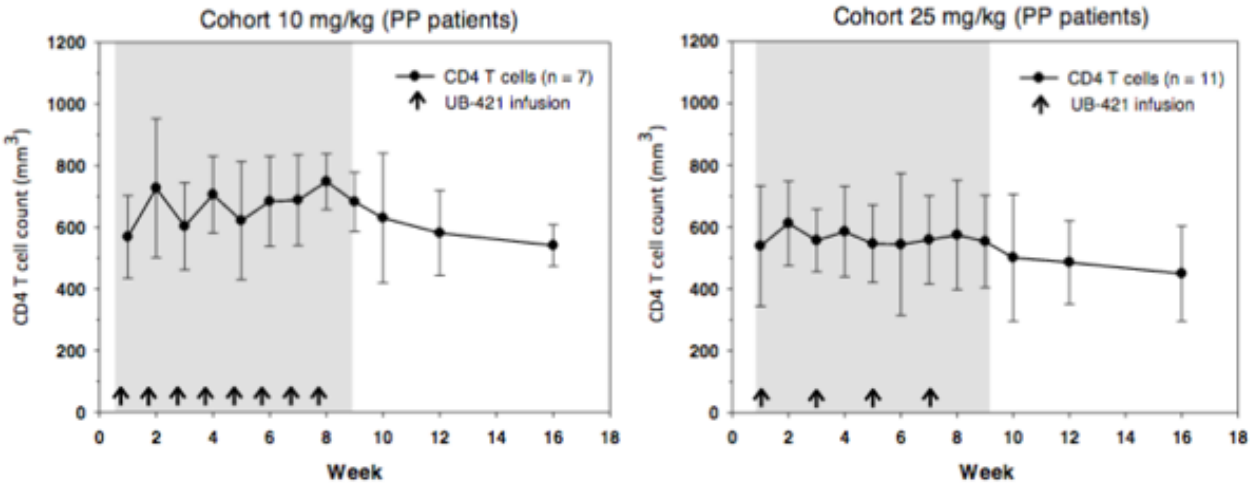
Serum UB-421 Concentration, CD4-Receptor Occupancy, and Viral Suppression with UB-421 Monotherapy during Analytic Treatment Interruption and after Reinitiation of ART.

Data are for 14 participants in Cohort 1 and 13 participants in Cohort 2. Panel A shows the time course of serum UB-421 concentrations. The troughs and peaks were measured by a validated enzyme-linked immunosorbent assay. The mean trough and peak concentrations at each visit are depicted here (also see Table S7 in the Supplementary Appendix); throughout the figure, triangles indicate mean values, and the vertical bars indicate standard deviations. Panel B shows the time course of free CD4 receptors left after UB-421 dose administration. The CD4 receptors on T cells were rapidly occupied (coated) by UB-421, leaving no free binding sites for the UB-421–Alexa488 probe, expressed as 0% mean fluorescence intensity (MFI); at the end of analytic treatment interruption, when UB-421 therapy was terminated and ART reinitiated, the free binding sites (unbound CD4 receptors) were once again available. Panel C shows the time course of plasma viremia after UB-421 dose administration.

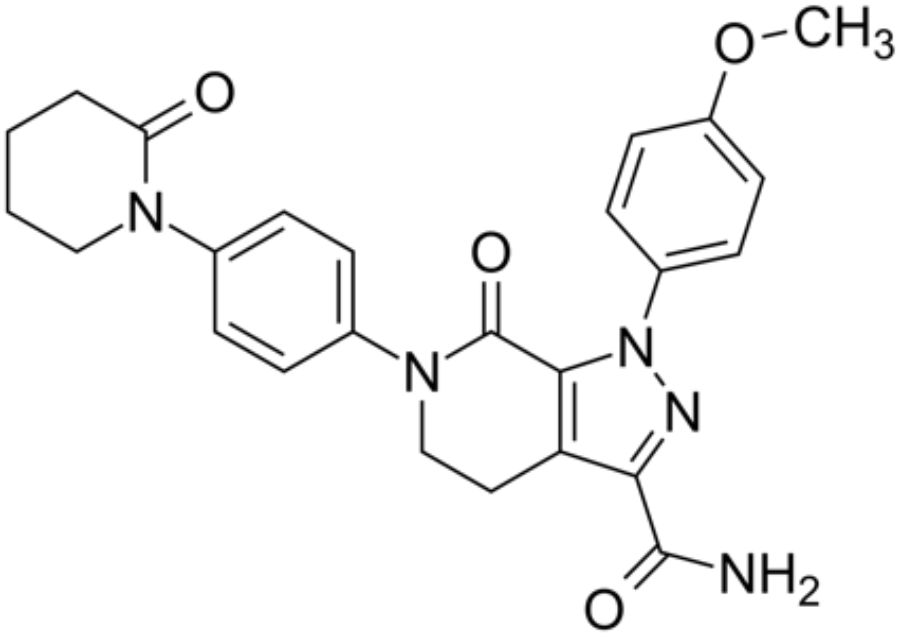
Discussion

In this study, UB-421 monotherapy maintained suppression of plasma viremia (<20 copies per milliliter) in the absence of ART for up to 8 weeks in participants receiving 10 mg per kilogram every week and for up to 16 weeks in participants receiving 25 mg per kilogram every 2 weeks. Occasional low-level viral blips, which did not require specific treatment, were detected in eight participants (28%). No evidence of HIV resistance to UB-421 was observed, but this small study of short duration has limited power to detect these changes. Future clinical studies with continued monitoring for drug-resistant strains during long-term administration of UB-421 are needed to properly assess this concern. In this small study, UB-421 monotherapy maintained viral suppression for up to 16 weeks without viral rebound in the absence of ART. Targeting a host viral receptor (CD4) complements direct antiviral strategies. Future studies are warranted to determine the longer-term safety and efficacy of UB-421 in HIV-infected persons.

Figure S13. Effects of UB-421 treatment on the absolute CD4$^+$ T cell number observed in the phase-IIa clinical trial with treatment-naïve HIV-infected patients



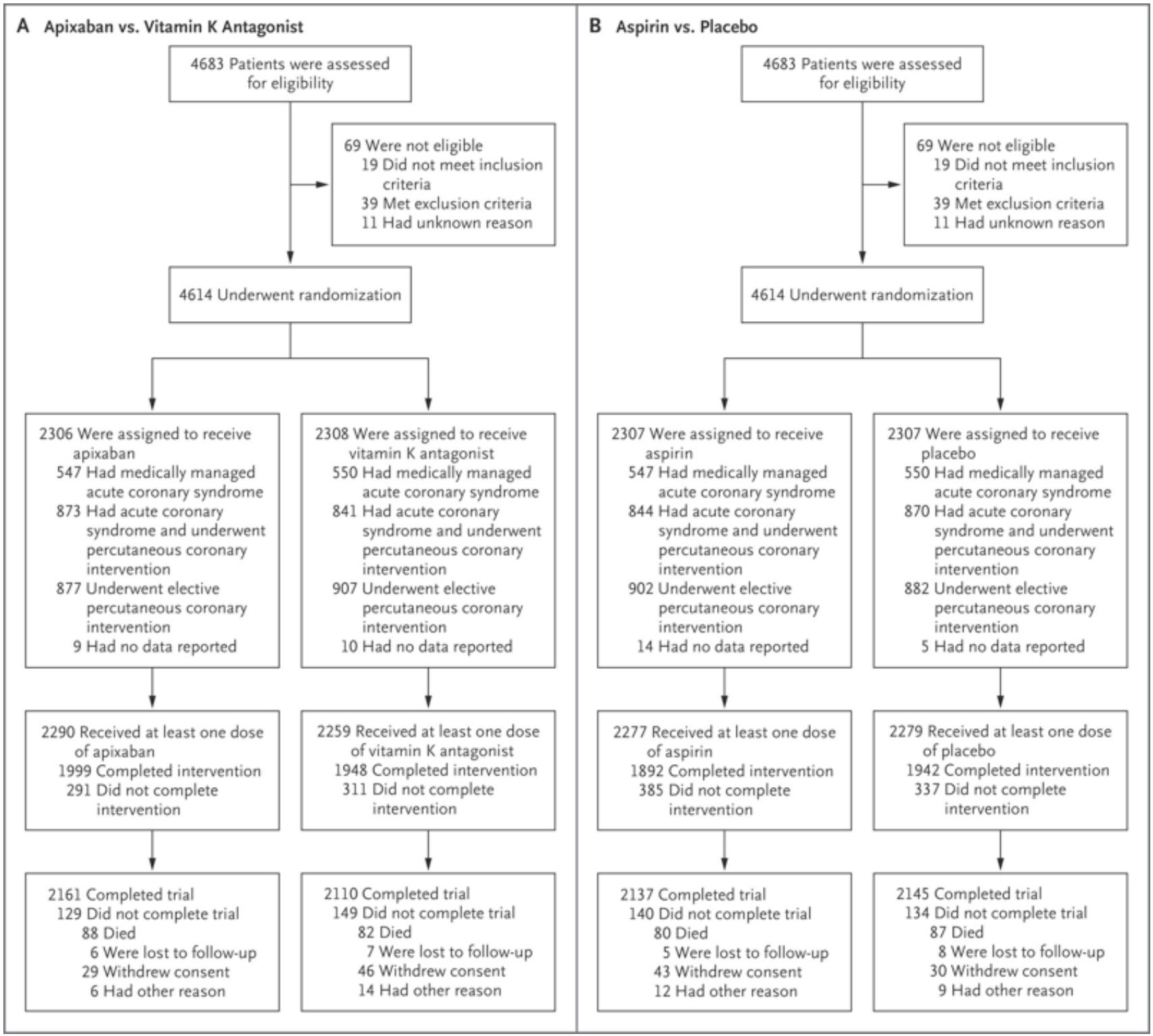
Apixaban ist ein Arzneistoff aus der Gruppe der Antikoagulanzien. Es hemmt die Thrombokinase (auch Faktor Xa) und damit die Blutgerinnung, weshalb Apixaban und die ähnlichen Arzneistoffe Betrixaban, Edoxaban und Rivaroxaban auch als direkte Faktor-Xa-Hemmer (Xabane) bezeichnet werden. Die Substanz wurde in einer Kooperation zwischen den Firmen Pfizer und Bristol-Myers Squibb entwickelt. Apixaban ist (etwa als Filmtablette à 2,5 mg) oral wirksam und wurde 2011 EU-weit unter dem Namen Eliquis zur Prophylaxe von venösen Thromboembolien nach elektiven (nicht dringend notwendigen) orthopädischen Operationen zugelassen; in Deutschland und der Schweiz: nach Hüft- und Knieersatzoperationen (Endoprothesen) bei Erwachsenen. Seit 20. Dezember 2012 ist Apixaban in der Europäischen Union auch zur Prävention von ischämischen Schlaganfällen (Hirninfarkt) und systemischen Embolien bei Erwachsenen mit nicht-valvulärem Vorhofflimmern zugelassen. Im Juli 2014 erhielt Apixaban in der EU zusätzlich die Zulassung zur Therapie und Rezidivprophylaxe bei Lungenembolien und Tiefen Venenthrombosen (TVT).

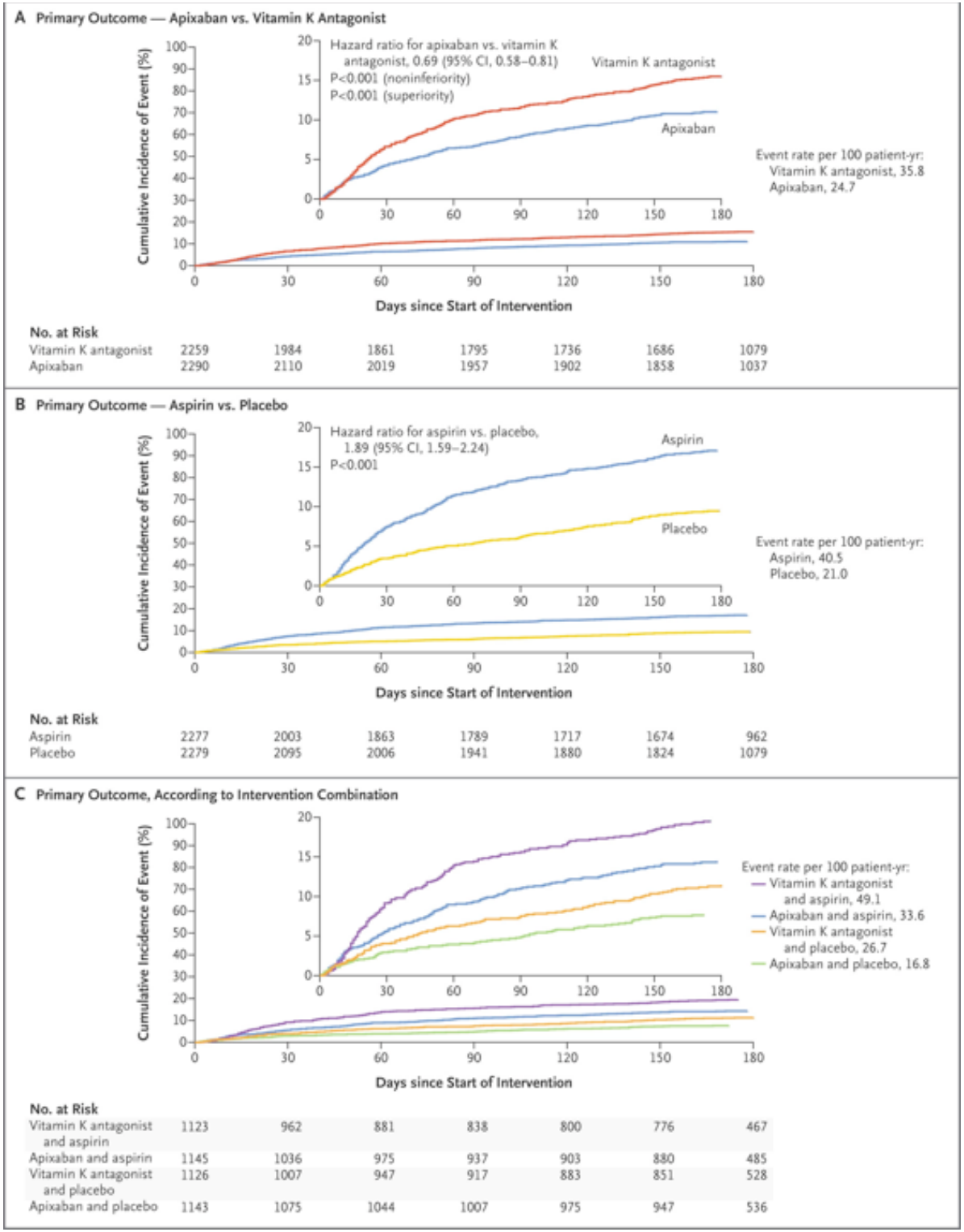


Antithrombotic Therapy after Acute Coronary Syndrome or PCI in Atrial Fibrillation

Appropriate antithrombotic regimens for patients with atrial fibrillation who have an acute coronary syndrome or have undergone percutaneous coronary intervention (PCI) are unclear. In an international trial with a two-by-two factorial design, we randomly assigned patients with atrial fibrillation who had an acute coronary syndrome or had undergone PCI and were planning to take a P2Y12 inhibitor to receive apixaban or a vitamin K antagonist and to receive aspirin or matching placebo for 6 months. The primary outcome was major or clinically relevant nonmajor bleeding. Secondary outcomes included death or hospitalization and a composite of ischemic events.

Characteristic	Apixaban (N=2306)	Vitamin K Antagonist (N=2308)	Aspirin (N=2307)	Aspirin-Matched Placebo (N=2307)	Total (N=4614)
Age — yr					
Median	70.4	70.9	70.8	70.6	70.7
Interquartile range	64.1–77.2	64.3–77.2	64.4–77.3	63.8–77.2	64.2–77.2
Female sex — no. (%)	670 (29.1)	667 (28.9)	696 (30.2)	641 (27.8)	1337 (29.0)
Race or ethnic group — no./total no. (%)†					
White	2097/2282 (91.9)	2087/2275 (91.7)	2082/2276 (91.5)	2102/2281 (92.2)	4184/4557 (91.8)
Black	29/2282 (1.3)	30/2275 (1.3)	29/2276 (1.3)	30/2281 (1.3)	59/4557 (1.3)
Asian	70/2282 (3.1)	70/2275 (3.1)	74/2276 (3.3)	66/2281 (2.9)	140/4557 (3.1)
Native American	10/2282 (0.4)	6/2275 (0.3)	6/2276 (0.3)	10/2281 (0.4)	16/4557 (0.4)
Other	76/2282 (3.3)	82/2275 (3.6)	85/2276 (3.7)	73/2281 (3.2)	158/4557 (3.5)
Serum creatinine — no./total no. (%)‡					
<1.5 mg/dl	2101/2274 (92.4)	2051/2258 (90.8)	2078/2260 (91.9)	2074/2272 (91.3)	4152/4532 (91.6)
≥1.5 mg/dl	173/2274 (7.6)	207/2258 (9.2)	182/2260 (8.1)	198/2272 (8.7)	380/4532 (8.4)
CHA_2DS_2-VASc score§	3.9±1.6	4.0±1.6	3.9±1.6	3.9±1.6	3.9±1.6
HAS-BLED score¶	2.9±1.0	2.9±0.9	2.8±0.9	2.9±1.0	2.9±0.9
Hypertension leading to medication use — no. (%)	2042 (88.6)	2031 (88.0)	2031 (88.0)	2042 (88.5)	4073 (88.3)
Heart failure — no. (%)	975 (42.3)	998 (43.2)	982 (42.6)	991 (43.0)	1973 (42.8)
Diabetes mellitus — no. (%)	842 (36.5)	836 (36.2)	842 (36.5)	836 (36.2)	1678 (36.4)
Stroke, TIA, or thromboembolism — no./total no. (%)	326/2289 (14.2)	307/2292 (13.4)	297/2289 (13.0)	336/2292 (14.7)	633/4581 (13.8)
Concomitant $P2Y_{12}$ inhibitor at randomization — no./total no. (%)					
Clopidogrel	2105/2253 (93.4)	2060/2243 (91.8)	2075/2253 (92.1)	2090/2243 (93.2)	4165/4496 (92.6)
Prasugrel	27/2253 (1.2)	24/2243 (1.1)	31/2253 (1.4)	20/2243 (0.9)	51/4496 (1.1)
Ticagrelor	121/2253 (5.4)	159/2243 (7.1)	147/2253 (6.5)	133/2243 (5.9)	280/4496 (6.2)
Previous use of oral anticoagulant — no. (%)‖	1192 (51.7)	1070 (46.4)	1132 (49.1)	1130 (49.0)	2262 (49.0)
Qualifying index event — no./total no. (%)					
Acute coronary syndrome and PCI	873/2297 (38.0)	841/2298 (36.6)	844/2293 (36.8)	870/2302 (37.8)	1714/4595 (37.3)
Medically managed acute coronary syndrome	547/2297 (23.8)	550/2298 (23.9)	547/2293 (23.9)	550/2302 (23.9)	1097/4595 (23.9)
Elective PCI	877/2297 (38.2)	907/2298 (39.5)	902/2293 (39.3)	882/2302 (38.3)	1784/4595 (38.8)
No. of days from acute coronary syndrome or PCI to randomization**	6.7±4.2	6.6±4.2	6.7±4.3	6.5±4.1	6.6±4.2


A Apixaban vs. Vitamin K Antagonist
4683 Patients were assessed for eligibility
69 Were not eligible
19 Did not meet inclusion criteria
39 Met exclusion criteria
11 Had unknown reason
4614 Underwent randomization
2306 Were assigned to receive apixaban
547 Had medically managed acute coronary syndrome
873 Had acute coronary syndrome and underwent percutaneous coronary intervention
877 Underwent elective percutaneous coronary intervention
9 Had no data reported
2308 Were assigned to receive vitamin K antagonist
550 Had medically managed acute coronary syndrome
841 Had acute coronary syndrome and underwent percutaneous coronary intervention
907 Underwent elective percutaneous coronary intervention
10 Had no data reported
2290 Received at least one dose of apixaban
1999 Completed intervention
291 Did not complete intervention
2259 Received at least one dose of vitamin K antagonist
1948 Completed intervention
311 Did not complete intervention
2161 Completed trial
129 Did not complete trial
88 Died
6 Were lost to follow-up
29 Withdrew consent
6 Had other reason
2110 Completed trial
149 Did not complete trial
82 Died
7 Were lost to follow-up
46 Withdrew consent
14 Had other reason
B Aspirin vs. Placebo
4683 Patients were assessed for eligibility
69 Were not eligible
19 Did not meet inclusion criteria
39 Met exclusion criteria
11 Had unknown reason
4614 Underwent randomization
2307 Were assigned to receive aspirin
547 Had medically managed acute coronary syndrome
844 Had acute coronary syndrome and underwent percutaneous coronary intervention
902 Underwent elective percutaneous coronary intervention
14 Had no data reported
2307 Were assigned to receive placebo
550 Had medically managed acute coronary syndrome
870 Had acute coronary syndrome and underwent percutaneous coronary intervention
882 Underwent elective percutaneous coronary intervention
5 Had no data reported
2277 Received at least one dose of aspirin
1892 Completed intervention
385 Did not complete intervention
2279 Received at least one dose of placebo
1942 Completed intervention
337 Did not complete intervention
2137 Completed trial
140 Did not complete trial
80 Died
5 Were lost to follow-up
43 Withdrew consent
12 Had other reason
2145 Completed trial
134 Did not complete trial
87 Died
8 Were lost to follow-up
30 Withdrew consent
9 Had other reason



Kaplan–Meier Curves for Primary Outcome of Major or Clinically Relevant Nonmajor Bleeding.

The primary outcome was major or clinically relevant nonmajor bleeding as defined by the International Society on Thrombosis and Haemostasis. Insets show the same data on an enlarged y axis.

Table 2. Primary Safety and Secondary Efficacy Outcomes.*

Outcome	Apixaban	Vitamin K Antagonist	Hazard Ratio (95% CI)	P Value for Superiority
Anticoagulation-regimen comparison				
ISTH major or clinically relevant nonmajor bleeding†				
No. of patients with event/total no. (%)	241/2290 (10.5)	332/2259 (14.7)	—	—
Event rate per 100 patient-yr	24.7	35.8	0.69 (0.58–0.81)	<0.001
Death or hospitalization				
No. of patients with event/total no. (%)	541/2306 (23.5)	632/2308 (27.4)	—	—
Event rate per 100 patient-yr	57.2	69.2	0.83 (0.74–0.93)	0.002
Death or ischemic event‡				
No. of patients with event/total no. (%)	154/2306 (6.7)	163/2308 (7.1)	—	—
Event rate per 100 patient-yr	14.3	15.3	0.93 (0.75–1.16)	NS
Antiplatelet-regimen comparison	**Aspirin**	**Placebo**		
ISTH major or clinically relevant nonmajor bleeding				
No. of patients with event/total no. (%)	367/2277 (16.1)	204/2279 (9.0)	—	—
Event rate per 100 patient-yr	40.5	21.0	1.89 (1.59–2.24)	<0.001
Death or hospitalization§				
No. of patients with event/total no. (%)	604/2307 (26.2)	569/2307 (24.7)	—	—
Event rate per 100 patient-yr	65.7	60.6	1.08 (0.96–1.21)	NS
Death or ischemic event				
No. of patients with event/total no. (%)	149/2307 (6.5)	168/2307 (7.3)	—	—
Event rate per 100 patient-yr	13.9	15.7	0.89 (0.71–1.11)	NT

* The hazard ratios were calculated by the Cox proportional-hazards model for time to the first event, stratified according to indication at enrollment and either the antiplatelet regimen (in the analysis of the anticoagulant-regimen comparison) or the anticoagulant regimen (in the analysis of the antiplatelet-regimen comparison). All P values for superiority are two-sided. ISTH denotes International Society on Thrombosis and Haemostasis, NS not significant, and NT not tested.

† The result of the noninferiority test comparing the time to the first primary safety event in the apixaban group with that in the vitamin K antagonist group was significant (P<0.001).

‡ This analysis had the first nonsignificant result in the hierarchical testing procedure for the outcomes assessed in the anticoagulant-regimen comparison.

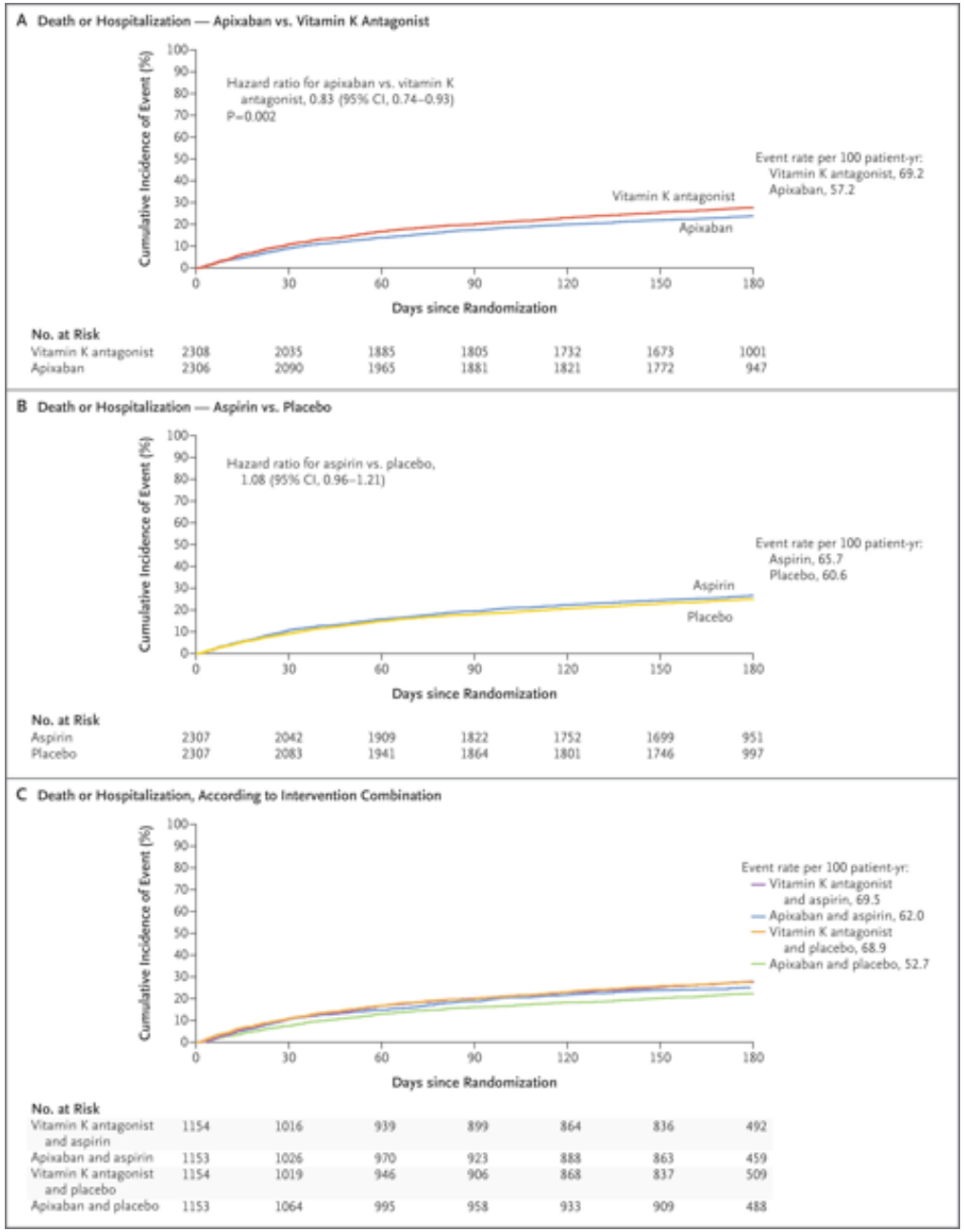
§ This analysis had the first nonsignificant result in the hierarchical testing procedure for the outcomes assessed in the antiplatelet-regimen comparison.

Table 3. Additional Safety and Efficacy Outcomes of Interest.*

Outcome	Anticoagulant-Regimen Comparison			Antiplatelet-Regimen Comparison		
	Apixaban	Vitamin K Antagonist	Hazard Ratio (95% CI)	Aspirin	Placebo	Hazard Ratio (95% CI)
Safety outcomes						
No. of patients in analysis	2290	2259		2277	2279	
ISTH major bleeding						
No. of patients with event (%)	69 (3.0)	104 (4.6)	—	108 (4.7)	65 (2.9)	—
Event rate per 100 patient-yr	6.7	10.5	0.64 (0.47–0.86)	11.1	6.5	1.70 (1.25–2.31)
Clinically relevant nonmajor bleeding						
No. of patients with event (%)	180 (7.9)	246 (10.9)	—	275 (12.1)	148 (6.5)	—
Event rate per 100 patient-yr	18.2	26.1	0.69 (0.57–0.84)	30.0	15.2	1.93 (1.58–2.36)
Intracranial hemorrhage						
No. of patients with event (%)	5 (0.2)	13 (0.6)	—	8 (0.4)	10 (0.4)	—
Event rate per 100 patient-yr	0.5	1.3	0.39 (0.14–1.12)	0.8	1.0	0.82 (0.32–2.07)
GUSTO severe or moderate bleeding						
No. of patients with event (%)	41 (1.8)	68 (3.0)	—	68 (3.0)	40 (1.8)	—
Event rate per 100 patient-yr	4.0	6.8	0.58 (0.39–0.86)	6.9	4.0	1.72 (1.17–2.55)
GUSTO severe bleeding						
No. of patients with event (%)	5 (0.2)	8 (0.4)	—	7 (0.3)	6 (0.3)	—
Event rate per 100 patient-yr	0.5	0.8	0.59 (0.19–1.81)	0.7	0.6	1.19 (0.40–3.53)
GUSTO moderate bleeding						
No. of patients with event (%)	37 (1.6)	64 (2.8)	—	63 (2.8)	37 (1.6)	—
Event rate per 100 patient-yr	3.6	6.4	0.56 (0.37–0.84)	6.4	3.7	1.73 (1.15–2.59)
TIMI major or minor bleeding						
No. of patients with event (%)	96 (4.2)	132 (5.8)	—	146 (6.4)	80 (3.5)	—
Event rate per 100 patient-yr	9.5	13.5	0.70 (0.54–0.91)	15.2	8.0	1.88 (1.43–2.47)
TIMI major bleeding						
No. of patients with event (%)	38 (1.7)	48 (2.1)	—	55 (2.4)	29 (1.3)	—
Event rate per 100 patient-yr	3.7	4.8	0.78 (0.51–1.20)	5.6	2.9	1.93 (1.23–3.03)
TIMI minor bleeding						
No. of patients with event (%)	80 (3.5)	118 (5.2)	—	126 (5.5)	71 (3.1)	—
Event rate per 100 patient-yr	7.9	12.0	0.65 (0.49–0.86)	13.1	7.1	1.82 (1.36–2.44)
Efficacy outcomes						
No. of patients in analysis	2306	2308		2307	2307	
Hospitalization						
No. of patients with event (%)	518 (22.5)	607 (26.3)	—	585 (25.4)	540 (23.4)	—
Event rate per 100 patient-yr	54.8	66.5	0.83 (0.74–0.93)	63.7	57.5	1.10 (0.98–1.24)
Death						
No. of patients with event (%)	77 (3.3)	74 (3.2)	—	72 (3.1)	79 (3.4)	—
Event rate per 100 patient-yr	7.0	6.7	1.03 (0.75–1.42)	6.6	7.2	0.91 (0.66–1.26)
Death from cardiovascular causes						
No. of patients with event (%)	57 (2.5)	54 (2.3)	—	53 (2.3)	58 (2.5)	—
Event rate per 100 patient-yr	5.2	4.9	1.05 (0.72–1.52)	4.8	5.3	0.92 (0.63–1.33)
Stroke						
No. of patients with event (%)	13 (0.6)	26 (1.1)	—	20 (0.9)	19 (0.8)	—
Event rate per 100 patient-yr	1.2	2.4	0.50 (0.26–0.97)	1.8	1.7	1.06 (0.56–1.98)
Myocardial infarction						
No. of patients with event (%)	72 (3.1)	80 (3.5)	—	68 (2.9)	84 (3.6)	—
Event rate per 100 patient-yr	6.6	7.4	0.89 (0.65–1.23)	6.3	7.8	0.81 (0.59–1.12)
ARC definite or probable stent thrombosis						
No. of patients with event (%)	14 (0.6)	18 (0.8)	—	11(0.5)	21 (0.9)	—
Event rate per 100 patient-yr	1.3	1.6	0.77 (0.38–1.56)	1.0	1.9	0.52 (0.25–1.08)
Urgent revascularization						
No. of patients with event (%)	40 (1.7)	44 (1.9)	—	37 (1.6)	47 (2.0)	—
Event rate per 100 patient-yr	3.7	4.1	0.90 (0.59–1.38)	3.4	4.3	0.79 (0.51–1.21)

* Safety outcome analyses assessed the patients on an as-treated basis, and efficacy outcome analyses assessed patients according to their randomized group assignment. The hazard ratio was calculated by the Cox proportional-hazards model for time to the first event, stratified according to the indication at enrollment and either the antiplatelet regimen (in the analysis of the anticoagulant-regimen comparison) or the anticoagulant regimen (in the analysis of the antiplatelet-regimen comparison). ARC denotes Academic Research Consortium, GUSTO Global Use of Strategies to Open Occluded Arteries, and TIMI Thrombolysis in Myocardial Infarction.

Kaplan–Meier Curves for the Composite of Death or Hospitalization.



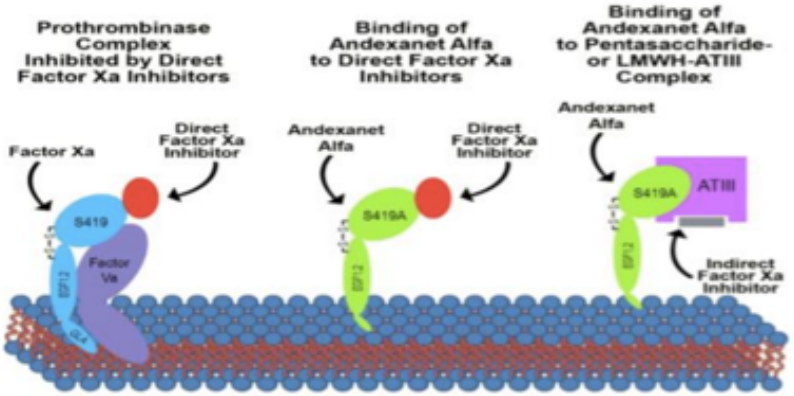
Discussion

The current trial was specifically designed to assess the independent effect of anticoagulant and antiplatelet therapy in patients with atrial fibrillation and recent acute coronary syndrome or PCI who were planning to receive a P2Y12 inhibitor. Apixaban led to a lower incidence of both bleeding and the composite of death or hospitalization than did a vitamin K antagonist; the latter result was driven by a lower incidence of hospitalization. The overall incidence of ischemic events was similar in the two groups. Aspirin led to a higher incidence of bleeding than placebo, and the rates of death or hospitalization and of ischemic events were similar in the two groups. A regimen of clopidogrel plus apixaban, at the dose labeled for stroke prevention, without aspirin was not associated with excess adverse events and appeared to be effective in this high-risk group of patients.

In conclusion, in patients with atrial fibrillation and a recent acute coronary syndrome or PCI treated with a $P2Y_{12}$ inhibitor, an antithrombotic regimen that included apixaban, without aspirin, resulted in less bleeding and fewer hospitalizations without significant differences in ischemic events than regimens that included a vitamin K antagonist, aspirin, or both.

Supported by Bristol-Myers Squibb and Pfizer.

Andexanet alfa ist ein Analogon von Faktor Xa und ein Antidot der Faktor Xa-Hemmer Rivaroxaban und Apixaban. In den USA ist es für die Behandlung nicht kontrollierbarer Blutungen unter Therapie mit Rivaroxaban oder Apixaban zugelassen. Andexanet alfa ist eine rekombinante und modifizierte Version des menschlichen, aktivierten Gerinnungsfaktor X.



In finance, valuation is the process of determining the present value (PV) of an asset. Valuations can be done on assets (for example, investments in marketable securities such as stocks, options, business enterprises, or intangible assets such as patents and trademarks) or on liabilities (e.g., bonds issued by a company). Valuations are needed for many reasons such as investment analysis, capital budgeting, merger and acquisition transactions, financial reporting, taxable events to determine the proper tax liability, and in litigation. Deutsch: die Abschätzung, die Wertermittlung

Accuracy of Valuations of Surgical Procedures in the Medicare Fee Schedule

The Relative Value Scale Update Committee (RUC) of the American Medical Association plays a central role in determining physician reimbursement. The RUC's role and performance have been criticized but subjected to little empirical evaluation. We analyzed the accuracy of valuations of 293 common surgical procedures from 2005 through 2015. We compared the RUC's estimates of procedure time with "benchmark" times for the same procedures derived from the clinical registry maintained by the American College of Surgeons National Surgical Quality Improvement Program (NSQIP). We characterized inaccuracies, quantified their effect on physician revenue, and examined whether re-review corrected them.

RUC

The RUC provided us with records dating from its inaugural meeting in May 1992 through 2015. The data included Current Procedural Terminology (CPT) codes of reviewed services, review outcomes, and estimates of service time from the physician surveys that were used in determining work RVUs.

NSQIP

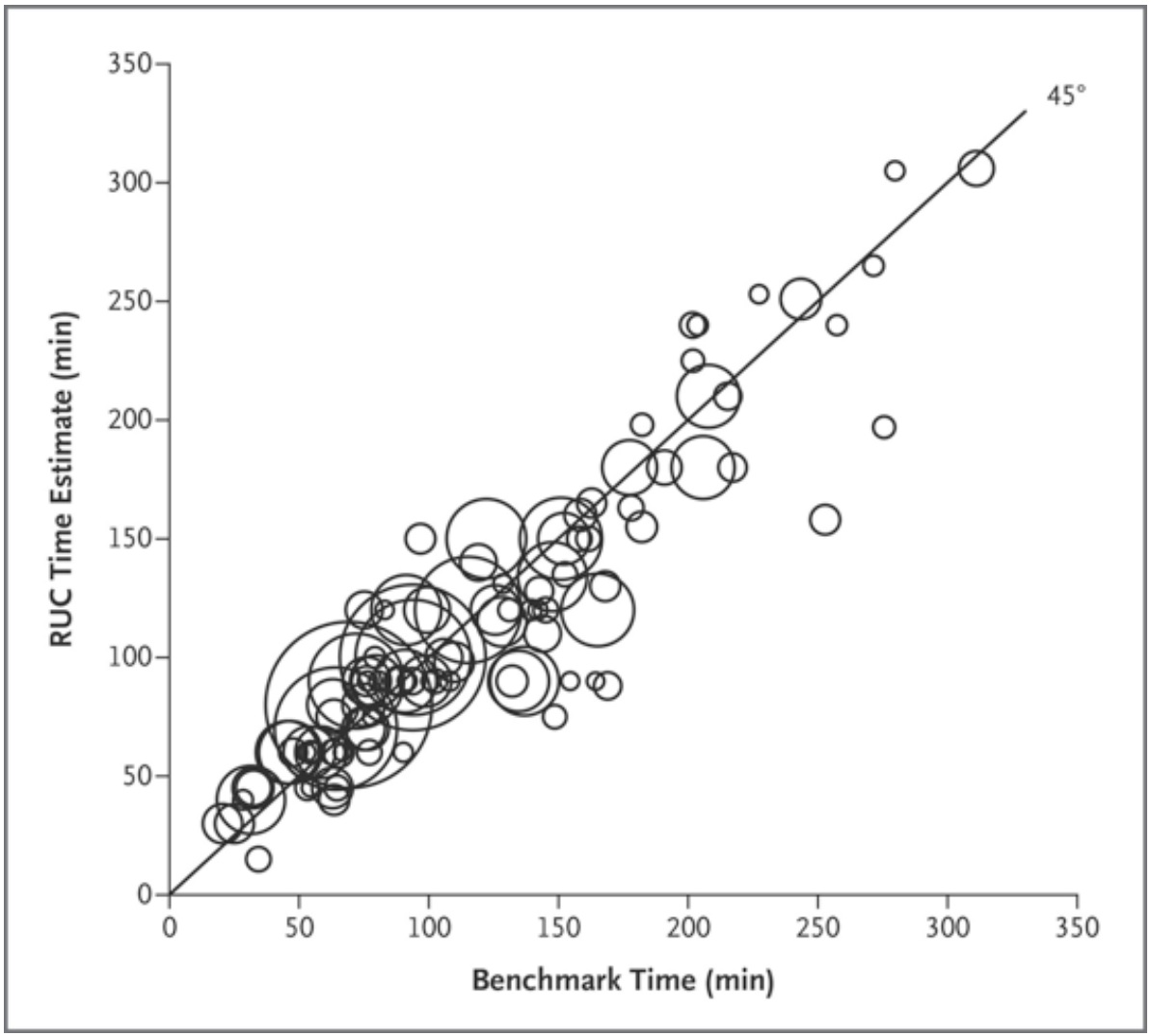
The NSQIP, established in the mid-1980s, has grown to encompass more than 600 participating hospitals that contribute data on surgical cases to a central clinical registry.

CMS

The Physician/Supplier Procedure Summary (PSPS) files are an annual summary of information on all claims for services and durable medical equipment submitted to Medicare's Part B fee-for-service program.

Study Sample

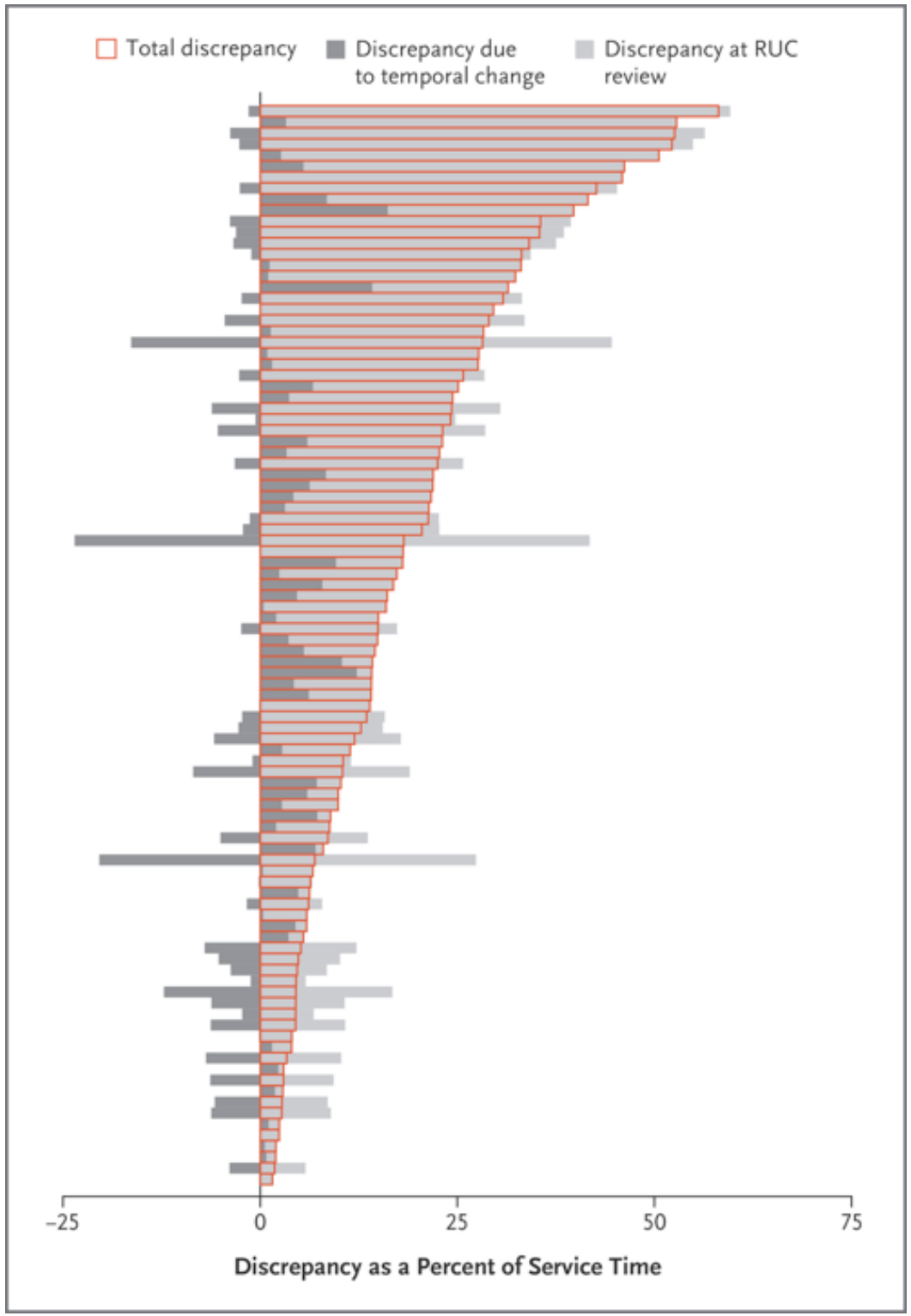
We used NSQIP data to identify the 300 most commonly performed surgical procedures. We then linked each procedure to its RUC intraoperative time estimates, NSQIP intraoperative times, and annual volume and charges from the PSPS files. RUC time estimates were missing for 7 procedures, leaving 293 procedures in our final study sample.



Relationship between RUC Time Estimates and Benchmark Times in 108 Reviews of Common Surgical Procedures.

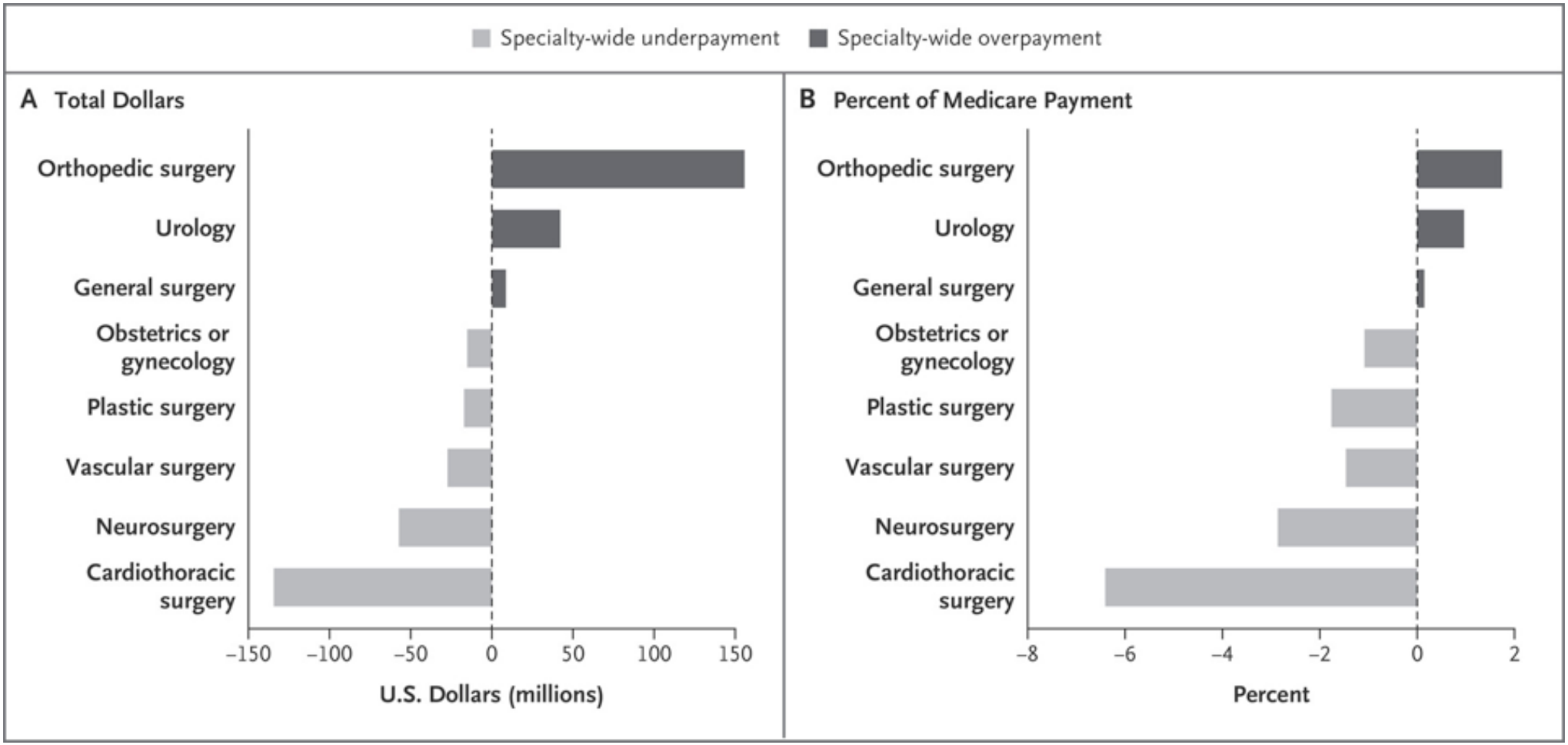
Each bubble represents a surgical procedure reviewed by the Relative Value Scale Update Committee (RUC) from 2005 through 2015. Bubble size represents the frequency with which the procedures were performed, as recorded in the clinical registry maintained by the American College of Surgeons National Surgical Quality Improvement Program (NSQIP). Benchmark times were defined as mean times in the NSQIP data for the relevant procedure and calendar quarter. The 45-degree line indicates equivalence between the RUC time and the benchmark time, and the distance of bubbles from this line indicates the degree of discrepancy between the two time values.

Eine Benchmark (von englisch benchmark oder bench mark) ist ein Vergleichsmaßstab. Benchmarking (sinngemäß „Maßstäbe vergleichen“) bezeichnet die vergleichende Analyse von Ergebnissen oder Prozessen mit einem festgelegten Bezugswert oder Bezugsprozess.



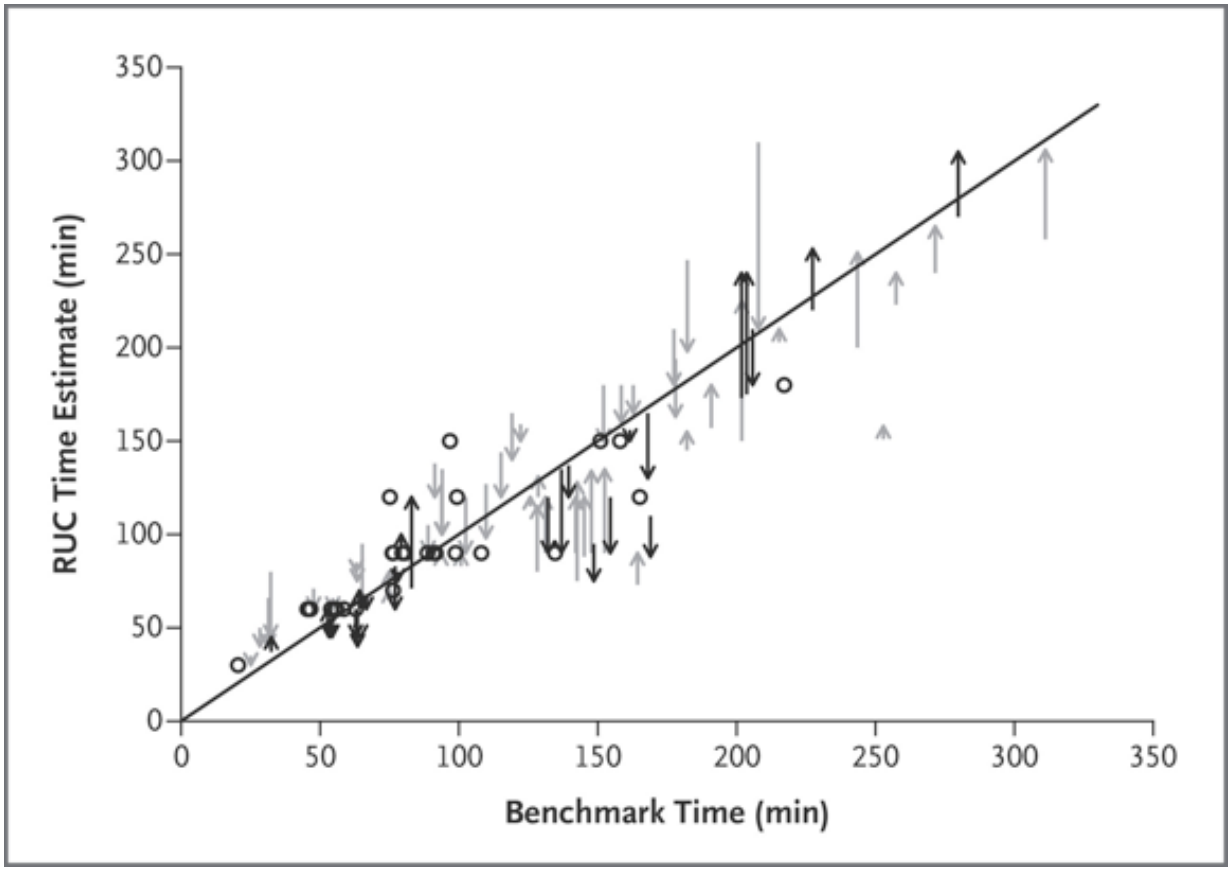
Discrepancies between RUC Time Estimates and Benchmark Times for 98 Common Surgical Procedures.

Shown are the components of discrepancy for each of 98 procedures performed, expressed as an average percentage deviation from the procedure's benchmark time over the period of observation. Each bar represents a procedure. The light gray segment of each bar represents the initial discrepancy at the time of review. The dark gray segments represent temporal changes in procedure times after review. Dark gray segments to the left of the zero line indicate temporal changes that decreased discrepancy from the initial discrepancy; dark gray segments to the right of the zero line indicate temporal changes that increased discrepancy from the initial discrepancy. The boxes outlined in red indicate the total discrepancy after adding temporal changes to or subtracting them from the initial discrepancy.



Effect of Inaccuracies in Time Estimates for 293 Procedures on Medicare Reimbursement for Eight Surgical Specialties, 2011–2015.

The bars show the differences, according to specialty, between actual Medicare payments and an estimate of counterfactual Medicare payments had the procedures been valued according to benchmark (NSQIP) times instead of RUC time estimates. Panel A shows the differences in dollars, and Panel B the differences as a percentage of all Medicare payments (i.e., for all services) made to physicians in the specialties. The dark gray bars to the right of the zero line indicate specialty-wide overpayment relative to the counterfactual amount. Light gray bars indicate specialty-wide underpayment.



Effect of RUC Re-Reviews on Extent of Discrepancies in Procedure Time, 2005–2015.

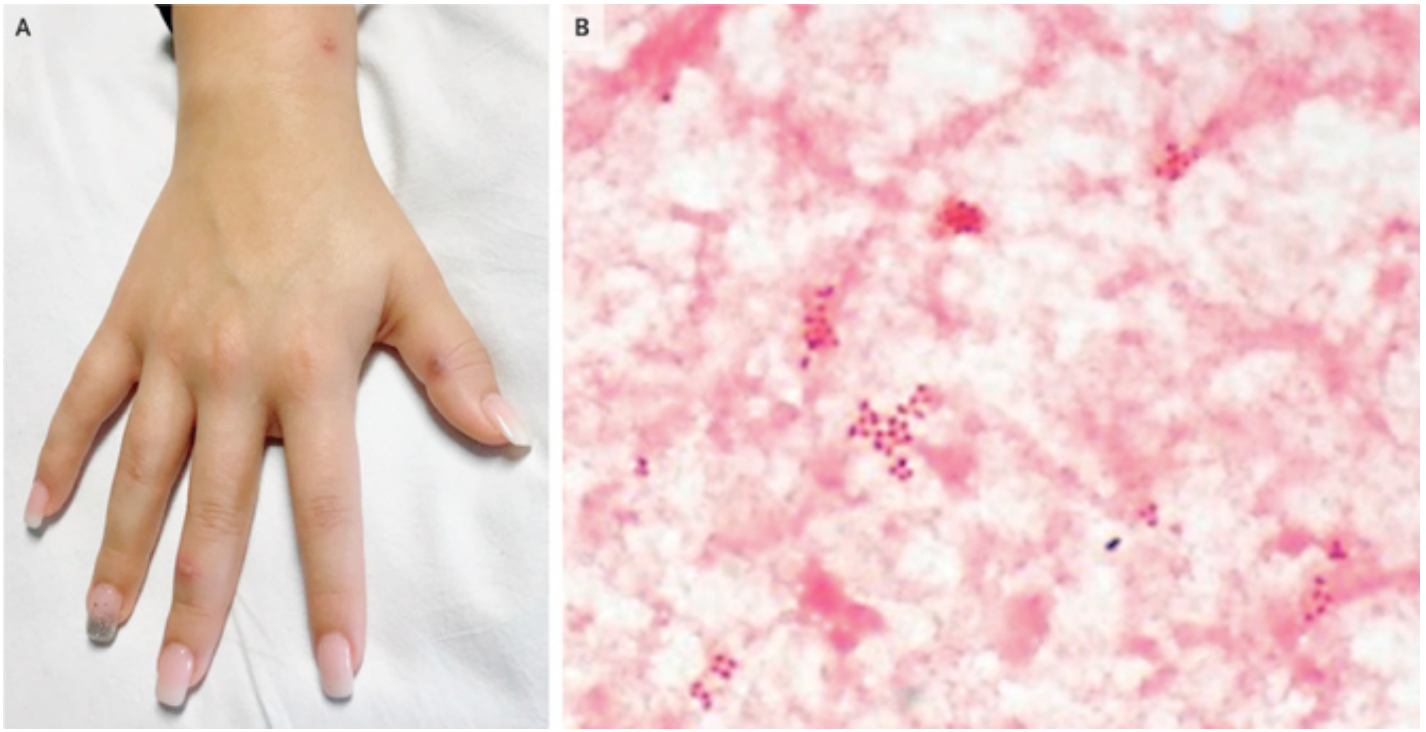
Each arrow and each dot represents a RUC re-review. The distance between the base of each arrow and the 45-degree line represents the size of the discrepancy between the RUC time measure used in the prevailing work RVU and the benchmark time (mean NSQIP) immediately before re-review. The distance between the tip of each arrow and the 45-degree line represents the size of the discrepancy between the new RUC time estimate used in the re-review and the benchmark time. The dots indicate re-reviews in which the discrepancy between the new RUC time and the benchmark time did not change. Six re-reviews conducted in 2005 through 2015 were excluded because their initial reviews were not conducted by the RUC and the time measures used in those reviews were not in our data.

Discussion

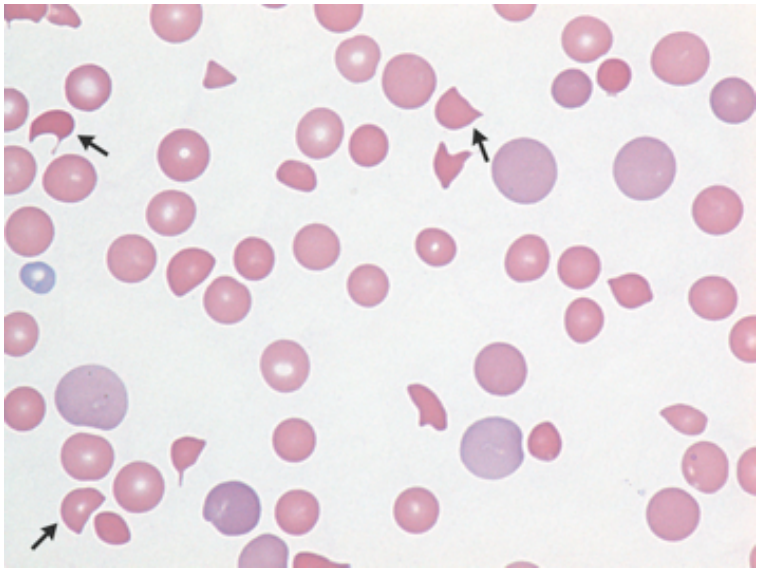
In this study, we analyzed estimates of the service times used to set reimbursement levels in the Medicare Physician Fee Schedule for the most commonly performed surgical procedures. By comparing RUC time estimates with times for the same procedures listed in a large registry of surgical times, we found discrepancies. These discrepancies varied across procedures in both size and direction, but we found no evidence that the RUC systematically overestimated or underestimated procedure times. For many procedures, the discrepancies changed substantially in size over time. Our analyses suggest that these inaccuracies had nontrivial distributional effects on surgeons' income from clinical practice. Re-reviews by the RUC helped to reduce the inaccuracies. However, only half the procedures in our sample underwent re-review in the years 2005 through 2015, and half of those re-reviews did not reduce inaccuracies.

However, the most striking limitation of the existing research — and a key motivation for our study — is its crude treatment of chronological time. Previous studies did not attempt to measure benchmark times at the same time that the RUC surveys were conducted, creating a legitimate reason for at least some discrepancy. More important, these studies focused on cross-sectional accuracy, largely ignoring longitudinal dimensions of accuracy. The size of the discrepancy between a procedure's RUC time estimate and its benchmark time typically expands or contracts over time, so effects cannot be fully understood without a longitudinal perspective.

The federal government is changing aspects of how it pays physicians. However, the approach used by CMS since 1992 to value physician services remains fundamentally intact. Reforms to that approach may improve the accuracy and fairness of reimbursement. Whether it is feasible to implement the necessary reforms within the existing institutional and procedural framework is a question that warrants careful consideration.



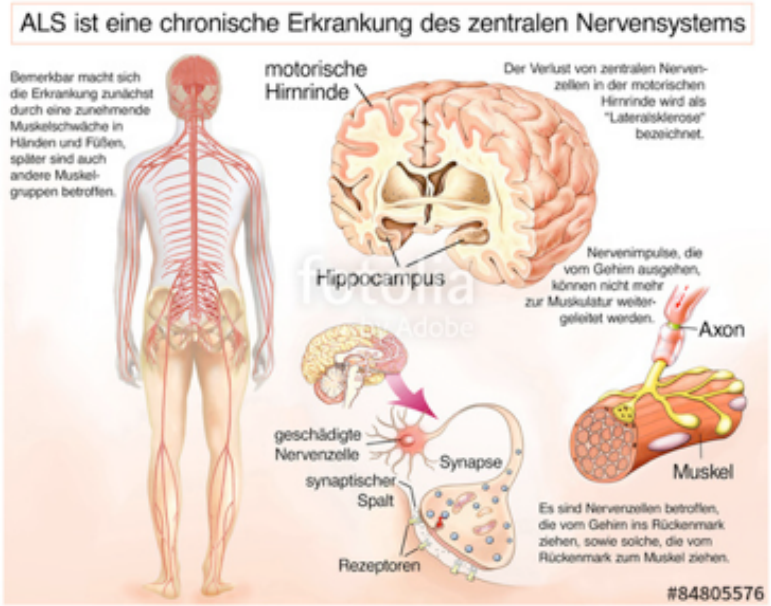
A 20-year-old woman presented to the emergency department with a rash involving the arms, legs, trunk, and scalp, which had erupted that morning. She also reported generalized muscle aches, fever, and pain in both ankles. Two weeks earlier, the patient had had vaginal intercourse with a new partner without barrier protection. The physical examination was notable for erythematous pustules near the wrist and on the fingers (Panel A) and on the trunk, scalp, and both ankles. There was mild swelling and pain with passive motion in the right ankle and tenosynovitis involving the tendons of both ankles. Given a high suspicion for disseminated gonococcal infection, treatment with ceftriaxone and azithromycin was initiated. Blood cultures grew gram-negative diplococci (Panel B) that were identified as Neisseria gonorrhoeae, which confirmed the diagnosis. The patient's symptoms abated with antibiotic treatment. At 3 months of follow-up, the patient was feeling well, with no recurrence of skin lesions or joint pain.

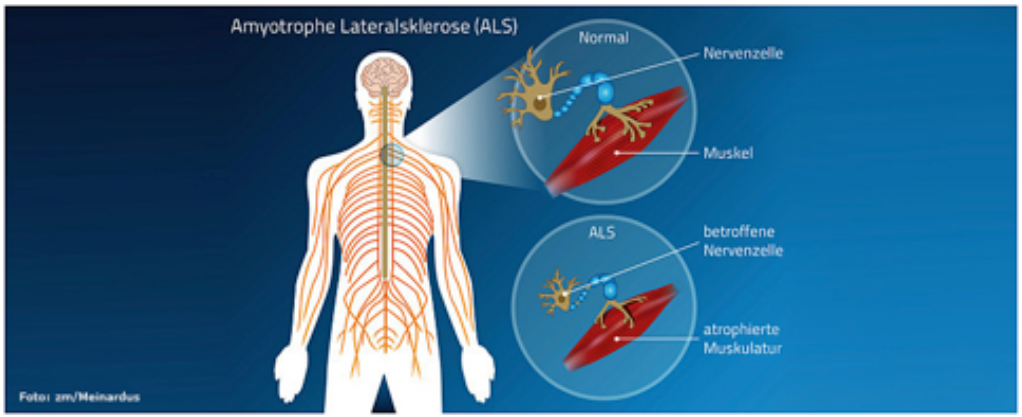


A 35-year-old man presented to the emergency department with a 2-day history of abdominal pain, headache, and brown urine. On examination, his temperature was 37.5° C. He was alert and oriented to time, place, and self, and he had no purpura or petechiae. Laboratory evaluation revealed a hemoglobin level of 8.6 g per deciliter (normal range, 13.7 to 17.5) and a platelet count of 6000 per cubic millimeter (normal range, 140,000 to 370,000). Levels of indirect bilirubin and lactate dehydrogenase were elevated, haptoglobin was undetectable, and the serum creatinine level was 1 mg per deciliter (88 μmol per liter; normal range, 0.6 to 1.3 mg per deciliter [57 to 115 μmol per liter]). Test results for infection with the human immunodeficiency virus were negative. A peripheral-blood smear showed numerous schistocytes (arrows). These findings were consistent with a microangiopathic hemolytic anemia. Plasma exchange for suspected thrombotic thrombocytopenic purpura was started immediately. Without the prompt initiation of treatment, mortality from thrombotic thrombocytopenic purpura is high. The patient underwent plasma exchange and received intravenous methylprednisolone for 5 days and had resolution of symptoms and an increased platelet count. The diagnosis was confirmed 2 days after initiation of treatment, with ADAMTS13 activity of 1%. He was discharged with instructions for tapering glucocorticoid treatment. Three months after discharge, he remained well.

Shruti Bhandari, M.D.
Rohit Kumar, M.D.
University of Louisville, Louisville, KY
s0bhan04@louisville.edu

Die amyotrophe Lateralsklerose (ALS) gehört zur Gruppe der Motoneuron-Krankheiten und ist eine nicht heilbare degenerative Erkrankung des motorischen Nervensystems. Sie wird auch amyotrophische Lateralsklerose oder myatrophe Lateralsklerose genannt, englisch auch Motor Neurone Disease, auch Lou-Gehrig-Syndrom oder nach dem Erstbeschreiber Jean-Martin Charcot Charcot-Krankheit.
Bei ALS kommt es zu einer fortschreitenden und irreversiblen Schädigung oder Degeneration der Nervenzellen (Neuronen), die für die Muskelbewegungen verantwortlich sind. Diese werden auch als motorische Neuronen oder Motoneurone bezeichnet. Es können sowohl die so genannten ersten Motoneurone betroffen sein, motorische Nervenzellen, die sich in der motorischen Hirnrinde (motorischer Kortex) befinden, als auch die als zweite Motoneurone bezeichneten Vorderhornzellen des Rückenmarks oder die motorischen Zellen des Hirnstamms in den Hirnnervenkernen. Die Fortsätze (Axone) der ersten Motoneurone ziehen zu den zweiten Motoneuronen, die wiederum mit ihren Fortsätzen zur Skelettmuskulatur ziehen und diese innervieren.
Die beiden Formen führen zu etwas unterschiedlichen Symptomen. Das Degenerieren der ersten Motoneurone führt zu einem erhöhten Muskeltonus (spastische Lähmung). Durch Schädigung der zweiten Motoneurone kommt es zu zunehmender Muskelschwäche (Parese bis Plegie), die mit Muskelschwund (Amyotrophie) einhergeht. Durch die Lähmungen der Muskulatur kommt es unter anderem zu Gang-, Sprech- und Schluckstörungen, eingeschränkter Koordination und Schwäche der Arm- und Handmuskulatur und dadurch zu einer fortschreitenden Einschränkung bei den Aktivitäten des täglichen Lebens.





A 60-Year-Old Man with Weakness and Difficulty Chewing

Six months before this presentation, weakness developed in the muscles of the patient's shoulders and arms, and he found it difficult to carry objects. He also noticed cramps in the muscles of his chest and shoulders.

Four months before this presentation, the patient began to have difficulty chewing food. He described mild difficulty chewing at the beginning of a meal, with the severity increasing during the meal.

The weakness and difficulty chewing persisted, and 5 weeks before this presentation, the patient was evaluated in a neurology clinic at another hospital. He reported excess salivation, slurred speech, mild constipation, and a weight loss of 3.6 kg over a period of 3 months. He had no associated pain, numbness, shortness of breath, memory deficits, or changes in bladder function or mood.



Detecting Atrophy and Fasciculations on Examination

On examination, the patient's speech was fluent, without dysarthria. There was no ophthalmoplegia or ptosis initially or with prolonged gaze. Results of formal testing of facial muscle power and jaw strength were normal. Motor testing revealed full, symmetric strength in the arms and legs, except for the strength on shoulder abduction and elbow flexion bilaterally, which was 4+ out of 5. Atrophy and fasciculations of the deltoid muscles were noted. Deep-tendon reflexes were 3+ and symmetric in the arms. Blood levels of electrolytes, glucose, vitamin B12 (cobalamin), copper, zinc, mercury, and arsenic were normal, as were results of tests of kidney, liver, and thyroid function. The complete blood count, erythrocyte-sedimentation rate, and creatine kinase level were normal. Screening tests for Lyme and syphilis antibodies were negative, as were tests for acetylcholine receptor binding, modulating, and blocking antibodies and antibodies to muscle-specific tyrosine kinase.

Computed tomography (CT) of the chest, performed after the intravenous administration of contrast material, was negative. Magnetic resonance imaging (MRI) of the head was performed without the administration of contrast material; T2-weighted images showed nonspecific, minimal, bilateral white-matter disease, a finding consistent with chronic small-vessel ischemic disease. MRI of the cervical spine revealed a normal cervical spinal cord and mild cervical spondylosis. Therapy with pyridostigmine was initiated, and the patient was referred to this hospital for further evaluation. On presentation to this hospital, the patient reported that pyridostigmine had had no effect on his weakness or chronic diplopia but that his difficulty chewing had improved. However, 5 weeks after the initiation of treatment, the difficulty chewing had worsened despite continued therapy with pyridostigmine. The patient reported new weakness in the legs, with difficulty rising from a seated position. He also reported increasing frequency of the fasciculations and one fall at home. He had a history of hypertension, treated Lyme disease, psoriasis, and a traumatic compression fracture of the thoracic spine.

Myopathy

Does this patient's mildly elevated creatine kinase level indicate myopathy? Elevated creatine kinase levels are not specific for myopathy and can be seen in neuropathic disorders, as well. For example, approximately 40% of patients with amyotrophic lateral sclerosis (ALS) have elevated creatine kinase levels, and the levels are typically 1 to 2 times the upper limit of the normal range.

Neuromuscular Junction Disorder

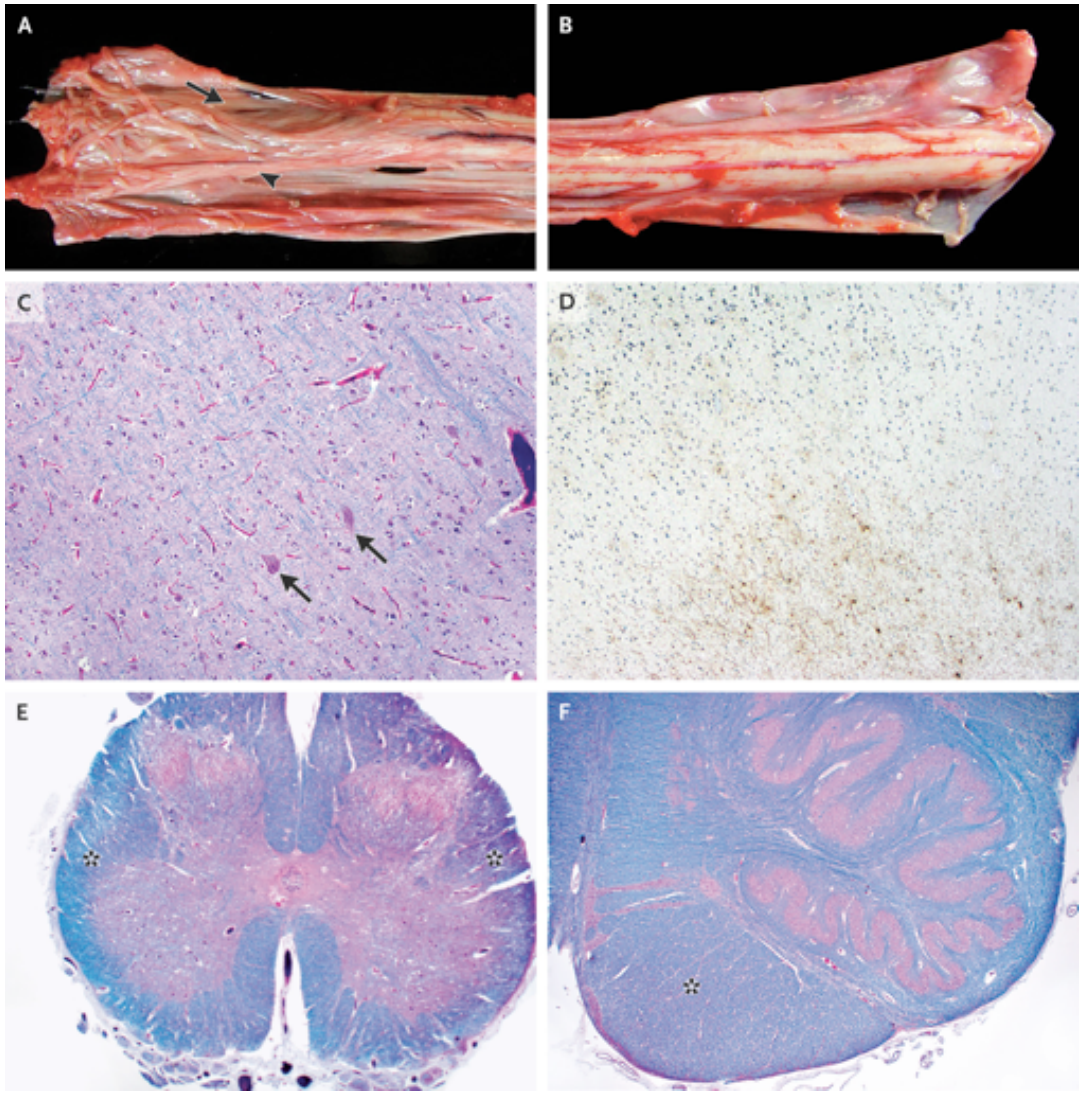
The patient reported difficulty chewing that would worsen over the course of a meal, a finding that could indicate fatigable weakness. Fatigable weakness is the hallmark of myasthenia gravis, an autoimmune disorder that affects the postsynaptic neuromuscular junction. The distribution of affected muscles in myasthenia gravis varies, but weakness of the proximal and bulbar muscles is common.

Neuropathy

Most neuropathies lead to predominantly distal weakness, but demyelinating neuropathies, such as chronic inflammatory demyelinating polyneuropathy, can cause proximal weakness. However, a neuropathy that would cause the degree of weakness that was seen in this patient would typically also cause sensory signs or symptoms, which were not seen in this patient.

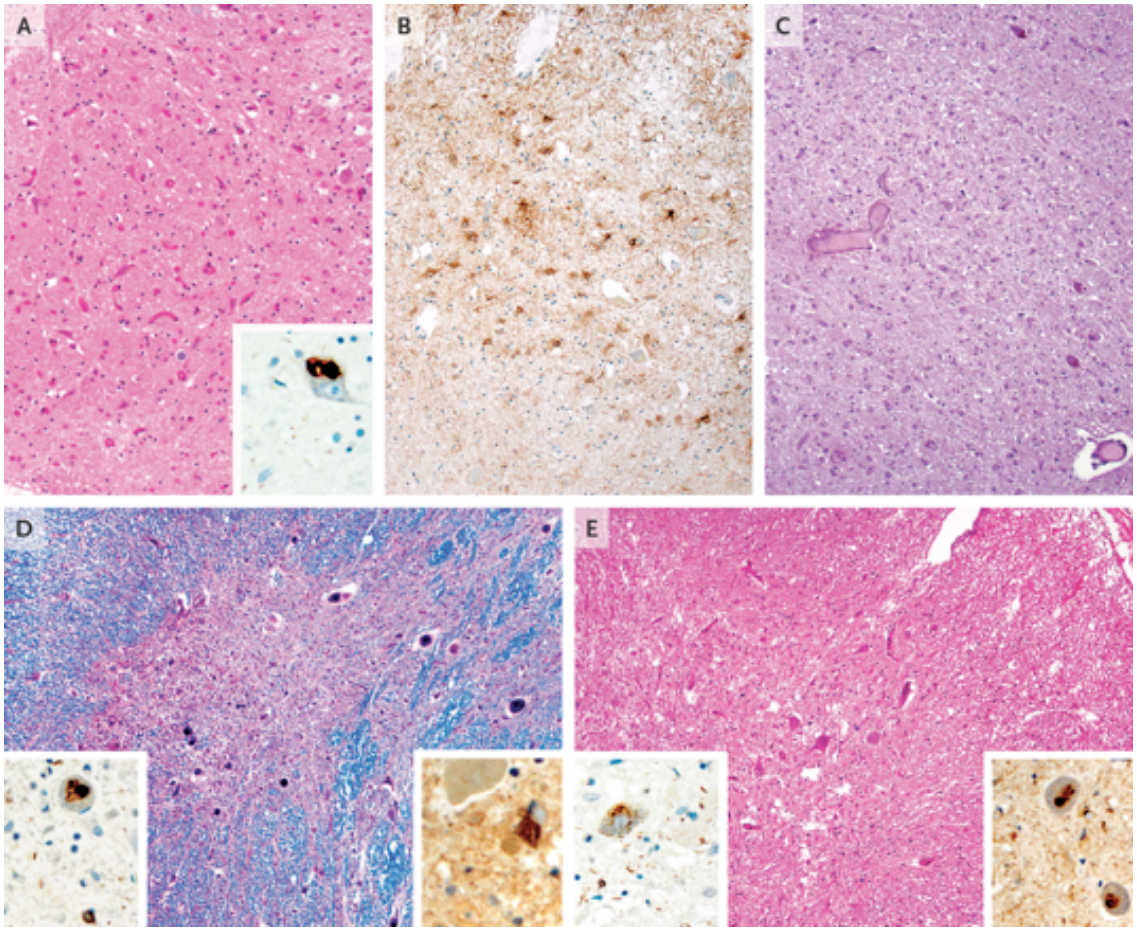
Motor Neuron Disease

The most common motor neuron disease to occur in this patient's age group is ALS, a degenerative disorder that affects both upper and lower motor neurons. The distribution of weakness in ALS varies. To receive a clinical diagnosis of ALS, the patient must have signs of both lower and upper motor neuron degeneration, progressive spread both within and between regions of the body, and no laboratory, electrodiagnostic, or imaging findings suggestive of alternative diagnoses.



Autopsy Specimens.

Gross photographs of the thoracolumbar and cervical spinal cord before fixation (Panels A and B, respectively) show that the anterior roots are thin, flat, and pale pink (Panel A, arrowhead) and the dorsal roots are round and white (Panel A, arrow). In the motor cortex, Luxol fast blue–hematoxylin and eosin staining (Panel C) shows that the overall cortical structure is retained, with some Betz cells visible (arrows), but staining for glial fibrillary acidic protein (Panel D) shows many reactive astrocytes in the deeper cortical layers. In the lumbar spinal cord and medulla (Panels E and F, respectively), Luxol fast blue–hematoxylin and eosin staining shows no loss of myelin staining in the corticospinal tracts (asterisks).



Additional Autopsy Specimens.

In the nucleus of the 12th cranial nerve, hematoxylin and eosin staining (Panel A) shows a reduction in motor neurons. Staining for TAR DNA-binding protein 43 (TDP-43) (Panel A, inset) shows inclusions in neurons and neurites in the neuropil. Staining for glial fibrillary acidic protein (Panel B) shows replacement gliosis. In the nucleus of the 5th cranial nerve, hematoxylin and eosin staining (Panel C) shows severe neuronal loss and gliosis. In the anterior horns of the cervical and lumbar spinal cord (Panels D and E, respectively), Luxol fast blue–hematoxylin and eosin staining (Panel D) and hematoxylin and eosin staining (Panel E) show greater loss of anterior-horn motor neurons in the cervical cord than in the lumbar cord. Staining for TDP-43 (Panels D and E, left insets) shows inclusions in remaining motor neurons and neurites in the neuropil, as does staining for ubiquitin (Panels D and E, right insets).

Anatomical Diagnoses

Motor neuron disease with TAR DNA-binding protein 43 proteinopathy.
Amyotrophic lateral sclerosis.
Acute bronchopneumonia.

β blockers to prevent decompensation of cirrhosis in patients with clinically significant portal hypertension (PREDESCI): a randomised, double-blind, placebo-controlled, multicentre trial

Summary

Background Clinical decompensation of cirrhosis is associated with poor prognosis. Clinically significant portal hypertension (CSPH), defined by a hepatic venous pressure gradient (HVPG) ≥10 mm Hg, is the strongest predictor of decompensation. This study aimed at assessing whether lowering HVPG with β blockers could decrease the risk of decompensation or death in compensated cirrhosis with CSPH.

Methods This study on β blockers to prevent decompensation of cirrhosis with portal hypertension (PREDESCI) was an investigator-initiated, double-blind, randomised controlled trial done in eight hospitals in Spain. We enrolled patients with compensated cirrhosis and CSPH without high-risk varices. All participants had HVPG measurements with assessment of acute HVPG-response to intravenous propranolol. Responders (HVPG-decrease ≥10%) were randomly assigned to propranolol (up to 160 mg twice a day) versus placebo and non-responders to carvedilol (≤25 mg/day) versus placebo. Doses were individually determined during an open-label titration period after which randomisation was done with 1:1 allocation by a centralised web-based system. The primary endpoint was incidence of cirrhosis decompensation (defined as development of ascites, bleeding, or overt encephalopathy) or death. Since death in compensated cirrhosis is usually unrelated to the liver, an intention-to-treat analysis considering deaths unrelated to the liver as competing events was done. This study is registered with ClinicalTrials.gov, number NCT01059396. The trial is now completed.

Findings Between Jan 18, 2010, and July 31, 2013, 631 patients were evaluated and 201 were randomly assigned. 101 patients received placebo and 100 received active treatment (67 propranolol and 33 carvedilol). The primary endpoint occurred in 16 (16%) of 100 patients in the β blockers group versus 27 (27%) of 101 in the placebo group (hazard ratio [HR] 0·51, 95% CI 0·26–0·97, p=0·041). The difference was due to a reduced incidence of ascites (HR=0·44, 95%CI=0·20–0·97, p=0·0297). The overall incidence of adverse events was similar in both groups. Six patients (four in the β blockers group) had severe adverse events.

Interpretation Long-term treatment with β blockers could increase decompensation-free survival in patients with compensated cirrhosis and CSPH, mainly by reducing the incidence of ascites.

	Placebo group (n=101)	β-blockers group (n=100)
Baseline characteristics		
Sex		
Male	64 (63%)	59 (59%)
Female	37 (37%)	41 (41%)
Age (years)	59 (11)	60 (10)
Cause of cirrhosis		
Alcohol	14 (14%)	19 (19%)
Hepatitis C virus	59 (58%)	54 (54%)
Alcohol and hepatitis C virus	8 (8%)	9 (9%)
NASH	8 (8%)	5 (5%)
Others	12 (12%)	13 (13%)
Diabetes	21 (21%)	22 (22%)
Dyslipidaemia	15 (15%)	12 (12%)
Arterial hypertension	34 (34%)	45 (45%)
Child-Pugh class		
A	81 (80%)	80 (80%)
B	20 (20%)	20 (20%)
C	0	0
Child-Pugh score	5·8 (0·9)	5·7 (0·9)
Model for end-stage liver disease score	6·8 (0·3)	6·6 (0·3)
Oesophageal varices*		
None	43 (43%)	44 (44%)
Small	58 (57%)	56 (56%)
Gastric varices†	1 (1%)	2 (2%)
Portal-systemic collaterals by ultrasound‡	11 (11%)	18 (18%)
Splenomegaly§	67 (66%)	56 (56%)
Liver stiffness, kPa¶	30·4 (16)	28·7 (13)
Weight, kg	76 (16)	76 (15)
BMI, kg/m²	27 (5)	27 (4)

(Table 1 continues in next column)

	Placebo group (n=101)	β-blockers group (n=100)
(Continued from previous column)		
Procedural characteristics		
Duration of follow-up (months)		
Mean	37 (16)	36 (16)
Median (IQR)	37 (27–47)	37 (26–47)
Lost to follow-up‖	4 (4%)	9 (9%)
Abstinence from alcohol**	88 (87%)	82 (82%)
Development of portal thrombosis	5 (5%)	3 (3%)
Liver transplantation††	1 (1%)	3 (3%)
Randomised to propranolol (or identical tablets of placebo)		
Number of patients	68 (67%)	67 (76%)
Dose (mg/day)		
Mean	95 (81)	95 (76)
Median (IQR)	80 (40–90)	80 (40–120)
Withdrawal‡‡	2	6
Randomised to carvedilol (or identical tablets of placebo)		
Number of patients	33 (33%)	33 (33%)
Dose (mg/day)		
Mean	20 (6)	19 (7)
Median (IQR)	18·8 (18·8–25)	18·8 (12·5–25)
Withdrawal§§	4	2

Values are mean (SD) or n (%), unless otherwise stated. NASH=non-alcoholic steatohepatitis. BMI=body-mass index. *None denotes absence of oesophageal varices on endoscopy and small varices denotes varices that were flattened by insufflation. †Patients with oesophageal and fundal varices (gastro-oesophageal varices type 2 according to Sarin's classification). ‡Among patients with portal-systemic collaterals, small oesophageal varices were present in 13 (72%) of 18 patients in the placebo group and in five (45%) of 11 in the β blockers group. §Spleen diameter >12 cm on ultrasound. ¶Liver stiffness by transient elastography. ‖For patients lost to follow-up, mean follow-up time in the placebo group was 18 months (IQR 14–24) and in the β-blockers group was 18 months (IQR 9–20). Ten (77%) of the 13 patients lost to follow-up had history of active or previous alcohol intake versus 78 (41%) of 188 who were not lost to follow-up; there were no other significant differences between patients lost and not lost to follow-up. **In the placebo group 17 (77%) of the 22 patients with alcoholic cause of cirrhosis (14 alcohol only and eight alcohol plus hepatitis C virus) were abstinent,

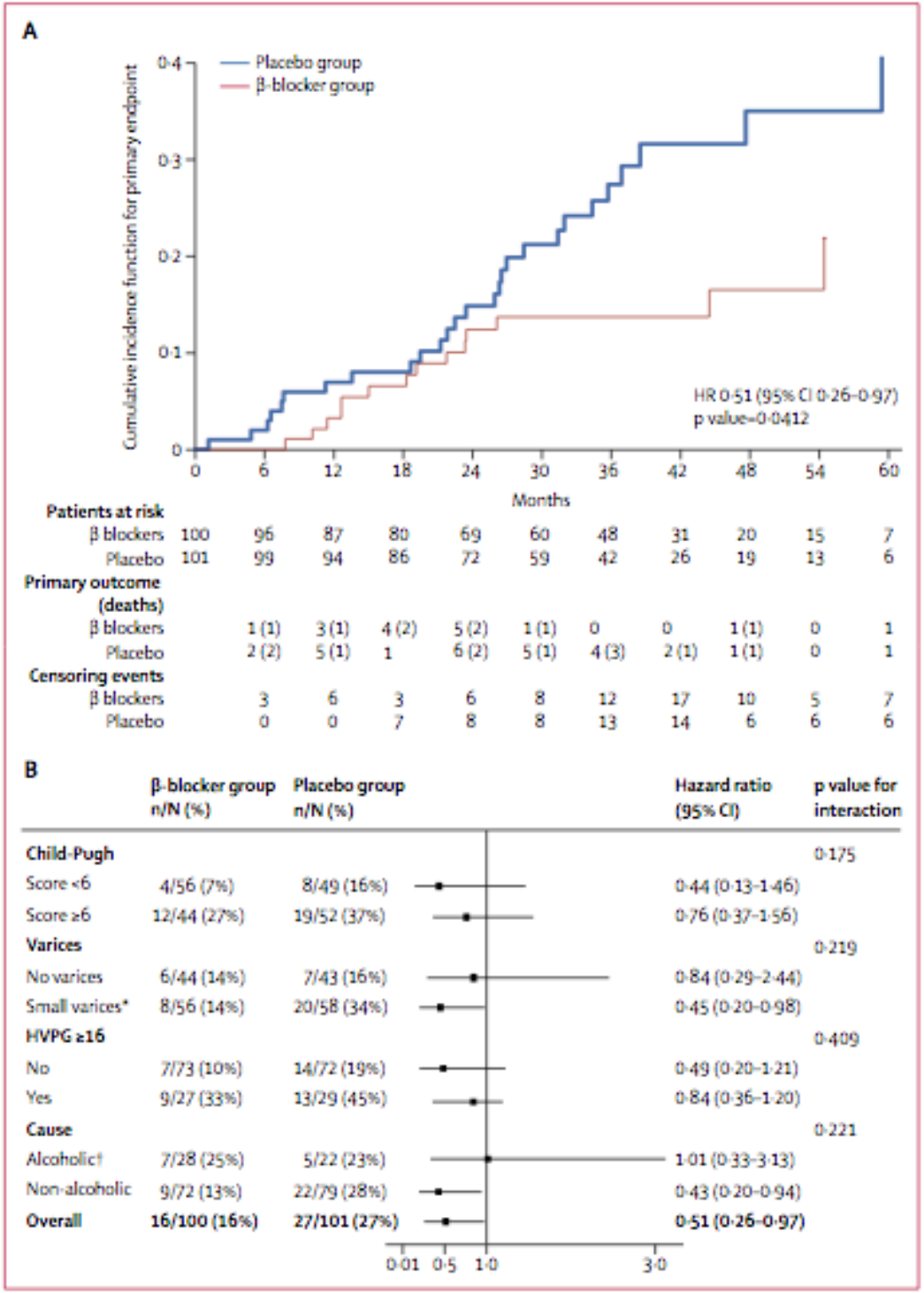


Figure 2: Primary endpoint (decompensation or death) according to treatment group

	Baseline	12 months follow-up	24 months follow-up	36 months follow-up	p values*
Patients†					
β blockers	100/100	78/88	44/69	22/40	..
Placebo	101/101	78/87	42/69	25/46	..
Hepatic venous pressure gradient					
Absolute values, mm Hg	..	..	..	..	p_{treat}<0·001; $p_{treat*time}$=0·075; p_{time}=0·98; $p_{stratum}$=0·94
β blockers	14·5 (14 to 15)	12·8 (12 to 14)	13·0 (12 to 14)	12·9 (12 to 14)	..
Placebo	14·8 (14 to 16)	15·0 (14 to 16)	14·9 (14 to 16)	14·6 (13 to 16)	..
Change from baseline, %					
β blockers	..	−12 (−15 to −8)	−10 (−12 to − 5)	−10 (−15 to −4)	..
Placebo	..	1·5 (−2 to 5)	1·2 (−3 to 6)	−0·9 (−6 to 5)	..
Cardiac output					
Absolute values, mm Hg	..	..	..	..	p_{treat}=0·049; $p_{treat*time}$=0·056; p_{time}=0·86; $p_{stratum}$=0·50
β blockers	6·0 (5·6 to 6·5)	5·3 (4·8 to 5·7)	5·4 (4·9 to 5·9)	5·5 (4·9 to 6·1)	..
Placebo	5·9 (5·5 to 6·4)	5·9 (5·5 to 6·4)	5·7 (5·1 to 6·1)	5·9 (5·3 to 6·5)	..
Change from baseline, %					
β blockers	..	−12 (−15 to −7)	−8 (−13 to −2)	−7 (−13 to −1)	..
Placebo	..	0·6 (−3 to 4)	−5 (−11 to −1)	−0·3 (−6 to 6)	..
Cardiac index					
Absolute values, mm Hg	..	..	..	..	p_{treat}=0·010; $p_{treat*time}$=0·074; p_{time}=0·29; $p_{stratum}$=0·58
β blockers	3·4 (3·1 to 3·6)	2·9 (2·7 to 3·2)	2·9 (2·7 to 3·3)	3·0 (2·7 to 3·4)	..
Placebo	3·2 (3.0 to 3.4)	3·5 (3·2 to 3·8)	3·2 (2·8 to 3·5)	3·2 (2·9 to 3·6)	..
Change from baseline, %					
β blockers	..	−15 (−21 to −7)	−11 (−19 to −3)	−10 (−20 to 0)	..
Placebo	..	11 (4 to 18)	−3 (−14 to 4)	−2 (−12 to 8)	..
Mean arterial pressure					
Absolute values, mm Hg	..	..	..	..	p_{treat}=0·007; $p_{treat*time}$=0·227; p_{time}=0·28; $p_{stratum}$=0·70
β blockers	98 (95 to 100)	92 (89 to 95)	92 (89 to 96)	95 (91 to 99)	..
Placebo	96 (93 to 98)	91 (88 to 94)	92 (88 to 95)	93 (88 to 97)	..
Change from baseline, %					
β blockers	..	−5 (−7 to 2)	−5 (−8 to −2)	−2 (−6 to 2)	..
Placebo	..	−3 (-5 to −1)	−2 (−5 to 1)	−2 (−5 to 2)	..
Heart rate					
Absolute values, mm Hg	..	..	..	..	p_{treat}=<0·001; $p_{treat*time}$=0·80; p_{time}=0·004; $p_{stratum}$<0·001
β blockers	74 (72 to 76)	61 (59 to 64)	62 (59 to 65)	60 (57 to 64)	..
Placebo	73 (71 to 75	72 (69 to 74)	69 (65 to 72)	71 (67 to 74)	..
Change from baseline, %					
β blockers	..	−16 (−19 to 14)	−16 (−18 to −12)	−17 (−21 to −13)	..
Placebo	..	−1 (−3 to 1)	−5 (−7 to −2)	−3 (−6 to 1)	..
Pulmonary artery pressure					
Absolute values, mm Hg	..	..	..	..	p_{treat}=0·81; $p_{treat*time}$=0·97; p_{time}=0·08; $p_{stratum}$=0·67
β blockers	16·5 (15 to 18)	17·3 (16 to 19)	18·6 (17 to 20)	21·6 (19 to 24)	..
Placebo	16·5 (15 to 18)	17·0 (15 to 18)	18·7 (17 to 21)	17·0 (15 to 19)	..
Change from baseline, %					
β blockers	..	7·5 (−1 to 16)	18 (5 to 29)	19 (17 to 21)	..
Placebo	..	5 (−3 to 13)	18 (5 to 31)	4 (−11 to 19)	..
Pulmonary wedge pressure					
Absolute values, mm Hg	..	..	..	..	p_{treat}=0·37; $p_{treat*time}$=0·89; p_{time}=0·35; $p_{stratum}$=0·10
β blockers	8·8 (8 to 10)	10·3 (9 to 11)	10·9 (9 to 12)	13·4 (11 to 15)	..
Placebo	9·7 (9 to 11)	10·0 (9 to 11)	10·6 (9 to 12)	10·1 (8 to 12)	..
Change from baseline, %					
β blockers	..	35 (21 to 53)	66 (39 to 93)	81 (46 to 117)	..
Placebo	..	13 (−7 to 32)	29 (1 to 57)	22 (−11 to 56)	..

(Table 1 coninues on next page)

	Placebo group (n=101)	β-blockers group (n=100)	Risk (95% CI)*	p value†
Decompensation or death				
Overall‡	27 (27%)	16 (16%)	0·51 (0·26–0·97)	0·0412
Secondary outcomes				
Ascites	20 (20%)	9 (9%)	0·42 (0·19–0·92)	0·030
Gastrointestinal bleeding	3 (3%)	4 (4%)	1·52 (0·34–6·82)	0·61
Overt hepatic encephalopathy	5 (5%)	4 (4%)	0·92 (0·40–2·21)	0·98
Death from any cause	11 (11%)	8 (8%)	0·54 (0·20–1·48)	0·23
Varices	56 (56%)	58 (58%)	1·15 (0·65–2·02)	0·72
High-risk varices§	25 (25%)	16 (16%)	0·60 (0·30–1·21)	0·15
Spontaneous bacterial peritonitis	4 (4%)	2 (2%)	0·49 (0·10–2·70)	0·40
Other bacterial infections¶	19 (19%)	15 (15%)	0·81 (0·41–1·59)	0·54
Hepatorenal syndrome	1 (1%)	1 (1%)	0·99 (0·06–15·96)	0·96
Hepatocellular carcinoma	17 (17%)	13 (13%)	0·76 (0·37–1·54)	0·43

Percentages are crude incidences of events occurring at any time during the follow-up. *Values indicate the hazard ratio of an outcome in the β-blockers group as compared with the placebo group. †Comparison of cumulative incidences by competing-risk analysis (differences assessed by Gray's test). ‡The absolute reduction in the incidence of the primary outcome was of 11% (95% CI 0–22). §Among patients with high-risk varices, oesophageal variceal ligation to prevent bleeding was performed in 18 (72%) of 25 patients in the placebo group versus 11 (69%) of 16 in the non-selective β-blockers group. ¶Including spontaneous bacterial peritonitis, and other documented bacterial infections during follow-up.

Table 3: **Long-term outcomes**

	Placebo group (n=101)	β blockers group (n=100)
Overall	88 (87%)	84 (84%)
Probably related to treatment*	30 (30%)	39 (39%)
Very probably related to treatment†	15 (15%)	16 (16%)
Total number of adverse events‡	45	57
Major adverse events§	2 (2%)	4 (4%)
Syncope	1	2
Bradyarrhythmia	0	1
Heart failure	0	1
Acute coronary syndrome	1	0
Minor adverse events¶	28 (28%)	36 (36%)
Weakness	17	23
Shortness of breath	2	4
Dizziness or hypotension	9	9
Bradycardia	2	3
Headache	1	2
Impotence	3	2
Gastrointestinal symptoms	3	2
Other	6	7

*Adverse events that were subjectively considered by the investigator to be probably related to drug treatment. †Adverse events that were subjectively considered by the investigator to be very probably related to drug treatment. ‡Some patients had more than one type of adverse event probably or very probably related to treatment: in the placebo group, 101 patients had 45 adverse events and in the β-blockers group 100 patients had 57 adverse events. §Adverse effects were considered severe if the health or safety of the patient was endangered. ¶In the placebo group, 28 patients had 43 minor adverse events. In the β-blockers group, 36 patients had 52 minor adverse events and, in this group, two patients had both minor and major complications.

Table 4: **Adverse outcomes**

Research in context

Evidence before this study

Liver cirrhosis evolves over time from a compensated to a decompensated stage, which is associated with a marked decline in life expectancy. Portal hypertension (PH) is the main determinant of the progression to clinical decompensation, defined by the occurrence of ascites, bleeding, or encephalopathy. A portal pressure gradient ≥10 mm Hg defines clinically significant PH (CSPH), since decompensation might appear after reaching this threshold. Indeed, CSPH is the strongest predictor of clinical decompensation. Non-selective β blockers (NSBB) lower portal pressure by decreasing portal venous inflow, which is increased in patients with CSPH, but much less in those without CSPH, in whom the response to NSBB is almost negligible. We searched PubMed, Embase and the Cochrane Library (Feb 28, 2018), for clinical trials evaluating drug therapies to prevent decompensation of cirrhosis, without language or date restrictions. We used the terms "compensated cirrhosis", "prevent decompensation", "prevent ascites", "prevent bleeding", "prevent encephalopathy", and "β-blockers". We identified numerous randomised controlled trials and meta-analyses showing that NSBB effectively prevent first variceal bleeding. Only one randomised controlled trial evaluated whether NSBB could prevent the development of varices in compensated cirrhosis, but this study failed to demonstrate any beneficial effect. This negative result might have been due to the fact that part of the patients included had no CSPH, and therefore were very unlikely to respond to NSBB and to develop decompensation. On the other hand, current European (Baveno VI) and American Association for the Study of Liver Diseases (AASLD) recommendations indicate that the aim of treatment of portal hypertension in patients with compensated cirrhosis should be to prevent decompensation, rather than focusing only on variceal bleeding. However, no randomised controlled trial with this endpoint has been conducted so far. The present cooperative, double-blind randomised controlled trial aimed at investigating whether long-term treatment of patients with compensated cirrhosis and CSPH with NSBB might prevent progression to clinical decompensation or death.

Added value of this study

The present double-blind randomised controlled trial is the first study showing that long-term treatment with NSBB decreases approximately by half the risk of clinical decompensation or liver-related death. This is mainly due to a decreased likelihood of developing ascites, which is the most common and severe decompensating event, for which previously there was no effective preventive drug therapy. As a likely explanation of the beneficial effects of therapy, the study shows that NSBB, but not placebo, significantly reduced the portal pressure gradient at each yearly control.

Implications of all the available evidence

Our finding that in patients with compensated cirrhosis and CSPH continued therapy with NSBB significantly reduces the incidence of decompensation or death represents a landmark innovation in the management of patients with cirrhosis. It has important implications in clinical practice, suggesting that patients with compensated cirrhosis should be screened for development of CSPH, and that therapy with NSBB should be started from its detection, which nowadays can be done quite confidently using non-invasive tools, such as transient elastography (alone or associated with platelet count or spleen diameter measurements). This new indication of NSBB might have a major impact on patients' outcomes, health-care burden and costs, which would likely influence future clinical guidelines. Future research should confirm that it is indeed possible to accurately detect CSPH in patients with compensated cirrhosis using simple non-invasive methods, and further define specific biomarkers of response to therapy.

Laser peripheral iridotomy for the prevention of angle closure: a single-centre, randomised controlled trial

Summary

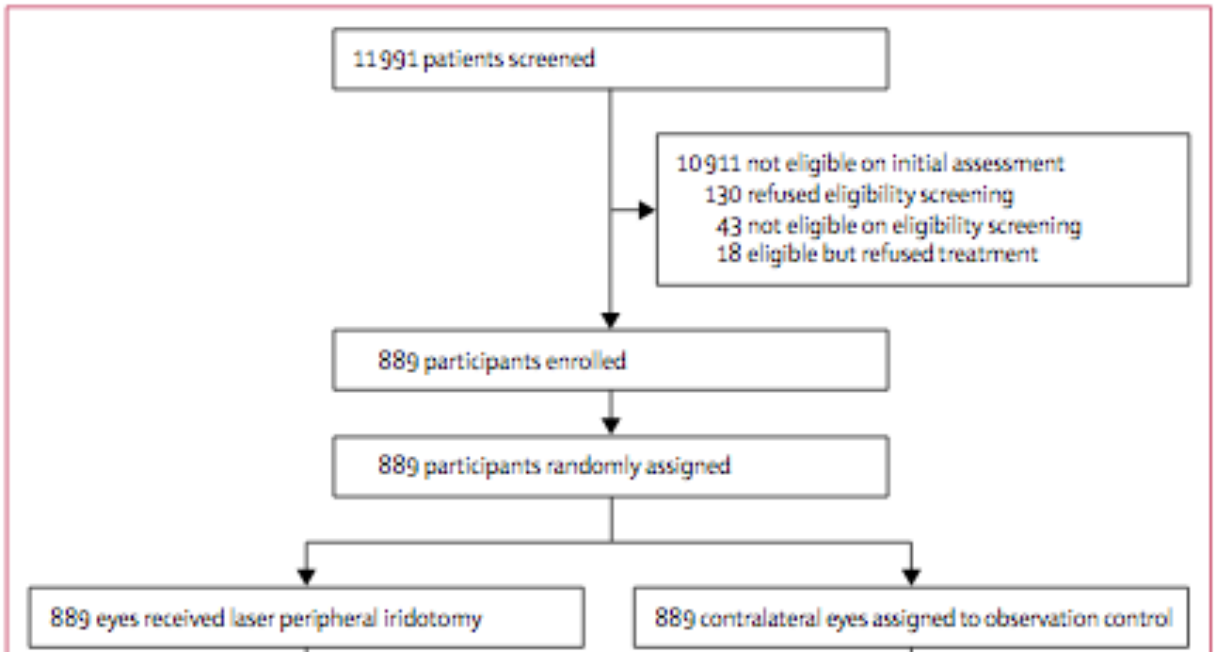
Background Primary angle-closure glaucoma affects 20 million people worldwide. People classified as primary angle closure suspects have a higher but poorly quantified risk of developing glaucoma. We aimed to assess efficacy and safety of laser peripheral iridotomy prophylaxis against primary angle-closure glaucoma in Chinese people classified as primary angle closure suspects.

Methods In this randomised controlled trial, bilateral primary angle closure suspects aged 50–70 years were enrolled at the Zhongshan Ophthalmic Center, a tertiary specialised hospital in Guangzhou, China. Eligible patients received laser peripheral iridotomy in one randomly selected eye, with the other remaining untreated. The primary outcome was incident primary angle closure disease as a composite endpoint of elevation of intraocular pressure, peripheral anterior synechiae, or acute angle-closure during 72 months of follow-up in an intention-to-treat analysis between treated eyes and contralateral controls. This trial is registered with the ISRCTN registry, number ISRCTN45213099.

Findings Of 11 991 screened individuals, 889 individuals were randomly assigned from June 19, 2008 (889 treated and 889 untreated eyes). Incidence of the primary outcome was 4·19 per 1000 eye-years in treated eyes compared with 7·97 per 1000 eye-years in untreated eyes (hazard ratio 0·53; 95% CI 0·30–0·92; p=0·024). A primary outcome event occurred in 19 treated eyes and 36 untreated eyes with a statistically significant difference using pair-wise analysis (p=0·0041). No serious adverse events were observed during follow-up.

Interpretation Incidence of angle-closure disease was very low among individuals classified as primary angle closure suspects identified through community-based screening. Laser peripheral iridotomy had a modest, albeit significant, prophylactic effect. In view of the low incidence rate of outcomes that have no immediate threat to vision, the benefit of prophylactic laser peripheral iridotomy is limited; therefore, widespread prophylactic laser peripheral iridotomy for primary angle-closure suspects is not recommended.

Funding Fight for Sight, the Sun Yat-Sen University 5010 Project Fund, Moorfields Eye Charity, and the National Natural Science Foundation of China.



	Laser peripheral iridotomy (n=889)	Control (n=889)
Spherical equivalent, diopter	2·11 (1·35)	2·14 (1·37)
Cup-to-disc ratio	0·40 (0·14)	0·40 (0·14)
Axial length, mm	22·49 (0·73)	22·49 (0·72)
Central anterior chamber depth, mm*	2·55 (0·22)	2·55 (0·22)
Lens thickness, mm	4·87 (0·33)	4·88 (0·32)
Goldmann applanation tonometry intraocular pressure, mm Hg		
Before provocative test	14·3 (2·6)	14·3 (2·6)
After provocative test	18·6 (3·2)	18·6 (3·2)
Limbal anterior chamber depth grade, n (%)†		
5%	31 (3%)	32 (4%)
15%	262 (30%)	271 (30%)
25%	557 (63%)	543 (61%)
40%	35 (4%)	38 (4%)
75%	4 (<1%)	5 (<1%)
Total angle width on Gonioscopy, score‡	5·33 (2·37)	5·34 (2·40)
Number of closed quadrants, n (%)		
2 quadrants	36 (4%)	31 (3%)
3 quadrants	114 (13%)	113 (13%)
4 quadrants	739 (83%)	745 (84%)
Lens Opacity Classification System III grading		
Nuclear opacity	2·30 (0·59)	2·30 (0·59)
Nuclear colour	2·17 (0·58)	2·18 (0·58)
Cortical opacity	0·84 (1·16)	0·85 (1·17)
Posterior subcapsular cataract	0·11 (0·30)	0·12 (0·33)

All values are mean (SD) unless stated otherwise. *Measured by ultrasound A-scan. †Evaluated using modified van Herick grading. ‡Total angle width was calculated by the sum of Shafer grading of all four quadrants (range from 0 to 16, larger number indicates wider angle).

Table 1: **Baseline characteristics of laser peripheral iridotomy-treated and control eyes**

	Laser peripheral iridotomy (n=889)	Control (n=889)	p value
Reach primary endpoint	19 (4·19 per 1000 eye-years)	36 (7·97 per 1000 eye-years)	0·021
2 weeks	1	1	..
6 months	5	3	..
18 months	5	6	..
36 months	3	6	..
54 months	2	11	..
72 months	3	9	..
Intraocular pressure measures >24 mm Hg	3 (0·66 per 1000 eye-years)	5 (1·11 per 1000 eye-years)	0·480
2 weeks	0	0	..
6 months	1	0	..
18 months	2	2*	..
36 months	0	2*	..
54 months	0	0	..
72 months	0	1*	..
Peripheral anterior synechiae ≥1 clock hour	15 (3·31 per 1000 eye-years)	30 (6·64 per 1000 eye-years)	0·024
2 weeks	0	0	..
6 months	4	3	..
18 months	3	5†	..
36 months	3	5†	..
54 months	2	11	..
72 months	3	6†	..
Acute attack	1 (0·22 per 1000 eye-years)	5 (1·11 per 1000 eye-years)	0·100
2 weeks	1§	1‡	..
6 months	0	0	..
18 months	0	0	..
36 months	0	1§	..
54 months	0	0	..
72 months	0	3	..

All values are number of events unless stated otherwise. p values were estimated by log-rank test for equality of survival function. Six participants reached endpoint in both eyes at the same visit and four reached endpoint in both eyes at two separate visits. *Three control eyes reached both intraocular pressure and peripheral anterior synechiae endpoint at the same visit. †Four control eyes reached both PAS endpoint and IOP or acute attack endpoint at the same visit. ‡Same individual with bilateral acute attack after dilation. §One control eye reached both PAS endpoint and acute attack endpoint at the same visit.

Table 2: **Primary outcomes at 72 months by intention-to-treat analysis**

	Laser peripheral iridotomy	Control	p value
Presenting visual acuity, logarithm of the minimum angle of resolution			
Baseline (n=889)	0·19 (0·17)	0·19 (0·17)	0·908
6 months (n=863)	0·15 (0·15)	0·16 (0·16)	0·016
18 months (n=836)	0·18 (0·16)	0·19 (0·17)	0·017
36 months (n=778)	0·21 (0·18)	0·22 (0·18)	0·093
54 months (n=695)	0·24 (0·18)	0·25 (0·19)	0·244
72 months (n=628)	0·29 (0·21)	0·28 (0·20)	0·121
Intraocular pressure, mm Hg			
Baseline (n=889)	15·07 (2·85)	15·09 (2·83)	0·673
6 months (n=863)	15·89 (2·66)	15·64 (2·64)	<0·001
18 months (n=837)	14·99 (2·71)	14·81 (2·79)	<0·001
36 months (n=777)	15·05 (2·35)	14·86 (2·37)	<0·001
54 months (n=695)	15·76 (2·38)	15·59 (2·33)	<0·001
72 months (n=628)	15·26 (2·47)	15·09 (2·44)	<0·001
Total angle width, score*			
Baseline (n=889)	5·33 (2·37)	5·34 (2·40)	0·858
6 months (n=863)	10·29 (2·82)	4·91 (2·42)	<0·001
18 months (n=837)	9·57 (2·85)	4·53 (2·22)	<0·001
36 months (n=777)	11·47 (3·38)	4·74 (2·99)	<0·001
54 months (n=695)	9·78 (3·59)	3·69 (2·60)	<0·001
72 months (n=628)	9·62 (3·41)	3·93 (3·09)	<0·001
Limbal anterior chamber depth, %†			
Baseline (n=889)	22·17 (7·46)	22·15 (7·78)	0·917
6 months (n=863)	38·33 (16·31)	20·10 (8·15)	<0·001
18 months (n=837)	42·19 (20·75)	19·10 (9·80)	<0·001
36 months (n=777)	38·90 (17·21)	19·05 (9·00)	<0·001
54 months (n=695)	33·16 (14·90)	16·71 (9·46)	<0·001
72 months (n=628)	31·85 (13·59)	17·01 (10·39)	<0·001

Included both eyes without reaching endpoint at each visit. All values are mean (SD). p values were estimated by paired t test. *Total angle width was calculated by the sum of Shafer grading of all four quadrants (range from 0 to 16, larger number indicates wider angle). †Limbal anterior chamber depth was evaluated by modified van Herick grading.

Table 4: **Clinical secondary endpoints at each visit**

		Laser peripheral iridotomy		
		No endpoint	Endpoint	**Total**
Control	No endpoint	844	9	853
	Endpoint	26	10	36
	Total	870	19	889

***Figure 2*: Pair-wise analyses of primary endpoint (intention-to-treat analysis) at 72 months**
p=0·0041 with McNemar's test.

See Online for appendix

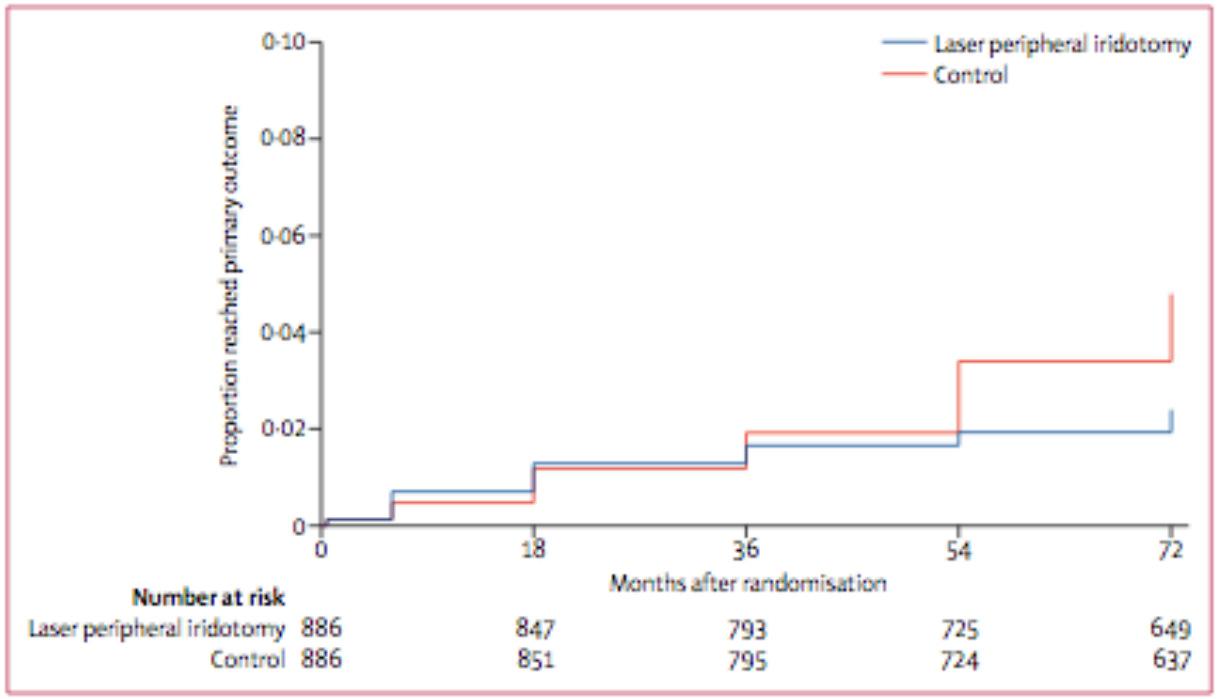


***Figure 3*: Kaplan-Meier plot of the study endpoint**

	Eyes that did reach endpoint, n=55, 3%	Eyes that did not reach endpoint, n=1723, 97%	Hazard ratio (95% CI)	p value
Univariate model				
Randomly assigned to laser peripheral iridotomy	34·5%	50·5%	0·53 (0·30-0·92)	0·024
Multivariate models				
Age, years (per 1 year older)	60·91 (5·76)	59·25 (4·97)	1·07 (1·01-1·13)	0·015
Female (*vs* male)	81·8%	82·9%	1·11 (0·55-2·24)	0·765
Randomly assigned to laser peripheral iridotomy (*vs* control)	34·5%	50·5%	0·52 (0·30-0·91)	0·023
Baseline intraocular pressure, mm Hg (per 1 mm Hg increase)	15·76 (3·02)	15·06 (2·83)	1·09 (0·99-1·19)	0·075
Total angle width*, score (per 1 score higher)	4·80 (2·37)	5·36 (2·38)	0·91 (0·82-1·02)	0·098
Limbal anterior chamber depth†, % (per 10% higher)	18·64 (8·41)	22·28 (7·57)	0·49 (0·34-0·71)	<0·001
Central anterior chamber depth‡, mm (per 1 mm deeper)	2·47 (0·24)	2·55 (0·22)	0·21 (0·06-0·72)	0·013
Lens thickness‡, mm (per 1 mm thicker)	4·95 (0·37)	4·87 (0·32)	1·57 (0·65-3·79)	0·318
Dark room prone provocative test, mm Hg (per 1 mm Hg increase)	3·76 (3·39)	4·27 (2·97)	0·94 (0·86-1·03)	0·199

All values are mean (SD) unless stated otherwise. Multivariable Cox proportional hazards models include laser peripheral iridotomy, age, gender, baseline intraocular pressure, and variables of interest. *Total angle width was calculated by the sum of Shafer grading of all four quadrants (range from 0 to 16, larger number indicates wider angle). †Limbal anterior chamber depth was evaluated by modified van Herick grading. ‡Central anterior chamber depth and lens thickness were measured by ultrasound A-scan.

***Table 3*: Baseline ocular biometrics and gonioscopic factors associated with endpoint at 72 months**

Research in context

Evidence before this study

We searched for studies published between database inception and June 30, 2018, in English in MEDLINE, PubMed, Embase, and the Cochrane Collaboration Database and hand searched the reference lists of important articles. We identified one systematic review that assessed nine randomised clinical trials and 24 non-randomised clinical trials and large case series. This review concluded that laser peripheral iridotomy should be recommended for treatment of affected and contralateral eyes of patients with acute angle-closure. Evidence was insufficient to advise prophylactic iridotomy for other angle-closure diseases, although this was widespread practice. A Cochrane review examining the benefits of laser iridotomy in management and prophylaxis of angle-closure disease was published on June 13, 2018. This review searched Cochrane CENTRAL (2017, Issue 9), which contains the Cochrane Eyes and Vision Trials Register, MEDLINE Ovid, Embase Ovid, PubMed, LILACS, ClinicalTrials.gov, and the International Clinical Trials Registry Platform (search date Oct 18, 2017). This review noted that our trial and one other similar trial in Singapore were ongoing, and that robust data on the benefit of prophylactic laser iridotomy was scarce.

Added value of this study

This large randomised controlled trial provides the first robust evidence on the use of laser peripheral iridotomy as prophylaxis against primary angle-closure disease and associated glaucoma. At the annual data monitoring meeting before all participants completed the 18-month follow-up visit, we decided to extend the study from 36 months to 72 months and enrol additional participants, given the much smaller than predicted event rate. At the 72-month visit, laser peripheral iridotomy-treated eyes had a small but statistically significant benefit, with incidence of primary angle-closure disease in treated eyes of 4·2 cases per 1000 eye-years compared with 8·0 per 1000 eye-years in untreated eyes (hazard ratio 0·53, 95% CI 0·30–0·92).

Implications of all the available evidence

The incidence of angle-closure disease was very low among angle-closure suspects identified through community-based screening. Laser peripheral iridotomy had a modest, albeit significant, prophylactic effect. Most individuals who developed incident primary outcomes had no immediate threat to vision; therefore, the benefit of prophylactic laser peripheral iridotomy was small in this 72-month study. Widespread prophylactic laser peripheral iridotomy for primary angle-closure suspects is not recommended.

Three-dimensional visualisation of the fetal heart using prenatal MRI with motion-corrected slice-volume registration: a prospective, single-centre cohort study

Summary

Background Two-dimensional (2D) ultrasound echocardiography is the primary technique used to diagnose congenital heart disease before birth. There is, however, a longstanding need for a reliable form of secondary imaging, particularly in cases when more detailed three-dimensional (3D) vascular imaging is required, or when ultrasound windows are of poor diagnostic quality. Fetal MRI, which is well established for other organ systems, is highly susceptible to fetal movement, particularly for 3D imaging. The objective of this study was to investigate the combination of prenatal MRI with novel, motion-corrected 3D image registration software, as an adjunct to fetal echocardiography in the diagnosis of congenital heart disease.

Methods Pregnant women carrying a fetus with known or suspected congenital heart disease were recruited via a tertiary fetal cardiology unit. After initial validation experiments to assess the general reliability of the approach, MRI data were acquired in 85 consecutive fetuses, as overlapping stacks of 2D images. These images were then processed with a bespoke open-source reconstruction algorithm to produce a super-resolution 3D volume of the fetal thorax. These datasets were assessed with measurement comparison with paired 2D ultrasound, structured anatomical assessment of the 2D and 3D data, and contemporaneous, archived clinical fetal MRI reports, which were compared with postnatal findings after delivery.

Findings Between Oct 8, 2015, and June 30, 2017, 101 patients were referred for MRI, of whom 85 were eligible and had fetal MRI. The mean gestational age at the time of MRI was 32 weeks (range 24–36). High-resolution (0·50–0·75 mm isotropic) 3D datasets of the fetal thorax were generated in all 85 cases. Vascular measurements showed good overall agreement with 2D echocardiography in 51 cases with paired data (intra-class correlation coefficient 0·78, 95% CI 0·68–0·84), with fetal vascular structures more effectively visualised with 3D MRI than with uncorrected 2D MRI (657 [97%] of 680 anatomical areas identified *vs* 358 [53%] of 680 areas; p<0·0001). When a structure of interest was visualised in both 2D and 3D data (n=358), observers gave a higher diagnostic quality score for 3D data in 321 (90%) of cases, with 37 (10%) scores tied with 2D data, and no lower scores than for 2D data (Wilcoxon signed rank test p<0·0001). Additional anatomical features were described in ten cases, of which all were confirmed postnatally.

Interpretation Standard fetal MRI with open-source image processing software is a reliable method of generating high-resolution 3D imaging of the fetal vasculature. The 3D volumes produced show good spatial agreement with ultrasound, and significantly improved visualisation and diagnostic quality compared with source 2D MRI data. This freely available combination requires minimal infrastructure, and provides safe, powerful, and highly complementary imaging of the fetal cardiovascular system.

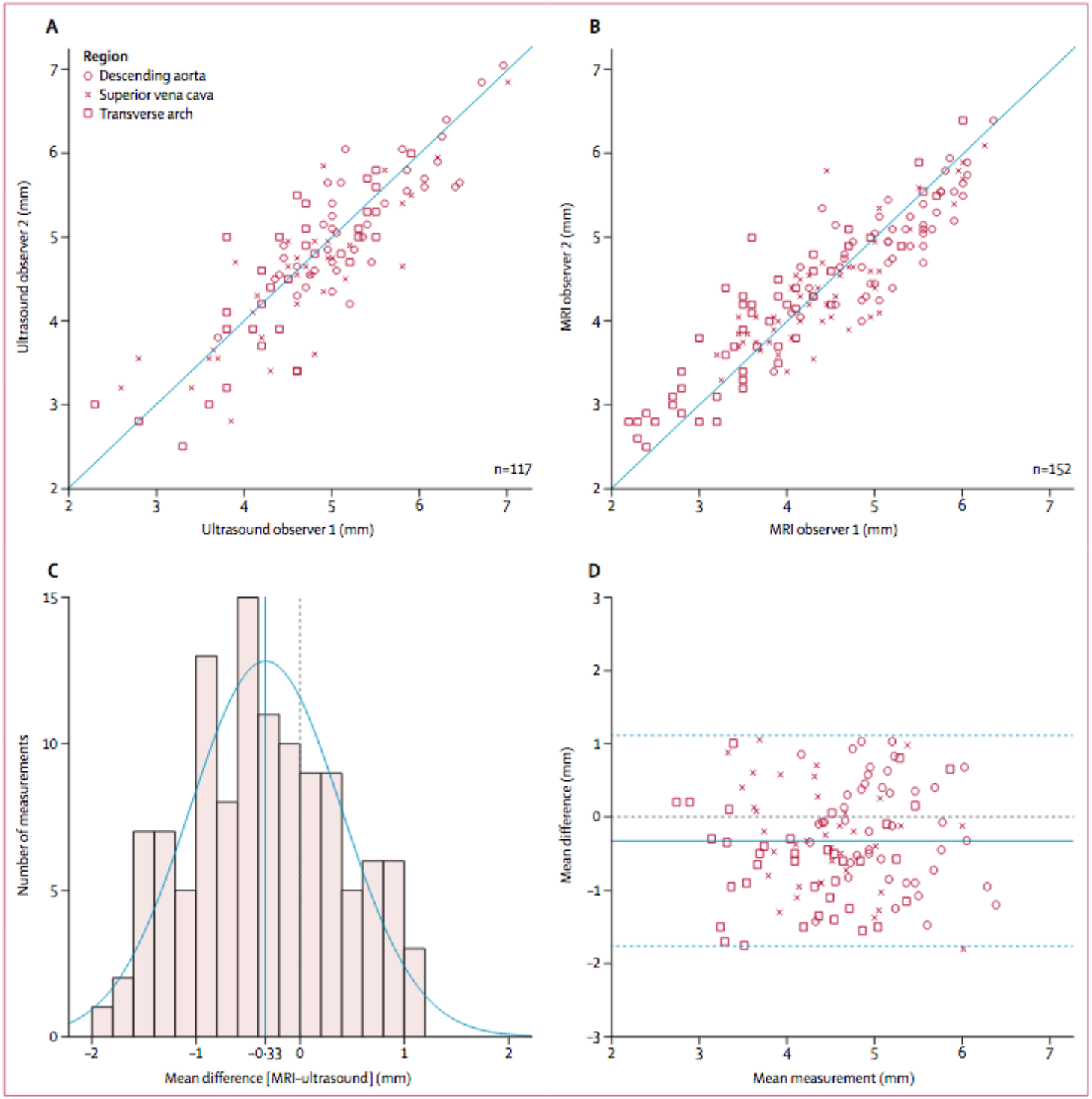


Figure 1: **Scatter plots comparing measurements from two independent observers for echocardiography (A) and MRI (B)**

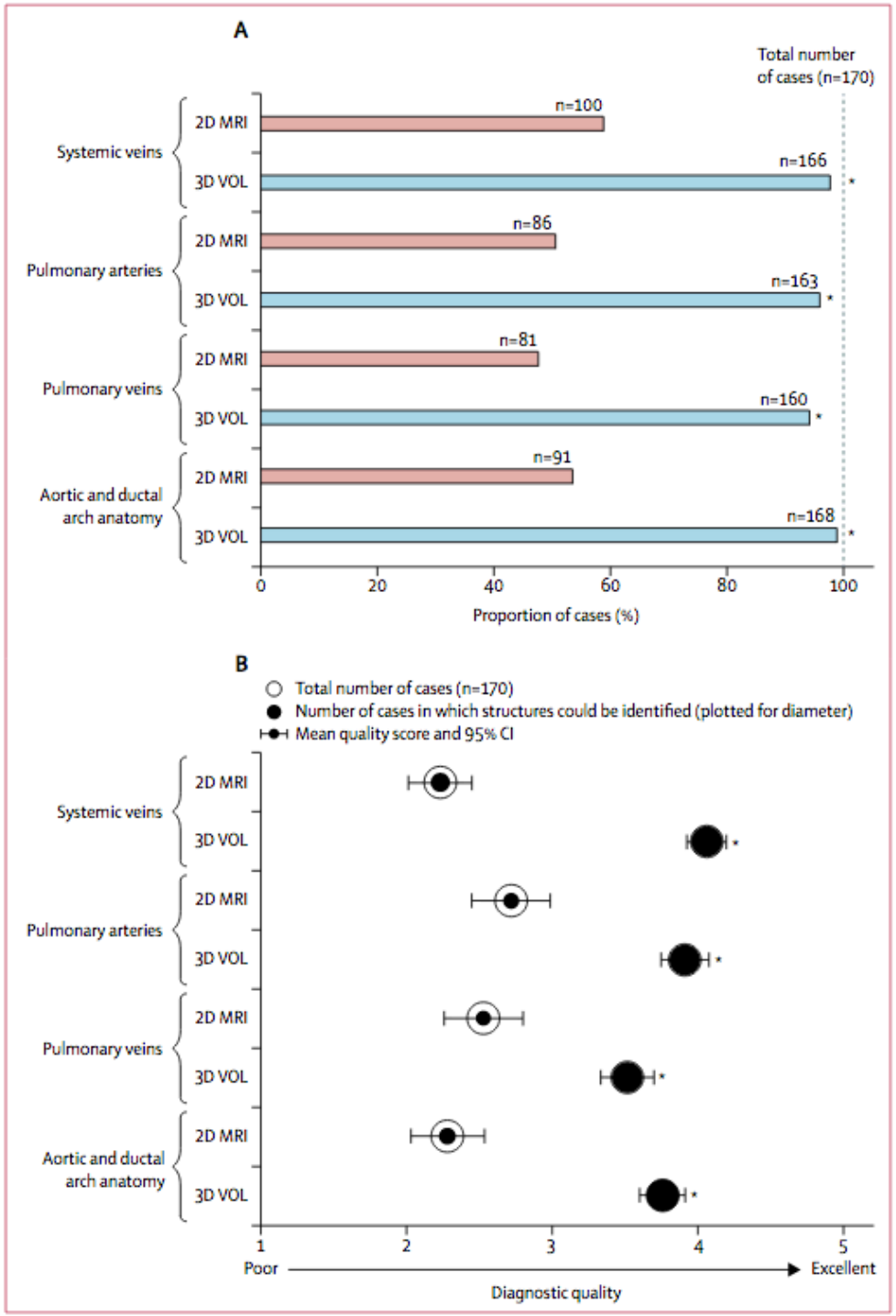


Figure 2: **Results of structured anatomical assessment from two independent observers, shown by anatomical category**

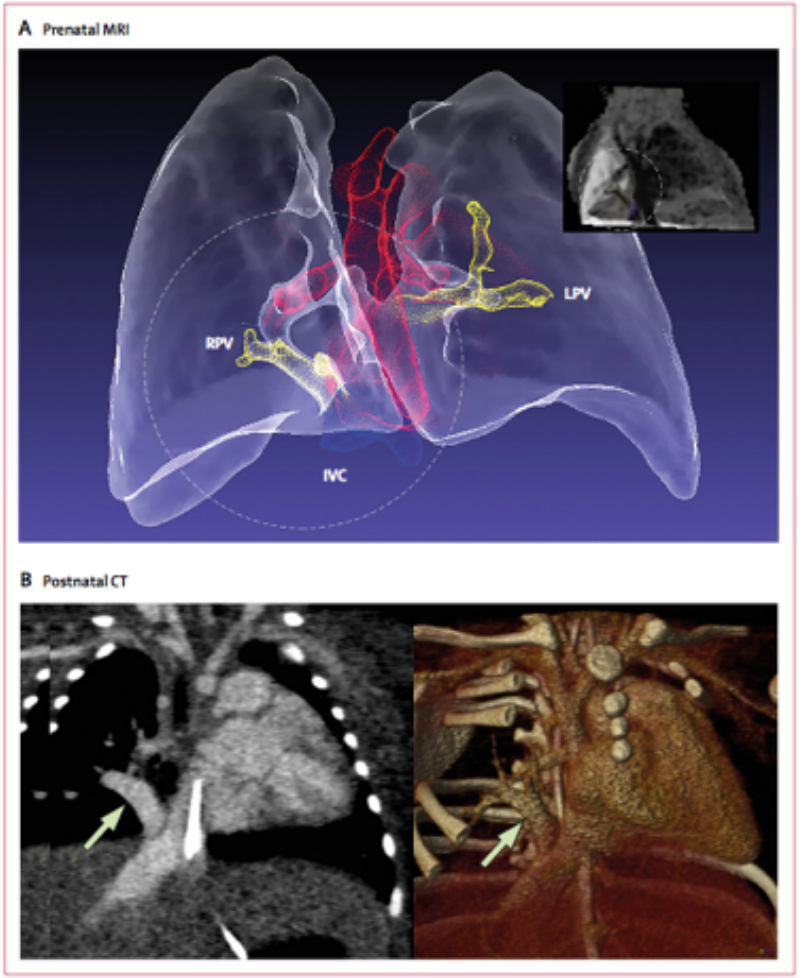


***Figure 4:* Example segmentation from motion-corrected 3D data, in a 33-week fetus referred because of abnormal right pulmonary veins on echocardiography**

(A) In this anterior projection of the lungs and major blood vessels, a single right pulmonary vein (RPV) can be seen draining anomalously to the inferior vena cava (IVC) in the circled area. A single left pulmonary vein (LPV) was also noted. Inset: minimum-intensity projection of the 0·7mm isotropic volume used to generate segmentation (RPV=yellow, IVC=blue). (B) All findings were confirmed postnatally by contrast-enhanced CT, with the anomalous vein indicated with an arrow. See video 4 for more detail.

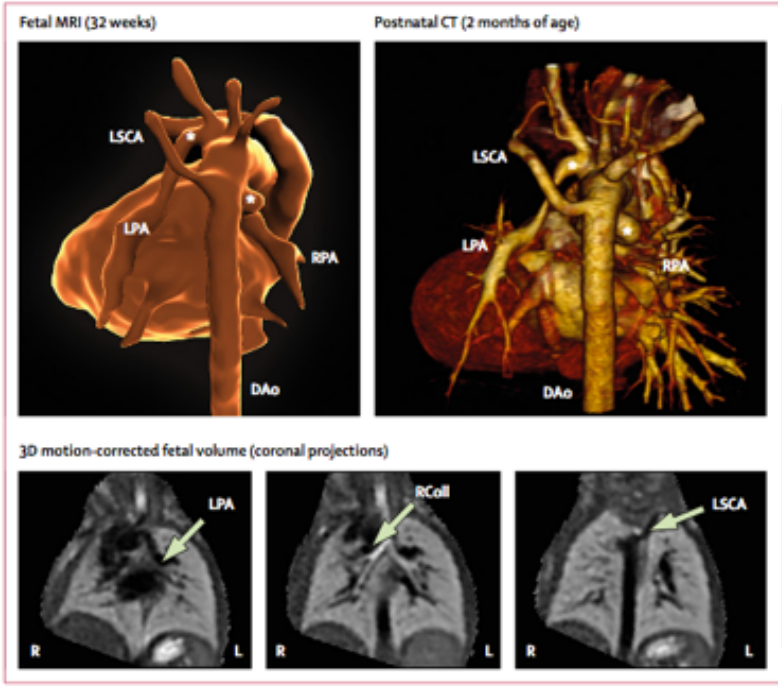


Figure 5: **Segmentation of a fetal heart from 3D data at 32 weeks in a fetus with pulmonary atresia and ventricular septal defect, right aortic arch, and disconnected pulmonary arteries**
Fetal MRI showed two large collateral arteries (asterisks): the left pulmonary artery (LPA) was supplied by a large collateral vessel originating close to the origin of the left common carotid artery, with the right pulmonary artery (RPA) supplied by a tortuous collateral or arterial duct from the underside of the aortic arch. The left subclavian artery (LSCA) was also noted to be aberrant. All findings were confirmed with postnatal CT at 2 months (right panel). The bottom panel shows three coronal planes of the original 3D motion-corrected fetal data. These images were used for pre-birth surgical planning and parental counselling. DAo=descending aorta. RColl=right collateral.

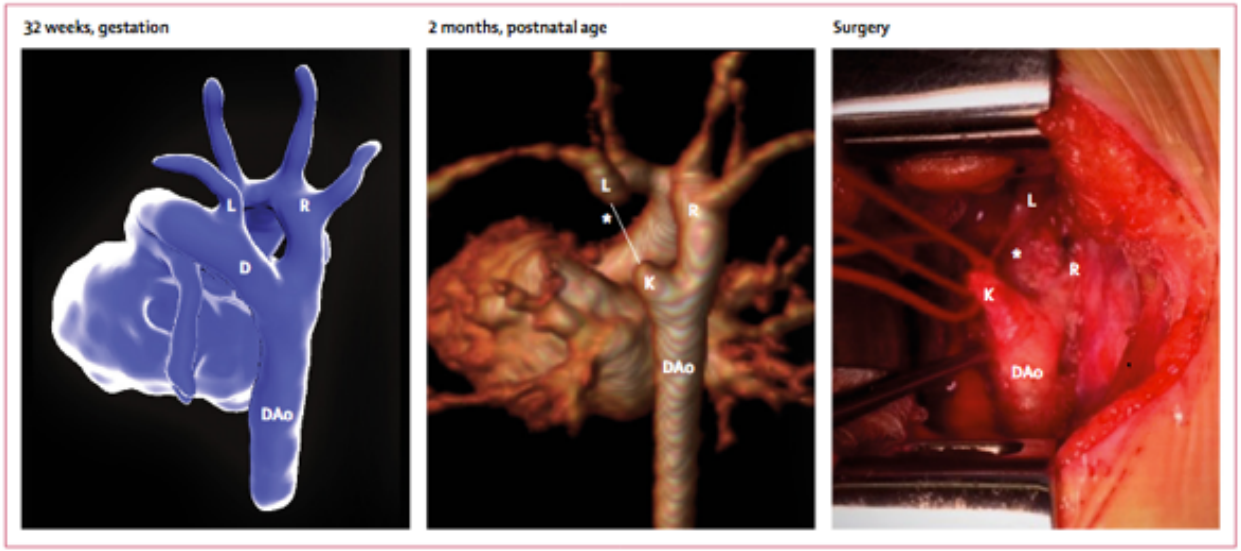


Figure 3: **Motion-corrected MRI data from a fetus with double aortic arch at 32 weeks**
Shown are the descending aorta (DAo), arterial duct (D), and left (L) and right (R) aortic arches. At 2 months postnatal age, contrast-enhanced MRI could show a right-sided arch (middle panel); however, a ligamentous remnant of the left arch was predicted on the basis of the fetal MRI findings (asterisk); this finding was confirmed at surgery (right panel). The distal remnant of the arterial duct—analogous to the diverticulum of Kommerell—is also seen (K). See video 3 for more detail.

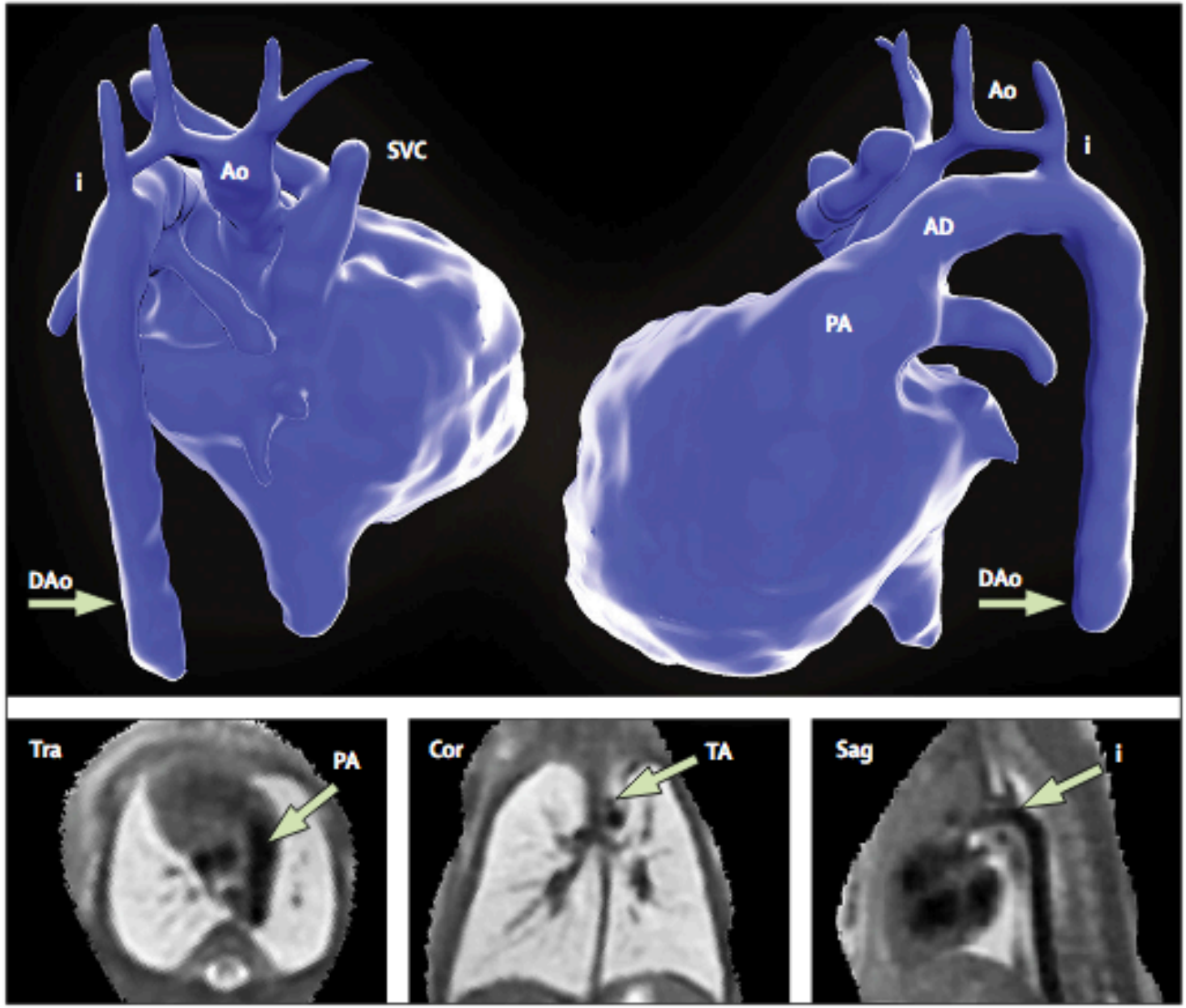


Figure 6: **Segmentation of motion-corrected MRI data of a fetus with suspected coarctation of the aorta at 33 weeks' gestation**

Posterior projection (top left) and left lateral projection (top right) are shown. The aorta (Ao), arterial duct (AD), descending aorta (DAo), aortic isthmus (i), and superior vena cava (SVC) are labelled. Coarctation was confirmed after birth and treated surgically. The bottom panel shows planes from the reconstructed 3D dataset in a transverse (Tra), coronal (Cor), and sagittal (Sag) orientation. See video 2 for more detail. TA=transverse arch. PA=pulmonary artery.

Research in context

Evidence before this study

The antenatal diagnosis of congenital heart disease has become routine in the UK and many other countries with the use of ultrasound, both at 20-week screening scans and at specialist fetal cardiac centres. However, some important aspects of congenital heart disease remain difficult to diagnose with ultrasound, even in the hands of experts, with no reliable alternative. Although several exploratory studies have investigated the potential of two-dimensional (2D) fetal MRI for cardiac imaging, uncontrolled fetal motion during acquisition is consistently cited as a cause of poor reliability, particularly when examining the small, complex three-dimensional (3D) structures of the fetal cardiovascular system. A reliable alternative to ultrasound has thus remained elusive. However, recent innovations in post-hoc image processing algorithms, enabled by advances in modern graphical processing units, have shown promising early results in a research setting, using multiple overlapping 2D MRI images to generate navigable, high-resolution 3D volumes of the brain and thorax in healthy fetuses. This combination has yet to be explored in clinical practice.

Added value of this study

By combining standard 2D fetal MRI images with novel motion-corrected slice-volume registration software, we were able to generate a high-resolution, 3D volume of the fetal heart in 85 fetuses with known congenital heart disease. Accuracy of the 3D dataset was validated by comparison with measurements made with paired ultrasound data, with structured clinical analysis showing a significantly better ability to visualise the fetal vascular anatomy compared with source 2D MRI images. In ten fetuses, new anatomical features were described that had previously been undetected, all of which were confirmed postnatally.

Implications of all the available evidence

The combination of standard fetal MRI sequences with novel, open-source image processing techniques is a reliable and accurate means of generating detailed 3D imaging of the fetal heart. These methods require minimal additional infrastructure and offer a safe, powerful, and highly complementary adjunct to ultrasound in the diagnosis of congenital heart disease before birth.

The relationships between democratic experience, adult health, and cause-specific mortality in 170 countries between 1980 and 2016: an observational analysis

Summary

Background Previous analyses of democracy and population health have focused on broad measures, such as life expectancy at birth and child and infant mortality, and have shown some contradictory results. We used a panel of data spanning 170 countries to assess the association between democracy and cause-specific mortality and explore the pathways connecting democratic rule to health gains.

Methods We extracted cause-specific mortality and HIV-free life expectancy estimates from the Global Burden of Diseases, Injuries, and Risk Factors Study 2016 and information on regime type from the Varieties of Democracy project. These data cover 170 countries and 46 years. From the Financing Global Health database, we extracted gross domestic product (GDP) per capita, also covering 46 years, and Development Assistance for Health estimates starting from 1990 and domestic health spending estimates starting from 1995. We used a diverse set of empirical methods—synthetic control, within-country variance decomposition, structural equation models, and fixed-effects regression—which together provide a robust analysis of the association between democratisation and population health.

Findings HIV-free life expectancy at age 15 years improved significantly during the study period (1970–2015) in countries after they transitioned to democracy, on average by 3% after 10 years. Democratic experience explains 22·27% of the variance in mortality within a country from cardiovascular diseases, 16·53% for tuberculosis, and 17·78% for transport injuries, and a smaller percentage for other diseases included in the study. For cardiovascular diseases, transport injuries, cancers, cirrhosis, and other non-communicable diseases, democratic experience explains more of the variation in mortality than GDP. Over the past 20 years, the average country's increase in democratic experience had direct and indirect effects on reducing mortality from cardiovascular disease (–9·64%, 95% CI –6·38 to –12·90), other non-communicable diseases (–9·14%, –4·26 to –14·02), and tuberculosis (–8·93%, –2·08 to –15·77). Increases in a country's democratic experience were not correlated with GDP per capita between 1995 and 2015 (ρ=–0·1036; p=0·1826), but were correlated with declines in mortality from cardiovascular disease (ρ=–0·3873; p<0·0001) and increases in government health spending (ρ=0·4002; p<0·0001). Removal of free and fair elections from the democratic experience variable resulted in loss of association with age-standardised mortality from non-communicable diseases and injuries.

Interpretation When enforced by free and fair elections, democracies are more likely than autocracies to lead to health gains for causes of mortality (eg, cardiovascular diseases and transport injuries) that have not been heavily targeted by foreign aid and require health-care delivery infrastructure. International health agencies and donors might increasingly need to consider the implications of regime type in their efforts to maximise health gains, particularly in the context of ageing populations and the growing burden of non-communicable diseases.

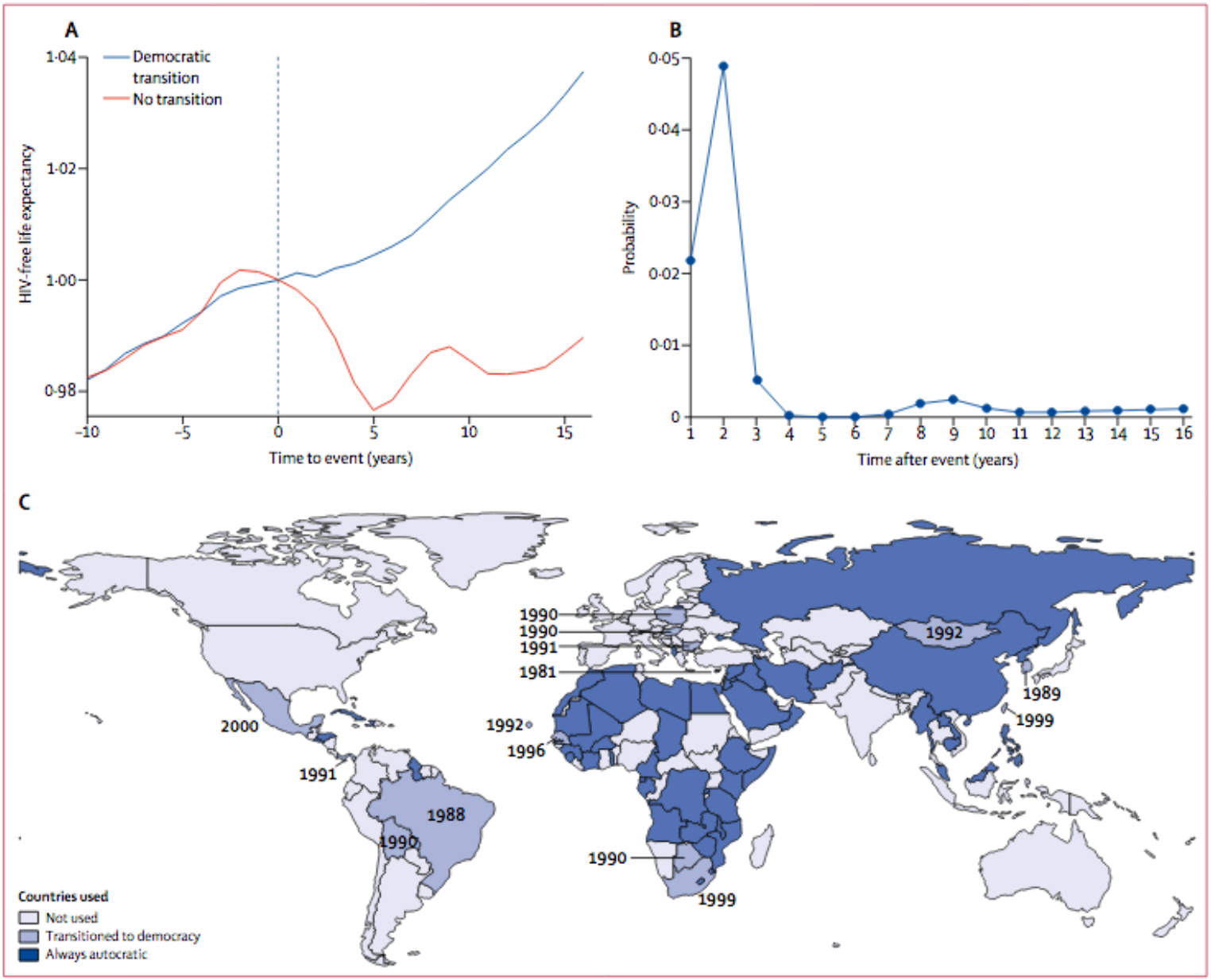


Figure 1: **The average effect of democratic transition on HIV-free life expectancy at age 15 years**

(A) The average effect on HIV-free life expectancy due to a democratic transition over 15 years. The blue line represents the normalised life expectancy in the 15 countries that underwent a democratic transition. The red line represents the normalised life expectancy in the corresponding synthetic countries that did not undergo a democratic transition. Year 0 is when the transition took place. Divergence after year 0 reflects the estimated average effect of democratic transitions. Life expectancy normalised to 1 in year 0. (B) The results of an empirical permutation test to determine if countries randomly might experience this improvement in HIV-free life expectancy. A low probability indicates that this improvement in life expectancy is unlikely to have happened by chance. (C) Democratising countries used in the synthetic control analysis are marked in blue, with year of transition noted. Continuously autocratic countries are in navy and countries that previously democratised or reverted back to autocracy are in light blue.

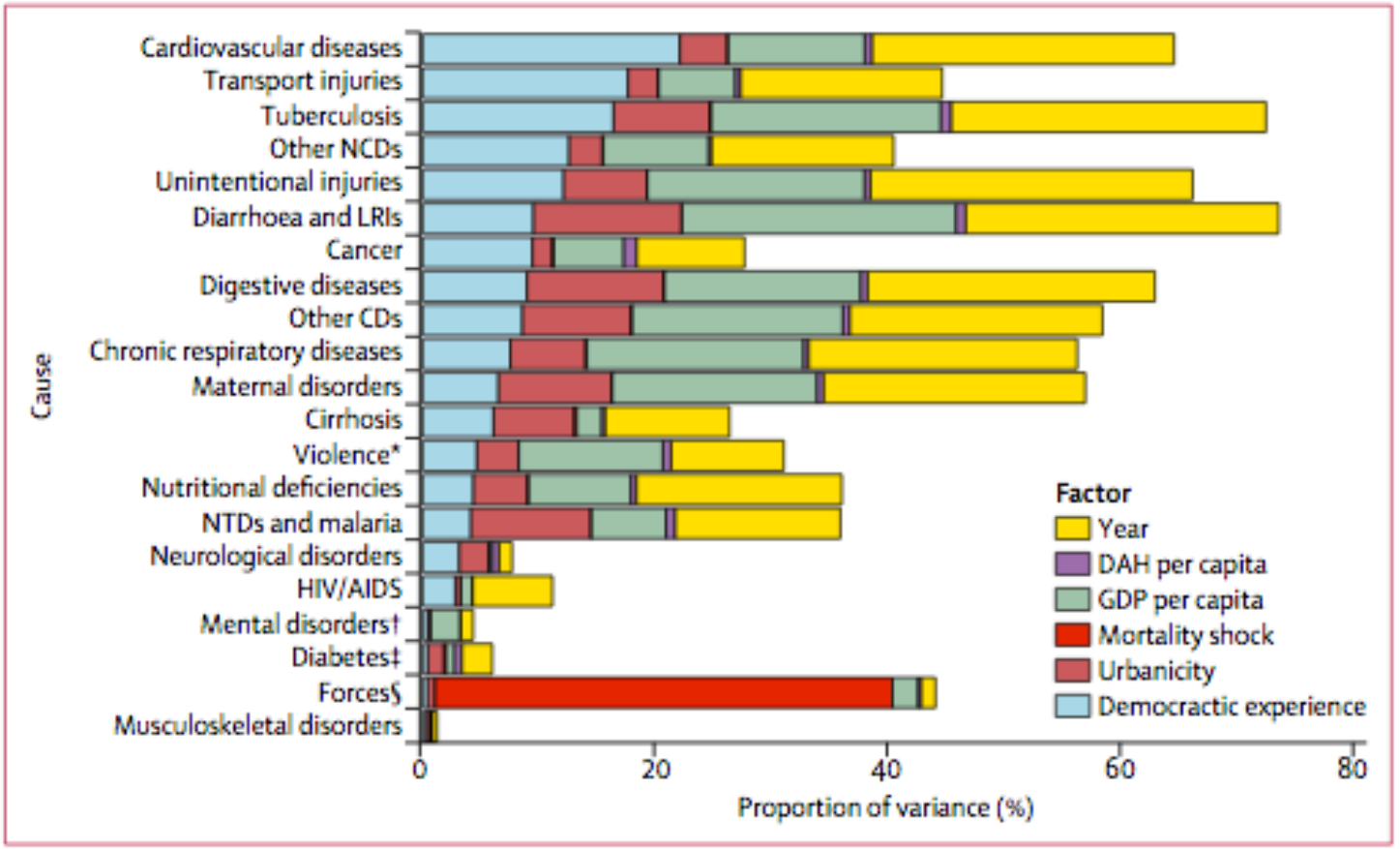


Figure 2: **Changes in mortality due to democracy and other determinants of health**

The proportion of variance in Global Burden of Disease Level 2 cause-specific, age-standardised mortality explained by democracy and other determinants of health such as gross domestic product (GDP) per capita, urbanicity, development assistance for health (DAH), and mortality shocks such as war. The sum of the variance explained by each variable is the r^2, which is the share of the variance of mortality explained by the model. NCDs=non-communicable diseases. LRIs=lower respiratory and other common infectious diseases. CDs=communicable diseases. NTDs=neglected tropical diseases. *Includes self-harm and interpersonal violence. †Includes substance use disorders. ‡Includes diabetes, urogenital, blood, and endocrine diseases. §Includes forces of nature, conflict, terrorism, and state violence.

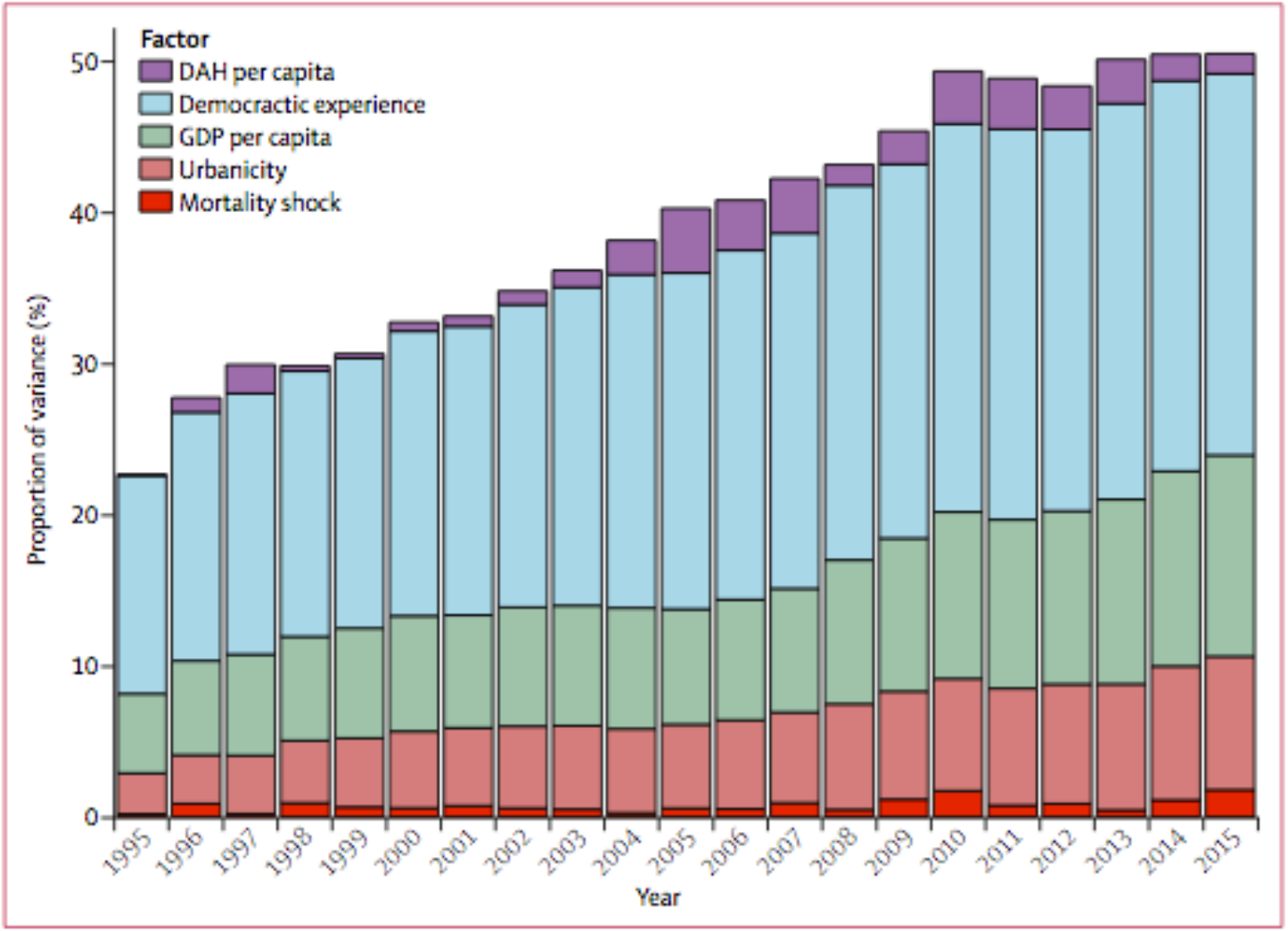


Figure 3: **Changes in cardiovascular disease across time**

The proportion of explained variance in age-standardised cardiovascular disease death rates across 188 countries from 1995 to 2015. DAH=development assistance for health. GDP=gross domestic product.

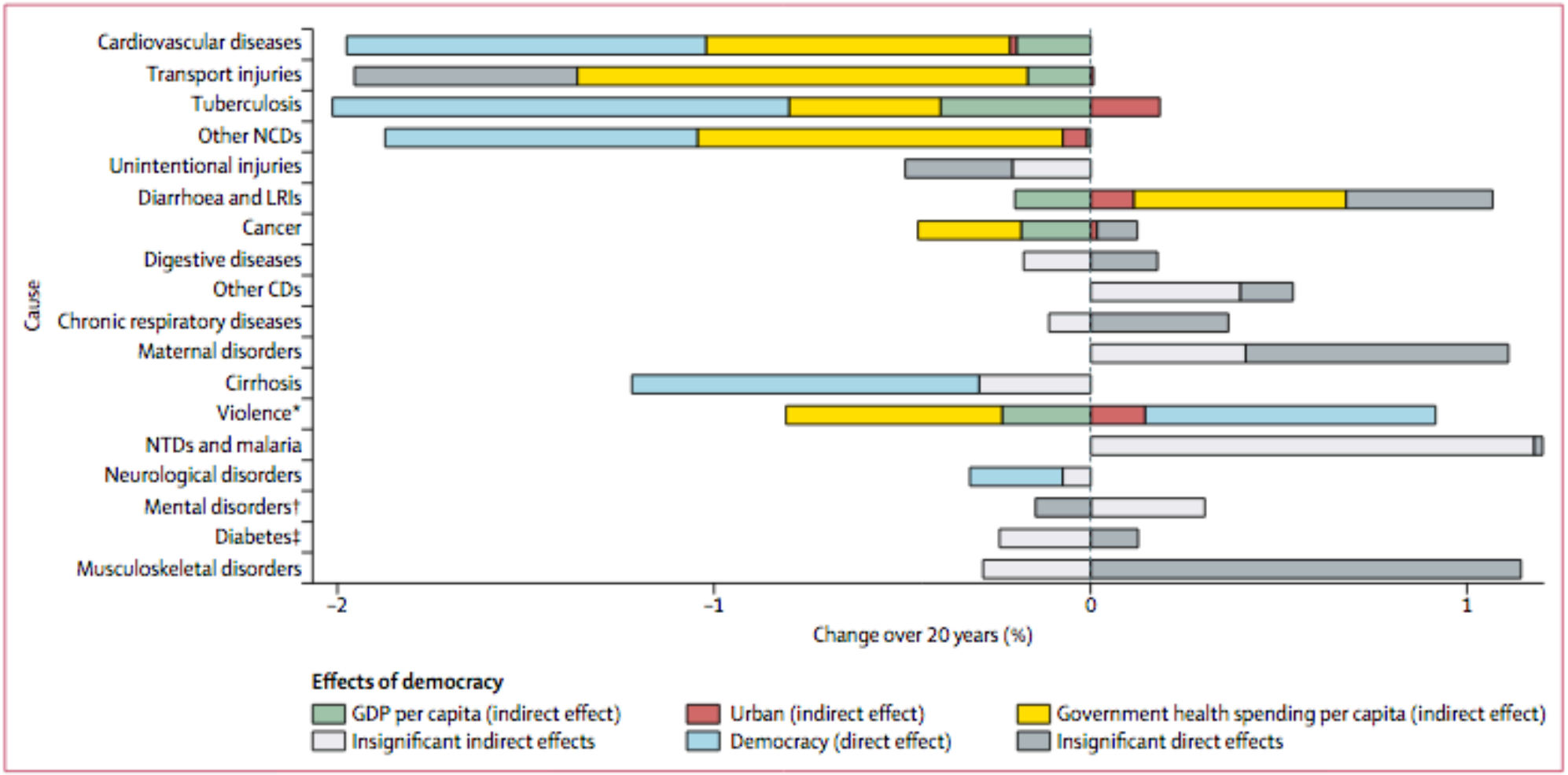


***Figure 4*: Long-term effect of democracy on country disease burden**

The estimated direct and indirect long-term effects of democracy on health from a structural equation model. The blue bars show the direct effect of democratic change on changes in health. The green, red, and yellow bars show the indirect effects of democratic change on changes in health due to resulting changes in gross domestic product (GDP) per capita, urbanicity, and government health expenditure as source. All changes are from 1995 to 2015. Results that were not statistically significant are shown in grey. HIV/AIDS and forces were omitted because of distortion of the x-axis of the graph, such that the other causes were not visible; all results are available in the appendix. NCDs=non-communicable diseases. LRIs=lower respiratory and other common infectious diseases. CDs=communicable diseases. NTDs=neglected tropical diseases. *Includes self-harm and interpersonal violence. †Includes substance use disorders. ‡Includes diabetes, urogenital, blood, and endocrine diseases.

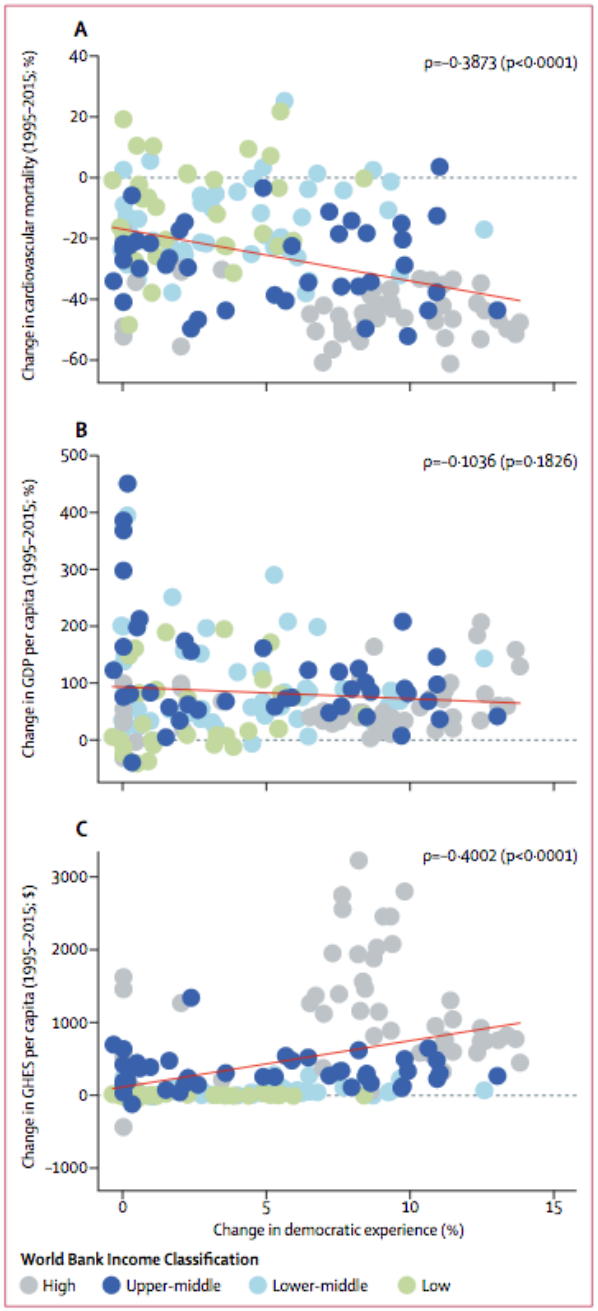


Figure 5: **Cross-country changes in democracy, cardiovascular disease, and health spending**
The relationships between changes in democracy and cardiovascular age-standardised death rates (A); changes in democracy and growth in gross domestic product (GDP) per person (B); changes in democracy and government health expenditure (GHES) as source (C). All panels show changes from 1995 to 2015. The red line is a linear fit through the bivariate relationship.

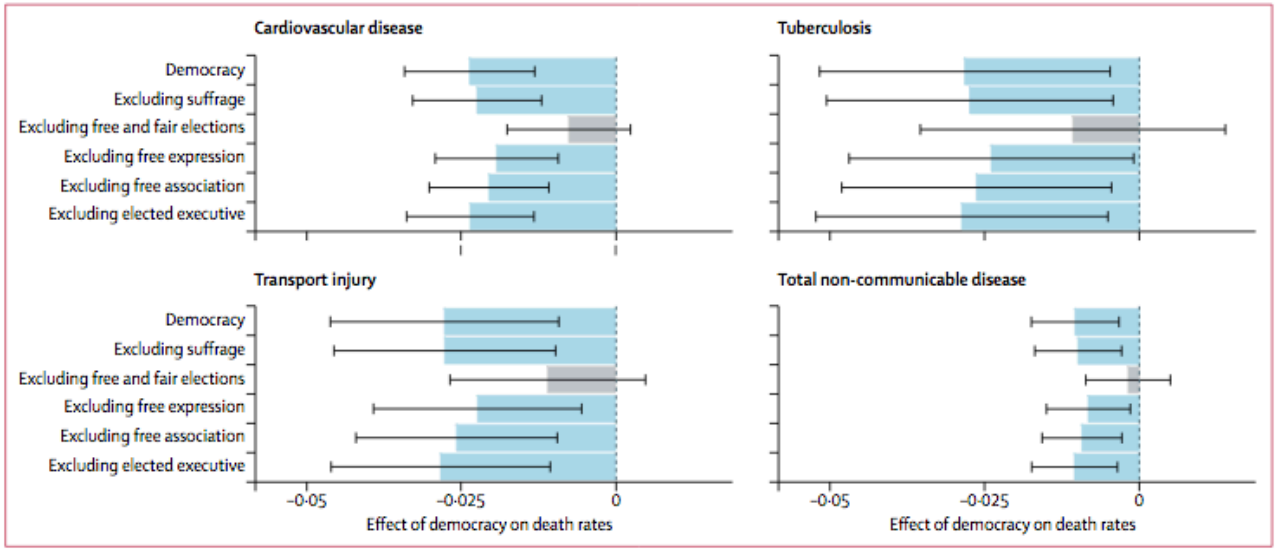


Figure 6: **Critical component of democracy for four causes**
The average effect of democracy on non-communicable disease, cardiovascular disease, tuberculosis, and transport injury age-standardised death rates using the leave-one-out strategy. The effect is measured as the percent change in death rates associated with a one-unit increase in democratic experience. The black lines indicate the 99% CI on the effect size. Blue bars indicate significant effects on health, whereas grey bars are insignificant (significance determined at p=0·01).

Research in context

Evidence before this study

Over the past 25 years, various cross-country studies have assessed whether democracy is related to improved population health. Almost all of these studies have limited their assessments to democracy's effect on mortality of infants and children younger than 5 years, or life expectancy at birth, primarily reflecting gains in child and infant health. The results of these studies largely support the notion that democracy is associated with better population health, but at least four studies have found no link between democracy and infant or child mortality. Critics of the methodological shortcomings of these democracy and health studies attribute the improved health outcomes to factors such as institutional capacity and country income, rather than regime type. Most studies of the allocation of development assistance to national governments have found that it remains uncorrelated with democratic governance and, in some instances, negatively correlated.

To identify studies that have investigated the relationship between democracy and population health, we searched, without date restrictions, Scopus, Google Scholar, and PubMed for all articles with "democracy" and "health" or "mortality" in the abstract or title. To the best of our knowledge, no other studies comprehensively assess the global effect of democratic governance on non-communicable diseases and injuries—health concerns that represent an increasing share of the disease burden in low-income and middle-income countries.

Added value of this study

This study brings updated, expanded, and improved data sources, a diverse set of methodologies, and a focus on non-communicable diseases, injuries, and adult health to the exploration of the relationship between democracy and health. To characterise the effect of democratic experience on country health burden, we leveraged estimates from the Global Burden of Diseases, Injuries, and Risk Factors Study (GBD) 2016, the University of Gothenburg's Varieties of Democracy project, and the Financing Global Health database. These data capture detailed political, economic, and population health information and enable us to construct a panel of data spanning 170 countries to assess the role of democracy, and its core components, on HIV-free life expectancy at age 15 years, cause-specific mortality, and health spending, and on the pathways connecting democratic rule to cause-specific health gains. In addition to broad population health measures, we used disaggregated cause-specific mortality estimates from GBD 2016.

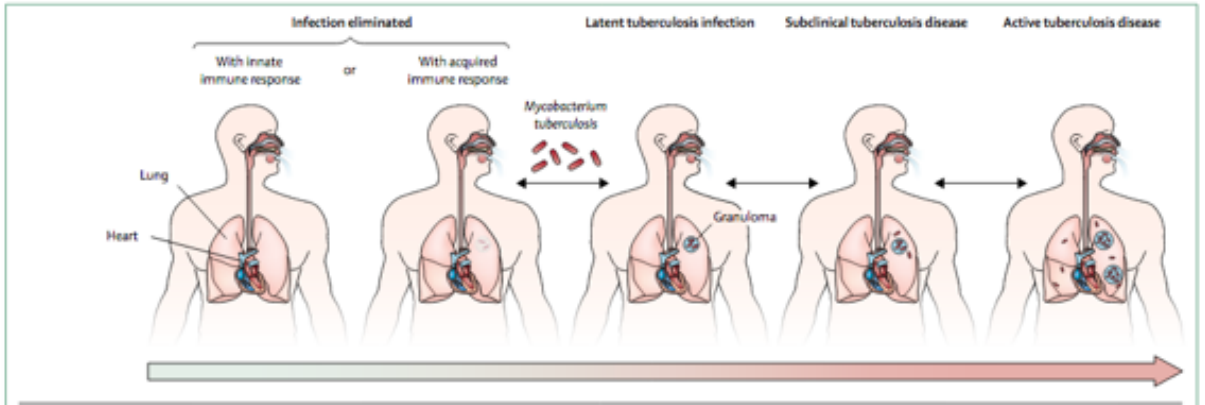
Implications of all the available evidence

Democratic governments have a greater incentive to improve adult health and reduce mortality from non-communicable diseases and injuries than their autocratic counterparts. These results are consistent with the perception that democracies are more apt than autocracies to implement proven treatment and prevention interventions for causes not heavily targeted by foreign aid and requiring health-care delivery infrastructure. Regular free and fair elections appear important for improving adult health and non-communicable disease outcomes, most likely by increasing government accountability. This study suggests that democratic institutions and processes might help to enhance and expand the effectiveness of global health programmes and initiatives, especially with regard to non-communicable diseases, injuries, and adult health.

Tuberculosis

Jennifer Furin, Helen Cox, Madhukar Pai

Tuberculosis remains the leading cause of death from an infectious disease among adults worldwide, with more than 10 million people becoming newly sick from tuberculosis each year. Advances in diagnosis, including the use of rapid molecular testing and whole-genome sequencing in both sputum and non-sputum samples, could change this situation. Although little has changed in the treatment of drug-susceptible tuberculosis, data on increased efficacy with new and repurposed drugs have led WHO to recommend all-oral therapy for drug-resistant tuberculosis for the first time ever in 2018. Studies have shown that shorter latent tuberculosis prevention regimens containing rifampicin or rifapentine are as effective as longer, isoniazid-based regimens, and there is a promising vaccine candidate to prevent the progression of infection to the disease. But new tools alone are not sufficient. Advances must be made in providing high-quality, people-centred care for tuberculosis. Renewed political will, coupled with improved access to quality care, could relegate the morbidity, mortality, and stigma long associated with tuberculosis, to the past.



TST	Negative	Positive	Positive	Positive	Usually positive
IGRA	Negative	Positive	Positive	Positive	Usually positive
Culture	Negative	Negative	Negative	Intermittently positive	Positive
Sputum smear	Negative	Negative	Negative	Usually negative	Positive or negative
Infectious	No	No	No	Sporadically	Yes
Symptoms	None	None	None	Mild or none	Mild to severe
Preferred treatment	None	None	Preventive therapy	Multidrug therapy	Multidrug therapy

Figure 1: **Spectrum of tuberculosis infection and disease**
Reproduced from Pai et al,[1] by permission of Springer Nature. IGRA=interferon-γ release assay. TST=tuberculin skin test.

	Class and mechanism of action	Phase completed and regulatory approval	Summary of findings	Adverse events	Drug–drug interactions and overlapping toxicities	Access and pricing[75]	Ongoing trials[76]
Bedaquiline[77–79]	Diarylquinoline; inhibits mycobacterial ATP synthase	Phase 2b US FDA, EMA, SAHPRA, multiple other countries	Significantly faster time to culture conversion; significantly higher culture conversion; significantly improved treatment outcomes when compared with placebo	QTc prolongation (moderate), hepatitis	Cannot use with efavirenz; use with protease inhibitors results in increased bedaquiline concentration but clinical significance not clear; cannot use with rifampicin; caution when used with other QTc prolonging agents	Available to <20% of individuals that need it; US$400 for a 6-month course via GDF	endTB (NCT02754765), TB PRACETCAL (NCT02589782), NiX-TB (NCT02333799), STREAM 2 (NCT02409290), NeXT (NCT02454205), ZeNix (NCT03086486), Janssen C211 (NCT02354014), ACTG 5343 (NCT02583048), Janssen Japan Trial (NCT02365623), SimpliciTB (NCT03338621), P11018 (NCT02906007)
Delamanid[80–85]	Nitroimidazole; inhibits mycolic acid synthesis	Phase 3 EMA, Japanese Regulatory Authority	Faster time to culture conversion compared with placebo; no differences in final outcomes but study did not have statistical power for detection	QTc prolongation (mild), generally well tolerated	No clinically significant drug–drug interactions	Available to <5% of individuals that need it; $1700 for a 6-month course from GDF	endTB, MDR-END (NCT02619994), ACTG 5453, Otsuka 213 (NCT01424670), Otsuka 233 (NCT01859923), Otsuka 232 (NCT01856634), IMPAACT 2005 (NCT03141060)
Pretomanid[86–88]	Nitroimidazole; inhibits mycolic acid synthesis, generates mycobacterial nitrogen oxide	Phase 2b; currently undergoing regulatory review	Has only been tested in combination regimens and not as a single agent	Hepatitis, animal studies show ocular and reproductive toxic events	No clinically significant drug–drug interactions	Not available	SimpliciTB, NiX-TB, TB PRACTECAL, ZeNix
Linezolid[89–111]	Oxazolidinone; inhibits mycobacterial protein synthesis	Phase 2b, phase 3 (non-placebo controlled); no registered indication for tuberculosis	Improved outcomes (in delayed-start trial and non-placebo controlled trials), significantly higher rates of culture conversion, and faster times to culture conversion in people who received linezolid at the start of treatment compared with those who had a delayed start	Toxic effects on bone marrow, peripheral neuritis, optic neuritis	Caution when used in patients on zidovudine due to overlapping toxic effects on bone marrow; caution when given with other drugs that are associated with peripheral neuropathy (eg, isoniazid); use with caution when given with other drugs associated with optic neuritis or neuropathy (eg, ethambutol)	$1·30 per tablet from GDF	endTB, NiX-TB, TB PRACTECAL, ZeNix, NeXT, MDR-END, MDR-PK2 (NCT02619994)
Sutezolid[93,94]	Oxazolidinone; inhibits mycobacterial protein synthesis	Phase 2a	Significant 14-day early bactericidal activity	No severe adverse events reported in 14-day early bactericidal activity trial	Not available	Not available	Obtained by the Medicines Patent Pool for further testing
Clofazimine[95,96]	Inhibits mycobacterial DNA synthesis, increases activity of mycobacterial phospholipase A2	Phase 3 (non-placebo controlled)	Improved treatment outcomes, significantly faster time to culture conversion, and higher rates of culture conversion compared with people that did not receive clofazimine	Skin discoloration, QTc prolongation	Caution when used with other QTc prolonging agents	$1·00 per tablet from GDF	endTB, STREAM 2, TB PRACTECAL
Carbapenems (imipenem-cilastatin, meropenem)[97]	β-lactams; inhibit mycobacterial cell wall synthesis	Phase 2a	Significant 14-day early bactericidal activity	Seizures, rash, hepatitis	Cannot use with penicillin allergy; must be given with clavulanic acid to be effective in tuberculosis; must be given intravenously	$3·10 for one 500 mg vial of imipenem; $0·14 for one 125 mg tablet of clavulanic acid (only available in combination with 875 mg amoxicillin)	None known

	Drugs	Comments
Group A	Levofloxacin or moxifloxacin; bedaquiline; linezolid	Include all three medicines (unless they cannot be used)
Group B	Clofazimine; cycloserine or terizidone	Add both medicines (unless they cannot be used)
Group C	Ethambutol; delamanid; pyrazinamde; imipenem-cilastatin or meropenem (both must be given with clavulanic acid); amikacin or streptomycin; ethionamide or prothionamide; para-aminosalicylic acid	Add to complete a four-drug to five-drug regimen and when medicines from groups A and B cannot be used

Table 2: **2018 WHO grouping of medications for second-line drug-resistant tuberculosis**[130]

	Description	Examples
Holistic care	Care that sees the patient as a whole and addresses multiple individual needs	Effective and integrated care of comorbidities such as diabetes, HIV, and harmful substance use[152]
Individualised care	Care that reflects each patient's needs, preferences, and concerns	The provision of individualised treatment for rifampicin-resistant tuberculosis based on detailed drug susceptibility testing[153]
Empowering care	Care that recognises patients as active consumers	Mechanisms for supporting self-administration of treatment[154]
Respectful care	Care that encourages informed decision making and self-determination	Patient choice in regimen composition is based on understanding of efficacy and adverse events[155]

Table 3: **Key attributes of patient-centred care for tuberculosis**[156]

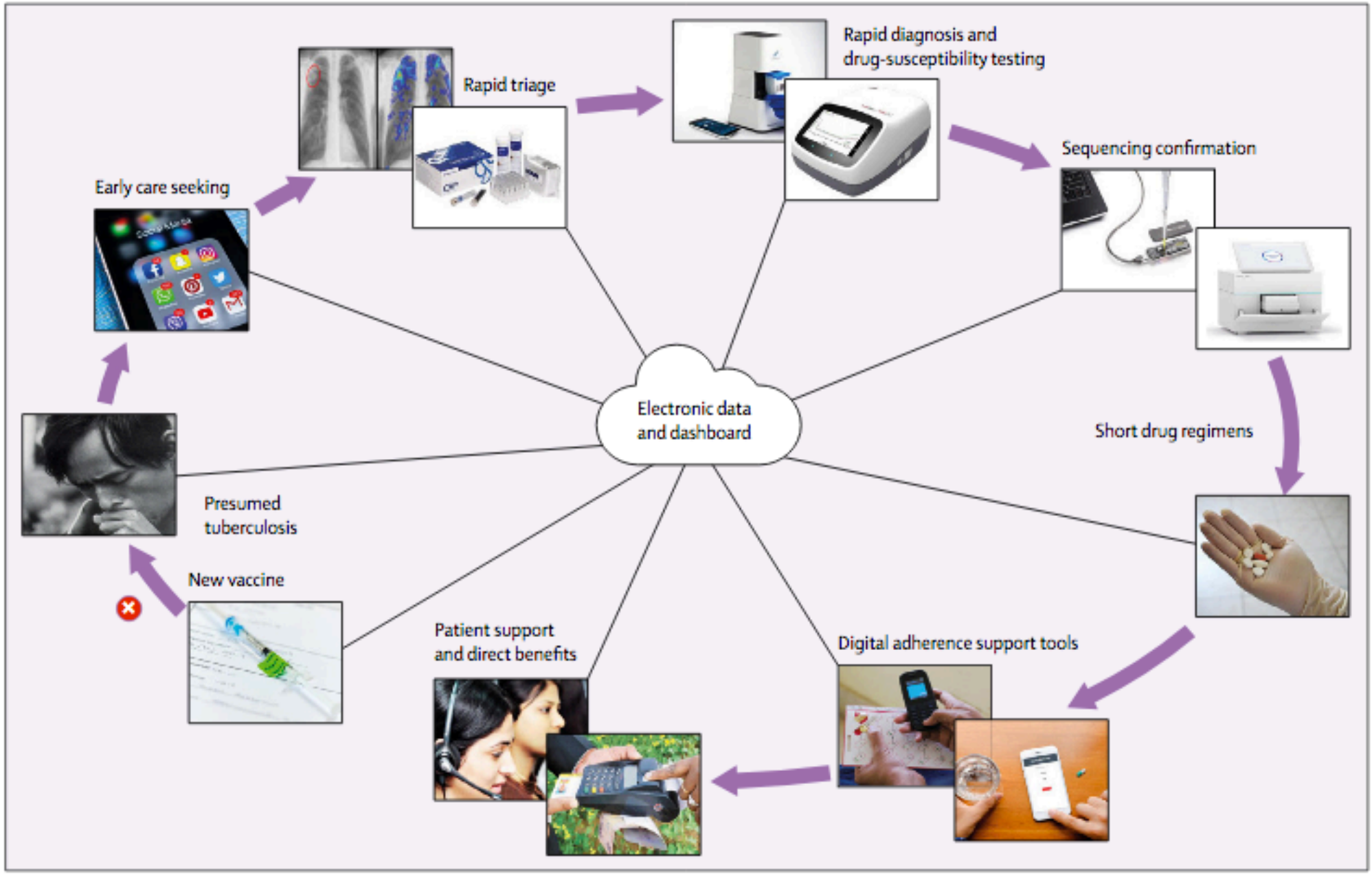


Figure 2: Schematic for a modern tuberculosis care delivery system

Tetanus

Lam Minh Yen, C Louise Thwaites

Tetanus is a vaccine-preventable disease that still commonly occurs in many low-income and middle-income countries, although it is rare in high-income countries. The disease is caused by the toxin of the bacterium *Clostridium tetani* and is characterised by muscle spasms and autonomic nervous system dysfunction. Global vaccination initiatives have had considerable success but they continue to face many challenges. Treatment for tetanus aims to control spasms and reduce cardiovascular instability, and consists of wound debridement, antitoxin, antibiotics, and supportive care. Recent research has focused on intravenous magnesium sulphate and intrathecal antitoxin administration as methods of spasm control that can avoid the need for ventilatory support. Nevertheless, without access to mechanical ventilation, mortality from tetanus remains high. Even with such care, patients require several weeks of hospitalisation and are vulnerable to secondary problems, such as hospital-acquired infections.

Tetanus (von altgriechisch τέτανος tetanos, deutsch ‚Spannung, Krampf'), auch Wundstarrkrampf genannt, ist eine häufig tödlich verlaufende Infektionskrankheit, welche die muskelsteuernden Nervenzellen befällt und durch das Bakterium Clostridium tetani ausgelöst wird. Die resistenten Sporen des Bakteriums kommen nahezu überall vor, auch im Straßenstaub oder in der Gartenerde. Die Infektion erfolgt durch das Eindringen der Sporen in Wunden. Unter anaeroben Bedingungen, also unter Sauerstoff-Abwesenheit, vermehrt sich das Bakterium und sondert Giftstoffe (Toxine) ab. Das proteolytische Toxin Tetanospasmin schädigt die muskelsteuernden Nervenzellen und verursacht dadurch die typischen Muskelkrämpfe. Das Toxin Tetanolysin ist herzschädigend.

***Panel 1:* Case definitions for maternal and neonatal tetanus[6]**

Maternal tetanus
Tetanus during pregnancy or within 6 weeks of the end of pregnancy (birth, miscarriage, or abortion)

Neonatal tetanus: suspected
Any neonatal death between 3 days and 28 days of age in which the cause of death is unknown; or any neonate reported as having neonatal tetanus between 3 days and 28 days of age, but for whom the disease is not investigated

Neonatal tetanus: confirmed
Any neonate with a normal ability to suck and cry during the first 2 days of life and who, between 3 days and 28 days of age, cannot suck normally, and becomes stiff or has spasms (ie, jerking of the muscles)

Panel 2: Ablett classification of tetanus severity[96]

Grade 1: mild

- Mild to moderate trismus
- Generalised spasticity
- No respiratory compromise
- No spasms
- Little or no dysphagia

Grade 2: moderate

- Moderate trismus
- Marked rigidity
- Mild to moderate but short spasms
- Moderate respiratory compromise with an increased respiratory rate (>30 breaths per min)
- Mild dysphagia

Grade 3: severe

- Severe trismus
- Generalised spasticity
- Reflex prolonged spasms
- Increased respiratory rate (>40 breaths per min)
- Apnoeic spells
- Severe dysphagia
- Tachycardia (>120 beats per min)

Grade 4: very severe

- Clinical features of grade 3 tetanus
- Violent autonomic disturbances involving the cardiovascular system
- Severe hypertension and tachycardia alternating with relative hypotension and bradycardia (either of which might be persistent)

	Interventions
General	
Wound	Wound debridement (U), antitoxin (L), intravenous immunoglobulin (U), antibiotics (L)
Circulatory	
Labile blood pressure and tachycardia	Sedation (VL), analgesia (VL), magnesium (L), calcium antagonists or β blockers (U), clonidine (U), opioids (VL)
Hypotension	Inotropes (U)
Thrombosis or embolism	Thromboprophylaxis (U)
Muscular	
Spasm	Benzodiazepines (L), magnesium (H), baclofen (L), botulinum toxin (VL), non-depolarising neuromuscular blocking agents (U)
Muscle wasting	Nutrition (U), physiotherapy (U)
Contractures	Nursing care (U), physiotherapy (U)
Respiratory	
Laryngeal spasm	Tracheostomy (U)
Increased secretions	Nursing care (U)
Aspiration	Antibiotics (U), nasogastric feeding tube (U)
Renal	
Acute kidney injury	Fluids (U), renal replacement therapy (U)
Rhabdomyolysis	Fluids (U), renal replacement therapy (U)
Urinary retention	Nursing (U)
Gastrointestinal	
Dysphagia	Nasogastric feeding (U)
Gastrointestinal stasis	Motility agents (U)
Gastrointestinal bleeding	Prophylaxis (U)
Other	
Hospital-acquired infection	Hand washing (VL)
Pressure ulceration	Nursing care (U)

Evidence for the efficacy of interventions is graded with the Grading of Recommendations Assessment, Development, and Evaluation tools and classified as high, low, or very low quality.[101] Interventions with no published supporting data but that are often applied and thought to be appropriate on the basis of expert opinion are ungraded. H=high. L=low. VL=very low. U=ungraded.

Table: **Clinical features, complications, and management of tetanus**

Panel 3: Presenting features on admission to hospital for non-neonatal tetanus

- Trismus (93–98%)
- Generalised muscle tension (94–95%)
- Muscle stiffness (96%)
- Dysphagia (83%)
- Dyspnoea (7%)
- Muscle spasms (46–80%)
- Body temperature >38·4°C (76%)
- Pulse ≥120 beats per min (34%)

Data are adapted from Tanon and colleagues[32] (n=499) and Thwaites and colleagues[34] (n=2421). The incidence of each feature is shown in parentheses.



Figure: Typical appearance of tetanus with trismus

	Interventions
General	
Wound	Wound debridement (U), antitoxin (L), intravenous immunoglobulin (U), antibiotics (L)
Circulatory	
Labile blood pressure and tachycardia	Sedation (VL), analgesia (VL), magnesium (L), calcium antagonists or β blockers (U), clonidine (U), opioids (VL)
Hypotension	Inotropes (U)
Thrombosis or embolism	Thromboprophylaxis (U)
Muscular	
Spasm	Benzodiazepines (L), magnesium (H), baclofen (L), botulinum toxin (VL), non-depolarising neuromuscular blocking agents (U)
Muscle wasting	Nutrition (U), physiotherapy (U)
Contractures	Nursing care (U), physiotherapy (U)
Respiratory	
Laryngeal spasm	Tracheostomy (U)
Increased secretions	Nursing care (U)
Aspiration	Antibiotics (U), nasogastric feeding tube (U)
Renal	
Acute kidney injury	Fluids (U), renal replacement therapy (U)
Rhabdomyolysis	Fluids (U), renal replacement therapy (U)
Urinary retention	Nursing (U)
Gastrointestinal	
Dysphagia	Nasogastric feeding (U)
Gastrointestinal stasis	Motility agents (U)
Gastrointestinal bleeding	Prophylaxis (U)
Other	
Hospital-acquired infection	Hand washing (VL)
Pressure ulceration	Nursing care (U)

Evidence for the efficacy of interventions is graded with the Grading of Recommendations Assessment, Development, and Evaluation tools and classified as high, low, or very low quality.[101] Interventions with no published supporting data but that are often applied and thought to be appropriate on the basis of expert opinion are ungraded. H=high. L=low. VL=very low. U=ungraded.

Table: Clinical features, complications, and management of tetanus

Panel 4: Ongoing areas of research for tetanus

Human antitoxin

- Consensus on the optimal dose for treatment
- Consensus on the optimal dose for prophylaxis
- Consensus on the optimal route of administration for treatment (intrathecal, intravenous, or intramuscular)

Spasm control

- Alternatives to neuromuscular blockade, mechanical ventilation, and benzodiazepine administration for tetanus treatment

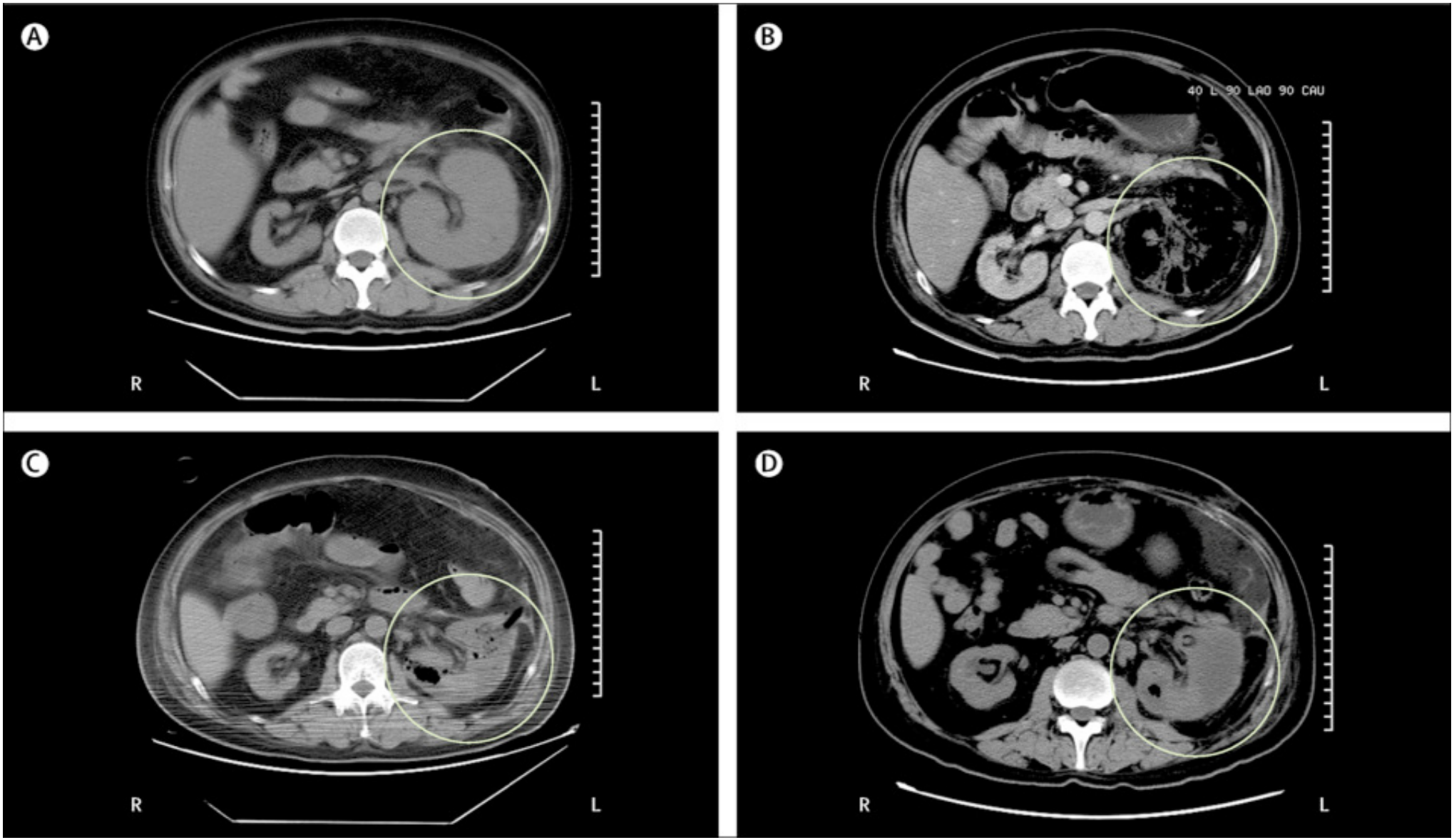
Autonomic nervous system dysfunction

- Identification of methods for sensitive and specific early detection



Conclusion

Tetanus is a severe disease that has high mortality in the absence of good intensive care treatment. Where intensive care is available, tetanus treatment is lengthy and costly. New and innovative interventions particularly suited to low-resource settings are needed. The disease cannot be eradicated, and continued efforts to strengthen and maintain vaccination programmes are required.



A size-altering kidney
Abdominal CT scan shows a diffusely swollen left kidney (A) and an enhanced CT scan shows the kidney expanded with gas (B). Repeated CT scans show decreases in the sizes of the left kidney (C and D).
Blood cultures + for gas-forming E. coli

A 54-Year-Old Man with Alcohol Withdrawal and Altered Mental Status

The patient was homeless but had recently been enrolled in an addiction treatment program in a residential clinical stabilization service. He reportedly left the program 4 days before admission to this hospital and then "blacked out" daily in tandem with drinking 0.5 to 1 gallon of vodka throughout the day. On the evening before admission, he decided to stop drinking alcohol. Approximately 10 hours later, he awoke on the ground without recollection of lying down; he had had vivid dreams and tremulousness and was worried that he may have had a seizure. He presented to the emergency department of this hospital.

On examination, the temperature was 36.7° C, the heart rate 108 beats per minute, the blood pressure 161/96 mm Hg, the respiratory rate 22 breaths per minute, and the oxygen saturation 98% while the patient was breathing ambient air. The weight was 55.4 kg, the height 142 cm, and the body-mass index (the weight in kilograms divided by the square of the height in meters) 27.5. The patient was described as restless, anxious, and flushed.

Folate, multivitamins, intravenous normal saline, thiamine, and lorazepam were administered during the next 10 hours. Phenobarbital was administered at a gradually tapering dose for management of alcohol withdrawal. On hospital day 5, the patient reported feeling anxious. That evening, a nurse found him to be acutely delirious, lethargic, and minimally responsive, even to sternal rub, just 1 hour after he had been awake and conversing; he had not left his room.

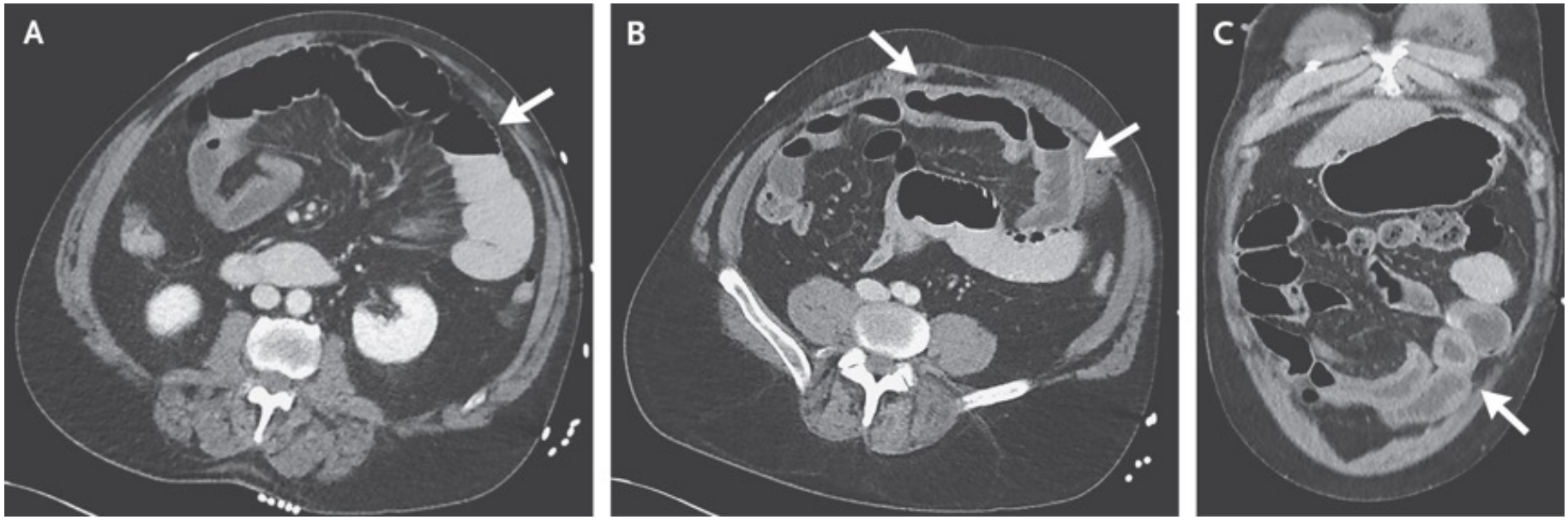
Variable	Reference Range, Adults†	On Evaluation, Hospital Day 1, 8 a.m.	On Admission, Hospital Day 1, 6 p.m.	Hospital Day 5, 7 p.m.	Hospital Day 6, Morning
Hemoglobin (g/dl)	13.5–17.5	15.9	13.3	15.6	15.6
Hematocrit (%)	41.0–53.0	47.4	39.1	45.4	44.7
White-cell count (per mm³)	4500–11,000	8390	8720	11,070	15,430
Differential count (%)					
Neutrophils	40–70	75.4	63.5	66.4	81.9
Lymphocytes	22–44	14.1	21.2	22.5	12.6
Monocytes	4–11	8.2	12.6	7.2	3.6
Eosinophils	0–8	0.5	1.4	1.1	0.1
Basophils	0–3	0.7	0.8	1.1	0.5
Immature granulocytes	0.0–0.9	1.1	0.5	1.7	1.3
Platelet count (per mm³)	150,000–400,000	504,000	360,000	436,000	508,000
Mean corpuscular volume (fl)	80.0–100.0	80.2	79.8	78.1	76.1
Sodium (mmol/liter)	135–145	138	140	139	140
Potassium (mmol/liter)	3.4–5.0	3.7	3.6	3.5	3.5
Chloride (mmol/liter)	100–108	98	102	101	104
Carbon dioxide (mmol/liter)	23–32	19	22	18	22
Urea nitrogen (mg/dl)	8–25	17	13	14	12
Creatinine (mg/dl)	0.60–1.50	0.93	0.66	1.24	1.15
Glucose (mg/dl)	70–110	243	143	139	148
Calcium (mg/dl)	8.5–10.5	9.4	8.6	9.3	9.1
Lactate (mmol/liter)	0.5–2.2	5.1	1.3	1.7	2.4
Ethanol (mg/dl)	Negative	136		Negative	
Protein (g/dl)					
Total	6.0–8.3	8.4		7.6	7.8
Albumin	3.3–5.0	4.1		4.1	4.3
Alanine aminotransferase (U/liter)	10–55	30		47	38
Aspartate aminotransferase (U/liter)	10–40	33		33	20
Alkaline phosphatase (U/liter)	45–115	134		140	126
Bilirubin (mg/dl)					
Total	0.0–1.0	0.3		0.2	0.2
Direct	0.0–0.4	<0.2		<0.2	<0.2
Creatine kinase (U/liter)	60–400	67		31	
Prolactin (ng/ml)	0.1–15.2	20.6		39.6	28.5

Na = 140, Cl = 104, CO2 content = 22, Lactate = 2.4

Na – (Cl+HCO3) = 14 mmol/L

A fingerstick glucose measurement was 151 mg per deciliter (8.4 mmol per liter). Examination revealed tachycardia with a heart rate of 107 beats per minute (as compared with 78 beats per minute 6 hours previously), tachypnea with a respiratory rate of 30 breaths per minute, an oxygen saturation of 95% while he was receiving oxygen through a nasal cannula at a rate of 2 liters per minute, and new abdominal distention without tenderness; he had no tremors, seizure, incontinence, or tongue trauma. Naloxone was administered but had no effect. An electrocardiogram showed sinus tachycardia. Results of repeat laboratory tests are shown. Urinalysis was again normal. (The first had shown „trace ketones). A chest radiograph was normal, as was a CT scan of the head that was obtained without the administration of contrast material. The neurology service evaluated the patient. The next morning, the patient was more awake, alert to person and place, and responsive to commands. An electroencephalogram showed generalized theta slowing, without epileptiform abnormalities. Later in the day, he was lethargic. He reported heartburn and nausea and vomited dark-brown material. Examination revealed abdominal distention and guaiac-positive, black stool. Urinalysis revealed trace ketones but was otherwise normal. Additional imaging studies were obtained.

Lipase (U/liter)	13–60	76			
Phosphorus (mg/dl)	2.6–4.5		1.7		2.8
Magnesium (mg/dl)	1.7–2.4		1.7		1.7
Beta-hydroxybutyrate (mmol/liter)	<0.4		0.1		
Acetaminophen (μg/dl)	0.0–25.0			<5.0	
Salicylates (mg/dl)	0.0–20.0			<0.3	
Tricyclic antidepressants	Negative			Negative	
Arterial blood gas					
Fraction of inspired oxygen				‡	
pH	7.35–7.45			7.40	
Partial pressure of carbon dioxide (mm Hg)	35–42			32	
Partial pressure of oxygen (mm Hg)	80–100			121	
High-sensitivity troponin T (ng/liter)	0–14				<6
Ammonia (μmol/liter)	12–48				46
Venous blood gas					
pH	7.30–7.40				7.45
Partial pressure of carbon dioxide (mm Hg)	38–50				31
Partial pressure of oxygen (mm Hg)	35–50				148
Routine urine toxicology screening	Negative for amphetamines, barbiturates, cannabinoids, cocaine, and opiates	Negative			Positive for barbiturates; negative for amphetamines, cannabinoids, cocaine, and opiates
Specific urine toxicology screening for drugs of abuse	Negative for 6-monoacetylmorphine, buprenorphine, methadone, and oxycodone				Negative



CT Scan of the Abdomen and Pelvis. Axial images (Panels A and B) and a coronal image (Panel C), obtained after the administration of oral and intravenous contrast material, show dilated loops of small bowel, with a segment of small-bowel wall thickening (arrows), but no changes consistent with bowel obstruction. These findings most likely represent enteritis with an associated ileus.
The surgery service evaluated the patient. A nasogastric tube was placed, with immediate return of 400 ml of dark-brown and “coffee grounds” material. Intravenous normal saline, vancomycin, cefepime, and metronidazole were administered.

What is the diagnosis? Cast your vote. What diagnostic test is most likely to be helpful? Submit a comment about this case and about what diagnostic test is indicated.

What is the most likely diagnosis in this case?

- Opioid overdose.
- Surreptitious ingestion of isopropyl alcohol.
- Acute pulmonary embolus.
- Stroke.
- Ingestion of ethylene glycol.
- D-lactic acidosis.

PCO_2 is 31

Only „trace“ ketones >2 h after symptoms

PO_2 is great

No localizing findings

Did not leave his room

Had no acidosis and no anion gap

Venous blood gas			
pH	7.30–7.40		7.45
Partial pressure of carbon dioxide (mm Hg)	38–50		31
Partial pressure of oxygen (mm Hg)	35–50		148
Routine urine toxicology screening	Negative for amphetamines, barbiturates, cannabinoids, cocaine, and opiates	Negative	Positive for barbiturates; negative for amphetamines, cannabinoids, cocaine, and opiates

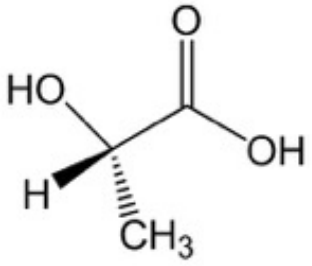
pH 7.45, H 35 nmol/L
pCO_2 31
HCO_3 21

No real acidosis

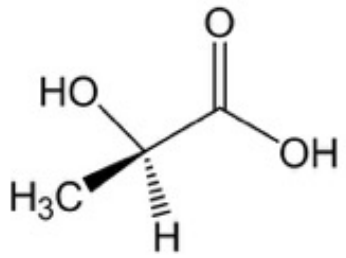
None of these choices really fit; they did not measure osmolality to look for an osmolar gap!

Lactate exists in two isomeric forms

The two lactate isomers are known as L-lactate and D-lactate; L-lactate rotates light clockwise (+) and D-lactate rotates light counterclockwise (-). This is reflected in the sometimes used nomenclature: D(-) lactate and L(+) lactate. Mammalian cells only contain L-LDH so that in humans the lactate produced is almost exclusively L-lactate. Some **bacteria** produce only D-lactate, some only L-lactate and others both forms.



L-lactic acid



D-lactic acid

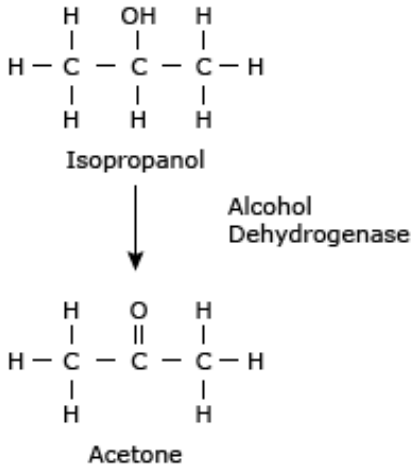
Short-bowel syndrome and d-lactac acidosis

Prior to 1979 it was presumed that all cases of hyperlactatemia and lactic acidosis were the result of increase in the predominant L-lactate isoform. In that year the first identified case of lactic acidosis resulting solely from increase in D-lactate rather than L-lactate was reported in a patient who 3 years previously had required life-saving surgery to remove a diseased section of his small intestine, This case provided the first evidence of the now established link between short-bowel syndrome and D-lactic acidosis.

Measurement of plasma lactate

Routine methods used to measure plasma lactate are based on measuring the product of enzymic action on lactate. One of two enzymes is commonly used for these analyses: lactate dehydrogenase, derived from animal tissue, and lactate oxidase derived from bacteria. Routinely, we cannot determine d-lactate

Isopropyl alcohol (isopropanol, 2-propanol, propan-2-ol) is commonly used as a disinfectant, antifreeze, and solvent, and typically comprises 70 percent of "rubbing alcohol." Like ethanol, isopropyl alcohol's precise mechanism of action in the central nervous system (CNS) remains uncertain. Isopropyl alcohol is metabolized by the alcohol dehydrogenase family of enzymes to acetone. Following ingestion of at least several grams, the elimination of acetone is slower than its formation, and this metabolic end-product accumulates. It is also responsible for the marked ketosis that is present in most isopropyl alcohol ingestions. Isopropyl alcohol is a secondary alcohol; as such, it is metabolized to a ketone (via alcohol dehydrogenase), rather than an aldehyde. Ketones cannot be oxidized to carboxylic acids. As a result, only very limited acidemia can occur; isopropyl alcohol is considerably less toxic than methanol or ethylene glycol.



Major effect and clinical course — Isopropyl alcohol manifests varying degrees of central nervous system (CNS) depression, ranging from inebriation with disinhibition, to sedation, to stupor and coma. These effects, due primarily to the parent alcohol (isopropyl alcohol), develop shortly after exposure, and peak within the first hour after ingestion. The absence of early symptoms excludes a significant isolated ingestion.

Osmolal gap — The osmolal gap provides important diagnostic information when quantitative serum testing for the toxic alcohols is not readily available.

Serum and urine ketones — Testing for serum and urine ketones using the nitroprusside reaction will be strongly positive in the presence of acetone. Low concentrations of serum ketones exclude any significant isopropyl alcohol exposure, provided at least **two hours** have transpired since ingestion. The hallmark of isopropyl alcohol metabolism is a marked ketonemia and ketonuria in the **absence** of metabolic acidosis.